

# New light on Galactic post-asymptotic giant branch stars. I. First distance catalogue

Shane B. Vickers,<sup>1,2\*</sup> David J. Frew,<sup>1,2</sup> Quentin A. Parker,<sup>1,2,3</sup> and Ivan S. Bojičić<sup>1,2,3</sup>

<sup>1</sup>Department of Physics and Astronomy, Macquarie University, NSW 2109, Australia

<sup>2</sup>Research Centre in Astronomy, Astrophysics and Astrophotonics, Macquarie University, NSW 2109, Australia

<sup>3</sup>Australian Astronomical Observatory, PO Box 915, North Ryde, NSW 1670, Australia

14 June 2018

## ABSTRACT

We have commenced a detailed analysis of the known sample of Galactic post-asymptotic giant branch (PAGB) objects compiled in the Toruń catalogue of Szczerba et al., and present, for the first time, homogeneously derived distance determinations for the 209 *likely* and 87 *possible* catalogued PAGB stars from that compilation. Knowing distances are essential in determining meaningful physical characteristics for these sources and this has been difficult to determine for most objects previously. The distances were determined by modelling their spectral energy distributions (SED) with multiple black-body curves, and integrating under the overall fit to determine the total distance-dependent flux. This method works because the luminosity of these central stars is very nearly constant from the tip of the AGB phase to the beginning of the white-dwarf cooling track. This then enables us to use a standard-candle luminosity to estimate the SED distances. For Galactic thin disk PAGB objects, we use three luminosity bins based on typical observational characteristics, ranging between 3500 and 12000  $L_{\odot}$ . We further adopt a default luminosity of 1700  $L_{\odot}$  for all halo PAGB objects. We have also applied the above technique to a further sample of 69 related nebulae not in the current edition of the Toruń catalogue. In a follow-up paper we will estimate distances to the subset of RV Tauri variables using empirical period-luminosity relations, and to the R CrB stars, allowing a population comparison of these objects with the other subclasses of PAGB stars for the first time.

**Key words:** planetary nebulae: general – stars: AGB and post-AGB – stars: evolution – catalogues – techniques: photometric – techniques: spectroscopic

## 1 INTRODUCTION

Pre-planetary nebulae (PPNe) are a very brief phase in the late-stage evolution of mid-mass stars ( $\sim 1 - 8 M_{\odot}$ ) between the asymptotic giant branch (AGB) and the planetary nebula (PN) phases (Kwok, Purton & Fitzgerald 1978; Kwok 1982; Balick & Frank 2002). The ejection of the tenuous envelope in the final superwind stage of AGB evolution (Renzini 1981) reaches rates of up to  $10^{-4} M_{\odot} \text{ yr}^{-1}$ , and leads to an increase in effective temperature of the central star. This rate of temperature increase is a strong function of the core mass (Schönberner 1983; Vassiliadis & Wood 1994, hereafter VW94) and ultimately determines if the core reaches a temperature high enough to photoionize the ejected matter as a planetary nebula (PN), before it disperses into the surrounding interstellar medium (ISM).

The relative scarcity of known Galactic PAGB objects ( $\sim 450$ ; Szczerba et al. 2007, 2012)<sup>1</sup> stems from the brevity of the PAGB

evolutionary stage (decades to a few thousand years), which for high core masses can be so brief that we are unlikely to observe these rapidly evolving objects (VW94; Blöcker 1995). The evolution of PPNe is typically characterised by a near constant bolometric luminosity, and a double-peaked spectral energy distribution (SED), manifest as a large infrared excess.

Understanding these objects is dependent on accurate distances, which are not available for most of the more poorly-quantified objects. Yet this phase is key to comprehending the shaping mechanisms of PNe (Balick & Frank 2002), as the dust shells around AGB stars, the precursors of PNe, have morphologies that are typically spherically symmetric (Corradi et al. 2003; Mauron & Huggins 2006; Cox et al. 2012; Mauron, Huggins & Cheung 2013), while imaging surveys of PNe show round morphologies to be in the minority (Balick 1987; Manchado et al. 1996; Górný et al. 1999; Parker et al. 2006; but see Jacoby et al. 2010). In order to better understand this conundrum, several imaging studies of PPNe have been undertaken over the last two decades, both at optical and infrared wavelengths (Sahai & Trauger 1998; Su et al. 1998; Hrivnak et al. 1999; Meixner et al. 1999; Sahai et al. 1999;

<sup>1</sup> Earlier compilations of PAGB stars were provided by Szczerba et al. (2001) and Kohoutek (2001).

Kwok et al. 2000; Ueta et al. 2000; Hrivnak et al. 2001; Gledhill 2005; Siódmiak et al. 2008; Lagadec et al. 2011a), with the goal of better understanding the shaping mechanisms of PPNe and PNe.

The central stars of dusty pre-PNe are invariably obscured making their identification difficult, and in contrast the dust shell is subordinate to the central star in many high-latitude objects. This variety of properties has led to a myriad of different identification schemes and criteria in their identification to date. These include the presence of an infrared (IR) excess (Zuckerman 1978; Parthasarathy & Pottasch 1986; Pottasch & Parthasarathy 1988; Hrivnak, Kwok & Volk 1989), including the utilization of IRAS colour-colour diagrams (e.g. Van der Veen & Habing 1988; Van der Veen, Habing & Geballe 1989; Preite-Martinez 1988; Manchado et al. 1989; Oudmaijer et al. 1992; Hu et al. 1993; García-Lario et al. 1997; Sahai et al. 2007). Identifying PAGB stars on the basis of their mid-IR spectra is also undertaken, including the presence of the distinctive  $21\text{ }\mu\text{m}$  feature in carbon-rich pre-PNe (Kwok, Volk & Hrivnak 1989; Cerrigone et al. 2011). More recently, surveys for new PAGB stars using near-IR photometric data (Ramos-Larios et al. 2009, 2012), and the related R CrB stars using either near- and mid-IR colours (Tisserand et al. 2011; Tisserand 2012), or ASAS-3 optical light curves (Tisserand et al. 2013), have been undertaken.

An improved understanding of this evolutionary phase is dependent on determining accurate distances to a large sample of objects, which can be used to furnish meaningful physical characteristics. Unfortunately at present, reliable distances have so far been determined for only a small fraction of these objects. It is therefore imperative that an accurate method for calculating distances to PAGB objects is determined. Since the PAGB phase is characterised by a near constant bolometric luminosity for their central stars, from the AGB-tip to the beginning of the white-dwarf cooling track (Paczyński 1971; Schönberner 1983; VW94; Blöcker 1995), we can use a standard-candle luminosity to estimate the distances to them. This is the main focus and legacy of this paper, described in detail in Section 3, below.

## 1.1 Nomenclature

For the benefit of the reader, we briefly describe the nomenclature that we have adopted in this paper. The generic term, PAGB star, includes all objects evolving from the AGB to the beginning of the white dwarf cooling track, with or without a surrounding nebula, though in practice, planetary nebulae (PNe) are defined separately (Kwok 1993, 2010; Frew & Parker 2010). With a few exceptions (e.g. Jacoby et al. 1997; Alves, Bond & Livio 2000), most Population II PAGB stars do not have extensive surrounding dust shells nor ionized PNe. We use the term pre-planetary nebulae (PPNe) to describe the non-ionized, dusty nebulae that scatter the light of their embedded central stars, and which emit in the thermal-IR (van der Veen & Habing 1989; Pottasch & Parthasarathy 1988). Spectra of their central stars range from B-type at the hot end to late-K or even early M-type at the cool end (Volk & Kwok 1989; van Hoof, Oudmaijer & Waters 1997; Van Winckel 2003). Once the effective temperature of the central star reaches about  $20\text{ kK}$ , the surrounding material is photoionized to produce a young PN. The term “transition object” is sometimes used to describe objects just commencing this process of ionization (Suárez et al. 2006; Cerrigone et al. 2008; Frew, Bojićić & Parker 2013), graphically demonstrated by the recent evolution of CRL 618 (Tafoya et al. 2013).

Ueta, Meixner & Bobrowsky (2000) classified resolved PPNe into two groups: the Star-Obvious Low-level Elongated (SOLE) nebulae, which have a visible nebula around an obvious central star,

and the DUst-Prominent Longitudinally EXtended (DUPLEX) objects, which typically have faint or even invisible central stars obscured by a dusty torus. These differences extend to other observed properties. In general the SOLE objects have bluer infrared colours than the dustier DUPLEX nebulae (Ueta et al. 2000; Siódmiak et al. 2008). Similarly the SEDs are different: the SEDs of the SOLE objects are typically two peaked, dominated by the stellar photosphere and the dust component, while the DUPLEX sources have a very prominent dust peak, with little or no optical peak (Siódmiak et al. 2008).

Siódmiak et al. (2008) also noted the different distributions in Galactic latitude of the two classes, and along with Meixner et al. (2002), suggested that the DUPLEX nebulae derive from more massive progenitor stars and are the natural precursors to bipolar PNe, which have been shown to have a lower scale-height than other PNe (Corradi & Schwarz 1995; Phillips 2001; Frew 2008). We will investigate this problem in more detail in a later paper in this series. It has become apparent that many PAGB stars have little or no dust around them, and these are generally thought to be of low mass (e.g. Alcolea & Bujarrabal 1991; Bujarrabal et al. 2013). Note that the “*likely*” PAGB section of the Toruń catalogue includes the UU Her variables (e.g. Sasselov 1984), named after the prototype UU Herculis, whose own classification is debatable (Klochkova et al. 1997). We consider these stars to be the lower-luminosity halo analogues of the old-disk “89 Herculis” stars (Gillett, Hyland & Stein 1970; Bujarrabal et al. 2007, and references therein).

Several other groups of uncommon stars are often classed as possible PAGB objects. These include the RV Tauri stars (Preston et al. 1963; Goldsmith et al. 1987; Van Winckel et al. 1999), pulsating yellow supergiants related to the Type II cepheids (Wallerstein 2002). The more luminous RV Tau stars are usually considered to be PAGB stars with low initial masses (Jura 1986; cf. Matsuura et al. 2002). For these stars, distances can be estimated using the period-luminosity (P-L) relation for Population II Cepheids (Alcock et al. 1998; Matsunaga et al. 2006; Soszyński et al. 2008; Matsunaga, Feast & Menzies 2009).<sup>2</sup> A detailed study of their distances and space distribution will be the subject of the second paper in this series (Vickers et al., in preparation). The hydrogen-deficient R Coronae Borealis stars (Clayton 1996, 2012), and their hotter kin, the extreme helium stars (e.g. Pandey et al. 2001; Jeffery 2008) will also be evaluated in that work.

## 1.2 Scientific Motivation

The compilation of the Toruń Catalogue of Galactic PAGB and related objects (Szczerba et al. 2007, 2012) now provides a central repository of information for all currently identified Galactic PAGB stars, facilitating a wider study of these objects. To date the general physical characteristics of PAGB objects have only been determined from relatively small samples, using well studied PAGB objects with ample data available. Prior to the Toruń catalogue, it was necessary to collect scattered photometric and spectroscopic data to find candidate PAGB stars; i.e. a source displaying canonical PAGB colours (van der Veen & Habing 1989; Pottasch & Parthasarathy 1988). This effectively meant that that a large-scale investigation of the Galactic PAGB population was not feasible.

<sup>2</sup> The less-luminous Type II Cepheids (W Vir and BL Her stars) are probably in an intermediate evolutionary phase between the blue horizontal branch and the base of the AGB, or are on a blue loop from the lower AGB (e.g. Maas, Giridhar & Lambert 2007). They are not considered further.

While some of the the data sets available in the Toruń catalogue are limited in quality, more recent all-sky surveys such as the AKARI (Astro-F) survey (Ishihara et al. 2010) and Wide-field Infrared Survey Explorer (WISE; Wright et al. 2010) survey provide photometric data that is more sensitive and of higher resolution than those previously utilised.

Here we present, for the first time, a homogenised catalogue of distances of all known Galactic PAGB objects available in the Toruń catalogue. Distances have been calculated using the observed SEDs, generated using the photometric and spectroscopic data gathered in the Toruń catalogue, as well as additional photometric data from recent all-sky surveys. Due to the narrow distribution of white dwarf masses (Vennes et al. 2002; Kleinman et al. 2013; and others), we have adopted assumed luminosities for specific sub-types rather than attempting to determine an individual luminosity for each object (see Section 3.1, below).

Our distance catalogue will allow new insights into this brief, poorly understood phase of late-stage stellar evolution by allowing a population study based on improved distance estimates. The paper will proceed as follows: in § 2 we outline the material used including additional data sources taken from the literature, and in § 3 we detail the method used for the SED derived distances. In § 4 we provide the reader with a sample table of the SED calculated distances, and a comparison of the results with independent literature distances. In § 6 we summarise our findings and give suggestions for future work. The resulting catalogue of distances as well as the fitted SEDs will be available in full as an online supplement.

## 2 THE TORUŃ CATALOGUE

The Toruń catalogue provides easy online access to processed photometric and spectroscopic data for the currently identified Galactic population of PAGB stars and related objects. With the advent of this compilation of all known such objects with associated flux data, our distance technique can be applied to them in their entirety, leading to a large-enough sample to exploit for scientific purposes. Prior to the Toruń catalogue the Galactic PAGB population was only available in subsets of ‘candidate’ objects. With the advent of this compilation of all known objects and flux data, our distance technique can be applied to the known PAGB population, leading to a large-enough sample to exploit for scientific purposes.

The catalogue is divided into five categories: (i) *very-likely* PAGB stars, (ii) RV Tauri stars, (iii) R Coronae Borealis / extreme Helium / Late thermal pulse stars, (iv) *possible* PAGB stars, and (v) *unlikely* PAGB objects. The data from the catalogue is summarised in Table 1. Hereafter, *likely* PAGB stars will be referred to simply as *PAGB*, R Coronae Borealis/extreme Helium/Late thermal pulse as R CrB/eHe/LTP, while the *possible* PAGB objects will be simply referred to as *possible*. We will present a distance catalogue of the R Tau and R CrB/eHe/LTP stars in a second paper (Vickers et al., in preparation), concentrating on the *likely* and *possible* PAGB objects in this work. *Unlikely* objects will in the main be not considered in this paper, except for some objects included in § 5.1.

The Toruń catalogue also includes optical fluxes from the Tycho-2 and Guide Star Catalogues (GSC; Høg et al. 2000; Lasker et al. 2008), along with Deep Near Infrared Survey of the Southern Sky (DENIS)  $IJK_s$  (Epchtein et al. 1999; Schmeja & Kimeswenger 2001) and Two Micron All Sky Survey (2MASS)  $JHK_s$  photometry (Cutri et al. 2003; Skrutskie et al. 2006). This is supplemented with mid-infrared (MIR) photometric data from the Infrared Astronomical Satellite (IRAS; Neugebauer et al. 1984) and

**Table 1.** Categories of PAGB objects in the Toruń Catalogue.

Category	Number
Likely Post-AGB	209
Possible Post-AGB	87
RV Tauri	112
R CrB / eHe / LTP	72
Unlikely Post-AGB	72
Total	465 <sup>a</sup>

<sup>a</sup>Excludes those objects categorised as unlikely PAGB stars.

the Mid Course Space Experiment 6C catalogues (MSX6C; Price et al. 2001).

For the 2MASS data we have excluded magnitudes with problematic quality flags of X, U, F and E, which leaves valid data with flags A, B, C and D, where  $\text{SNR} \geq 5$  for A, B and C flags (Cutri 2003). For the MSX6C data we have excluded data with quality flag 1 which removes all data with  $\text{SNR} \leq 5$  (Egan et al. 2003), while for the IRAS fluxes, we have removed all upper limits ( $FQUAL = 1$ ) across all four wavebands (Biechman et al. 1988).

### 2.1 Supplemental Data

Here we describe a number of additional data sources which we have used to supplement the data presented in the Toruń catalogue. The additional data includes data from several minor surveys, plus data that has been published since the most recent release of the Toruń catalogue (v 2.0; Szczepański et al. 2012). To gather much of these data, we interrogated the 5<sup>th</sup> edition of the Catalogue of Infrared Observations (Gezari, Pitts & Schmitz 1999, and references therein). This is a valuable source of literature data, but the catalogue includes both line and continuum fluxes, and data obtained using different aperture diameters, so in order to remove problematic fluxes we needed to carefully vet the data, object by object. We also utilised more recent MIR flux data from the literature for individual sources if available (e.g. Smith & Gehrz 2005; Hora et al. 2008; Lagadec et al. 2011a). Table 2 gives a comparison of the wavelengths and the angular resolution of the major surveys and catalogues that we have utilised. For consistency we have taken the zero magnitude fluxes from the SVO filter profile service<sup>3</sup>.

#### 2.1.1 Optical and Ultraviolet Photometry

From a perusal of the GSC magnitudes presented in the Toruń catalogue, it is clear there is significant confusion between stellar and nebular fluxes, such that the  $B$ ,  $V$  and  $R$ -band data differs from independent data in some cases by more than an order of magnitude. Therefore we have removed these data from the fitting process, substituting with  $UBVRI$  photometry extracted from the compilations of Mermilliod, Mermilliod & Hauck (1997) and Mermilliod (2006), supplemented with other data retrieved through the VizieR service<sup>4</sup> if available. The recently available AAVSO All-Sky Photometric Survey (APASS; Henden et al. 2012) was particularly useful for stars in the 10th to 17th visual magnitude range. A lack of

<sup>3</sup> <http://svo2.cab.inta-csic.es/theory/fps/fps.php>

<sup>4</sup> VizieR is hosted by the Centre de Données astronomiques de Strasbourg (CDS). See <http://vizier.u-strasbg.fr/viz-bin/VizieR>

**Table 2.** Table summarising the primary catalogues of flux data utilised in this study.

Survey/Catalogue	Wavebands ( $\lambda_{\text{eff}} \mu\text{m}$ )	Resolution	Reference
GALEX	FUV (0.15), NUV (0.23)	~4–6''	Morrissey et al. (2007)
TD-1	0.157, 0.197, 0.237, 0.274	~7'	Thompson et al. (1978)
ANS	0.155, 0.180, 0.220, 0.250, 0.330	2.5'	Wesselius et al. (1982)
Tycho-2	$B_T$ (0.44), $V_T$ (0.51)	~0.8''	Høg et al. (2000)
APASS	$B$ (0.44), $g'$ (0.47), $V$ (0.54), $r'$ (0.62), $i'$ (0.75)	~10''	Henden et al. (2012)
DENIS	$I$ (0.82), $J$ (1.25), $K_s$ (2.15)	1–3''	Epcstein et al. (1997)
UKIDSS	$Z$ (0.88), $Y$ (1.03), $J$ (1.25), $H$ (1.66), $K_s$ (2.15)	1''	Lawrence et al. (2007)
2MASS	$J$ (1.24), $H$ (1.66), $K_s$ (2.16)	2''	Skrutskie et al. (2006)
WISE	W1 (3.4), W2 (4.6), W3 (12), W4 (22)	6–12''	Wright et al. (2010)
COBE/DIRBE <sup>a</sup>	3.5, 4.9, 12, 25, 60	40'	Smith, Price & Baker (2004)
Spitzer (IRAC)	IRAC1 (3.6), IRAC2 (4.5), IRAC3 (5.8), IRAC4 (8.0)	≤2''	Fazio et al. (2004)
RAFGL	4.2, 11.0, 19.8, 27.4	3.5'	Price & Murdock (1983)
MSX6C	A (8.3), C (12.1), D (14.7), E (21.3)	18''	Price et al. (2001)
AKARI (IRC)	S9W (9.0), L18W (18.0)	~2''	Ishihara et al. (2010)
AKARI (FIS)	65, 90, 140, 160	30–50''	Ishihara et al. (2010)
IRAS	12, 25, 60, 100	0.5–2'	Neugebauer et al. (1984)
Spitzer (MIPS)	24, 70, 160	6–40''	Rieke et al. (2004); Carey et al. (2009)
Herschel (PACS)	blue (70), red (160)	5–35''	Pilbratt et al. (2010)
Herschel (SPIRE)	PSW (250), PMW (350), PLW (500)	5–35''	Pilbratt et al. (2010)
SCUBA	450, 850	8–14''	Holland et al. (1999)
Planck <sup>b</sup>	857 GHz (350), 545 GHz (550), 353 GHz (849)	5–30''	Planck Collaboration VI (2011)

**Notes:** <sup>a</sup>Other wavelengths have been excluded. <sup>b</sup>We have excluded data with a wavelength longer than 1 mm (217 GHz, 143 GHz, 100 GHz)

optical data is to be expected for dust enshrouded PAGB objects where the central star is almost entirely obscured. Because of this, APASS photometry was only available for about 40 objects.

We have collected  $ubvy$  Strömgren photometry from the  $ubvy - \beta$  Catalogue of Hauck et al. (1997). Here we have assumed that the Strömgren  $y$  band is equivalent to the Johnson  $V$ , and we have removed the  $u$  band photometry from the fitting procedure as it lies entirely below the Balmer discontinuity and does not lend itself to black body fitting (but would be useful for fitting model atmospheres).

We also utilised ultraviolet (UV) fluxes, which are needed to constrain the SEDs of the hotter PAGB stars. Our primary source of photometry is from the Galaxy Evolution Explorer (GALEX) mission (Morrissey et al. 2007), which covers most of the sky (excluding the Galactic plane) at a resolution of 4–6''. We have taken the GALEX magnitudes directly from the survey website<sup>5</sup>, or from the compilations of Bianchi et al. (2011a,b), which adopted 5-sigma depths of  $m_{AB} = 19.9$  for the FUV and  $m_{AB} = 20.8$  for the NUV. Since saturation in both the FUV and NUV detectors begins around  $m_{AB} = 15$  we checked all GALEX data brighter than 15th magnitude on the AB scale (Morrissey et al 2007). Data from the older TD-1 and Netherlands Astronomical Satellite (ANS) ultraviolet space missions (Thompson et al. 1978; Wesselius et al. 1982) were used to supplement the GALEX photometry. For the TD-1 data, we have only used data with a SNR  $\geq 10$ , necessarily restricting its use to fairly bright stars. For a single scan, the limit of the system is about 9th visual magnitude for a B-type star (Boksenberg et al. 1973). For the ANS data, only those objects are in the catalogue that have in at least one channel a SNR  $> 4$ , or in at least three channels a SNR  $> 3$ , were utilised.

### 2.1.2 Near- and Mid-infrared Photometry

From the Toruń catalogue we have used the given DENIS and 2MASS NIR data and supplemented this with recent  $JHK$  observations of heavily obscured objects from Ramos-Larios et al. (2012). These newly acquired data are up to 7 mag deeper than DENIS ( $K_s = 13.5$ ; Epcstein et al. 1997) and 2MASS ( $K_s = 14.3$ ; Skrutskie et al. 2006) going to a depth of  $K_s \sim 20.4$ , making these data useful for fainter Galactic PAGB stars. In addition, we also interrogated the UKIRT Deep Infrared Sky Survey (UKIDSS; Lawrence et al. 2007) to obtain  $ZYJHK_s$  magnitudes for fainter objects. UKIDSS is much more sensitive than 2MASS, with a  $K_s$  depth of 18.4–21.0 mag. We used the latest public data releases (DR) from the various UKIDSS surveys; the Large Area Survey (LAS; DR9), Galactic Clusters Survey (GCS; DR9), Deep Extragalactic Survey (DXS; DR9) and the Galactic Plane Survey (GPS; DR6). In several cases, we noted that incorrect NIR data has been incorporated into the Toruń catalogue, especially for objects at low latitude in crowded fields. We corrected these data accordingly, after perusal of a range of multi-wavelength images taken from our new Macquarie database (Bojičić et al. 2014, in preparation).

While the UKIDSS data supersedes 2MASS for faint objects, the saturation limits (~12 mag; Lucas et al. 2008) are significantly fainter than for 2MASS (~5 mag for a 51 ms exposure; Cutri 2003), so the UKIDSS data is not usable for many bright PAGB stars. Similarly, we have removed DENIS  $I$ ,  $J$  and  $K_s$  data brighter than the nominal saturation limits of 10, 8, and 6.5 mag respectively, where those data do not agree with other NIR data. Where the DENIS  $K_s$  magnitudes differ significantly from the 2MASS  $K_s$  magnitudes, we uniformly adopt the 2MASS data. As the WISE 3.4, 4.6 and 11.6  $\mu\text{m}$  wavebands are also prone to saturation for brighter objects, we have chosen to fit the black body curves through those WISE data only if there exists agreement between the WISE and other MIR data.

We also have IRAC MIR fluxes from the *Spitzer Space Tele-*

<sup>5</sup> <http://galex.stsci.edu/GR6/>

scope Galactic Legacy Infrared Mid-Plane Survey Extraordinaire (GLIMPSE; Fazio et al. 2004), as reported by Hora et al. (2008), Cerrigone et al. (2009), and others, plus archival data from the Revised Air Force Geophysics Laboratory (RAFGL) survey at wavelengths of 4.2, 11.0, 20.0 and 27.0  $\mu\text{m}$  (Price & Murdock 1983); see also Kleinmann, Gillett & Joyce (1981), for a review. We have also utilised five of the ten infrared bands of the *Cosmic Microwave Background Explorer* (COBE) Diffuse Infrared Background Experiment (DIRBE) point source catalogue (Smith, Price & Baker 2004), at 3.5, 4.9, 12, 25, and 60  $\mu\text{m}$ . Due to the large ( $42'$ ) beam size we have restricted our use of the DIRBE data to bright ( $F_{12} \geq 150 \text{ Jy}$ ), high latitude ( $|b| \geq 5^\circ$ ) objects (e.g. Smith 2003) leaving us with data for  $\sim 10$  objects.

While IRAS (Neugebauer et al. 1984) has been the most influential instrument in the discovery and identification of PAGB objects, the survey has been superseded in the MIR, first by MSX6C (Price et al. 2001) and then by the AKARI and WISE MIR surveys. The MSX survey, while of higher resolution and sensitivity than IRAS, only covered the Galactic plane. Compared to IRAS, the AKARI satellite operated over six NIR to far-infrared (FIR) passbands. The InfraRed Camera (IRC) provides photometry in two wavebands (*S9W* and *L18W*), while the far-infrared surveyor (FIS) operated at wavelengths of 65, 90, 140 and 160  $\mu\text{m}$ . AKARI is up to ten times more sensitive than the IRAS 12 and 25  $\mu\text{m}$  bands (Ishihara et al. 2010) and covers 90% of the sky. AKARI surveyed the sky in the mid-infrared with greater resolution than that of IRAS.

Using VizieR we extracted AKARI IRC and FIS data whilst excluding data from unconfirmed sources or those with a flux measurement considered to be unreliable i.e.  $FQUAL < 3$ . In addition to the IRAS fluxes collected in the Toruń catalogue we have queried VizieR for IRAS data (IPAC 1986) for the 69 additional objects. WISE surveyed 99% of the sky with greater sensitivity than all previous mid-infrared surveys (Wright et al. 2010). While IRAS had two far-infrared bands, WISE has two mid-infrared bands (3.4 and 4.6  $\mu\text{m}$ ) that IRAS does not. We have excluded those WISE data which are considered upper limits ( $SNR \leq 2$ ).

### 2.1.3 Far-infrared Photometry

In order to constrain the far-IR during the SED fitting process we have included sub-mm fluxes where available. Several data sets, including from the Kuiper Airborne Observatory (KAO), were extracted from Gezari et al. (1999, and references therein). We also utilised 450 and 850  $\mu\text{m}$  fluxes (Holland et al. 1999) obtained with the Submillimetre Common-User Bolometer Array (SCUBA) on the James Clerk Maxwell Telescope (JCMT). We have also made use of publicly-released data from the Herschel Space Observatory (Pilbratt et al. 2010), using 70 and 160  $\mu\text{m}$  fluxes from the Photodetector Array Camera and Spectrometer (PACS; Poglitsch et al. 2010) and 250, 350, 500  $\mu\text{m}$  fluxes from the Spectral and Photometric Imaging Receiver (SPIRE; Griffin et al. 2010), largely taken from the Mass loss for Evolving StarS (MESS) program (Groenewegen et al. 2011).

We also used 857, 545 and 353 GHz fluxes for a few objects from the Early Release Compact Source Catalogue (Planck Collab-

oration VI, 2011) of the Planck<sup>6</sup> mission (Planck Collaboration I, 2011).

### 2.1.4 Spectroscopy

We supplemented the photometric data with spectroscopic data where available. However this data was not used in the fitting process as the spectra are usually not normalised; the spectral data have been retained on the plots for illustrative purposes. UV spectra from the *International Ultraviolet Explorer* (IUE) were downloaded from the MAST website.<sup>7</sup> We generally excluded the IUE high dispersion spectra (due to bad data flags) and any other spectra with a low signal-to-noise ratio. We averaged the remaining long and short wavelength spectra before overplotting on the SED fits.

We also included both *Infrared Space Observatory* (ISO) and IRAS Low Resolution Spectrometer (LRS) spectra (see, e.g. Kwok, Volk & Bidelman 1997), when available for the objects in our sample. The LRS spectra used in the Toruń catalogue were extracted from Kevin Volk's Home Page<sup>8</sup> just as we have done for the additional objects used in the literature comparison (see later). The LRS spectra have been absolutely calibrated according to the procedure followed by Volk & Cohen (1989) and Cohen et al. (1992). For objects with available 2–45  $\mu\text{m}$  ISO Short Wave Spectrometer (SWS) spectra we have extracted and over plotted these data where appropriate.

## 3 METHODOLOGY

Here we outline the SED-based procedure used to calculate a set of homogenised distances for the currently known Galactic PAGB objects. In general, the SED technique for distance determinations has only been applied since the 1980s, after the infrared fluxes from the IRAS mission were published (Neugebauer et al. 1984; Beichman et al. 1988). Prior to that time, distance-dependent luminosities were determined for the bipolar nebulae CRL 2688 and CRL 618 (Ney et al. 1975; Westbrook et al. 1975), based on the limited thermal-IR data available, and before the nature of these objects was entirely clear (Cohen et al. 1975; Humphreys, Warner & Gallagher 1976; Zuckerman et al. 1976; Cohen & Kuhí 1977). The first real attempt at measuring SED-based distances for an ensemble of PPNe was by Zuckerman (1978). Now, the availability of flux data supplied by the Toruń catalogue, as well as additional recent flux data, provides us with the necessary tools to use the same SED modelling technique as for example, demonstrated in van der Veen et al. (1989), Kwok, Volk & Hrivnak (1989), Su, Hrivnak & Kwok (2001), De Ruyter et al. (2005, 2006), Sahai et al. (2007), and Gielen et al. (2011). This method requires the assumption of a ‘standard candle’ luminosity, statistically representative of PAGB stars, though with caveats, as we explain in detail below.

Most pre-PNe are seen to have a double-peaked SED comprised of a central star component and a cool dust component arising from the reprocessing of UV photons from the central star into IR photons from the detached circumstellar envelope (CSE), as in

<sup>6</sup> Planck (<http://www.esa.int/Planck>) is a project of the European Space Agency (ESA) with instruments provided by two scientific consortia funded by ESA member states, with contributions from NASA (USA) and telescope reflectors provided by a collaboration between ESA and a scientific consortium led and funded by Denmark.

<sup>7</sup> <https://archive.stsci.edu/iue/search.php>

<sup>8</sup> [http://www.iras.ucalgary.ca/~volk/getlrs\\_plot.html](http://www.iras.ucalgary.ca/~volk/getlrs_plot.html)

Kwok (1993). In some cases the presence of either a cool stellar companion or a Keplerian dust disk can be seen by an increase in the NIR flux (Dominik et al. 2003; De Ruyter et al. 2005; Van Winckel et al. 2006, 2009). We assumed in all cases that the observed SED can be expressed as a combination of one or more Planck functions. No object required more than three Planck functions to model the observed IR energy distribution.

Furthermore, due to the large amount of data on more than 200 catalogued stars, and the resulting statistical nature of the project, a number of simplifying assumptions were necessary in our approach. We used a combination of Planck functions at different temperatures rather than taking a more detailed radiative transfer approach, such as was done for the Red Rectangle by Men'shchikov et al. (2002). We only used broadband continuum fluxes, ignoring spectroscopic features such as silicate absorption and emission bands and any fine-structure lines (e.g. Engelke, Kraemer & Price 2004). Finally, in order to calculate the total distance-dependent flux of each object we have assumed an isotropic flux distribution, ignoring both the nebular morphology and orientation of each object which would inherently alter the flux distribution (Su, Hrivnak & Kwok 2001).

### 3.1 Assumed Luminosity

It has been shown several times in the literature (Vennes et al. 2002; Liebert et al. 2005; Kepler et al. 2007) that thin-disk white dwarfs (WDs), which are the direct progeny of most PNe and their precursor PAGB stars, have a narrow mass distribution around  $\sim 0.6 M_{\odot}$ . Tremblay, Bergeron & Gianninas (2011) found a mean mass of DA white dwarfs of  $0.613 M_{\odot}$  from Sloan Digital Sky Survey (SDSS; Adelman-McCarthy et al. 2006) DR4 data. In a more recent survey of  $\sim 2200$  hot ( $T_{\text{eff}} > 13000$  K) DA white dwarfs found in the SDSS, Kleinman et al. (2013) found that the disk DA white dwarf population can be divided into three distinct populations with mass peaks at  $0.39$ ,  $0.59$  and  $0.82 M_{\odot}$ , and population fractions of  $6\%$ ,  $81\%$  and  $13\%$  respectively. The lower mass peak can be excluded from further analysis here, on the grounds that single-star evolution cannot account for such low-mass remnants within a Hubble time. The higher mass WDs have also been suggested to be a product of binary evolution, and possibly represent white dwarf mergers (Jeffery, Karakas & Saio 2011; Kleinman et al. 2013), though the WDs derived from single higher-mass progenitors will also contribute to this mass bin. Independently, the empirical mass distribution of PN central stars have also been estimated by Stasińska, Gorny & Tylenda (1997) and Gesicki & Zijlstra (2007), who determine a range of  $0.55 - 0.65 M_{\odot}$ , and  $0.61 \pm 0.02 M_{\odot}$ , respectively.

In this paper, we adopt a mass of  $0.61 \pm 0.02 M_{\odot}$  to represent the mean core mass during the PAGB evolutionary stage for the nearby *intermediate-age* population of the thin disk, which we expect produced the majority of local PNe (Frew & Parker 2006; Frew 2008). Using the core mass / luminosity relation of VW94, this translates to an approximate PAGB luminosity of  $L_{\star} \approx 6000 \pm 1500 L_{\odot}$ . This does not imply that all catalogued PPNe have this luminosity, just that they are statistically likely to fall in this luminosity range. Indeed, given the wide range of PN morphologies and ionized masses (Frew & Parker 2010), and the diversity of central star photospheric compositions observed in the solar neighbourhood (e.g. Frew 2008; Frew et al. 2014a), this may a somewhat simplistic approach. Interestingly, the luminosity distribution function for PAGB stars observed in the Large Magellanic Cloud (LMC) by van Aarle et al. (2011) is much broader, between adopted extrema of  $\sim 1000$  and  $35000 L_{\odot}$ . This result is possibly

due to contamination issues and uncertain selection biases at play, manifest when comparing a local disk-dominated sample with a colour-selected and flux-limited LMC sample.

In light of the Kleinman et al. results, we endeavour to divide the Galactic population of PAGB stars into several subpopulations of different ages, to refine our distance estimates, especially for objects at low Galactic latitude. The high-mass objects are potentially the objects with the largest distance uncertainties. The extreme OH/IR stars are generally considered to be the descendants of the highest-mass progenitors (e.g. Justtanont et al. 2013). These are evolved, dust-enshrouded AGB stars with very strong 1612 MHz OH maser emission (Johansson et al. 1977; te Lintel Hekkert et al. 1989; Sevenster 2002), and are thought to produce the small homogeneous class of OHPNe, after photoionization has commenced (Zijlstra et al. 1989; Uscanga et al. 2012).

García-Hernández et al. (2007) propose that heavily obscured OHPNe descend from such high-mass progenitor stars, that could represent a link between OH/IR stars with extreme outflows and collimated bipolar PN. García-Hernández et al. (2007) adopted  $L = 10000 L_{\odot}$  for this class of stars. However, on the assumption that hot-bottom burning (HBB) of dredged-up carbon to nitrogen only occurs in stars heavier than  $4.0 - 5.0 M_{\odot}$  (Boothroyd, Sackmann & Ahern 1993; Mazzitelli et al. 1999; Izzard et al. 2004; McSaveney et al. 2007; Karakas et al. 2009), then at a minimum,  $L = 20000 L_{\odot}$  is more appropriate for the oxygen-rich AGB stars that are produced. On the other hand, there is some evidence that substantial nitrogen enrichment, at least at the amounts needed to make a Type I PN ( $N/O > 0.8$ , following Kingsburgh & Barlow 1994), may occur at masses less than this, down to stars with initial masses of  $\sim 3.0 M_{\odot}$ , or even less (Karakas et al. 2009; Parker et al. 2011).

Accordingly, we divide the young and intermediate-age (carbon star) populations at an initial mass of  $3.0 M_{\odot}$ , corresponding to a turn-off age of  $\sim 5 \times 10^9$  years (cf. Wood, Bessell & Fox 1983). However, recent observations in the inner disk of M 31 (Boyer et al. 2013) suggests that there is a metallicity threshold above which carbon stars (with  $C/O > 1$ ) cannot be produced through dredge-up processes. If the same threshold exists in the inner disk and Bulge of our Galaxy, then the presence of oxygen-rich stars there cannot be used as an indicator of high-mass progenitors. In light of this, we use a high luminosity ( $> 20000 L_{\odot}$ ) only for objects with an unambiguous isotopic signature of HBB; i.e. with low values of the  $^{18}\text{O}/^{17}\text{O}$  and  $^{12}\text{C}/^{13}\text{C}$  ratios (Imai et al. 2012; Justtanont et al. 2013; Edwards & Ziurys 2013), or a high N/O ratio in shock-ionized optical knots. Other criteria, such as nebular expansion velocities (e.g. Barnbaum, Zuckerman & Kastner 1991), need caution in their interpretation.

For the  $\sim 20$  low-mass Galactic thick-disk objects we have identified (from kinematics and/or distances from the disk mid-plane), we adopt an approximate age of 10 Gyr (Ramírez & Alende Prieto 2011; Hansen et al. 2013) and a progenitor mass of  $1.0 M_{\odot}$ . Using an average of the white dwarf initial-to-final mass relations (IFMRs) of Kalirai et al. (2008) and Renedo et al. (2010), we then estimate a core mass of  $0.53 M_{\odot}$ , leading to an assumed luminosity of  $1700 L_{\odot}$  (following VW94). For the more metal-poor Population II stars of the Galactic halo, we assume an age of 11–13 Gyr (Kalirai 2012; Hansen et al. 2013) and that the  $0.8 M_{\odot}$  progenitor stars produced white dwarfs with a mass of  $0.53 - 0.55 M_{\odot}$  (Kalirai et al. 2009; Kalirai 2012). From this mass we estimate a mean PAGB luminosity of  $2000 L_{\odot}$  (VW94) for this population. This luminosity is consistent with observations of ‘yellow’ PAGB stars in globular clusters (Alves, Bond & Onken 2001).

When considering the appropriate luminosity to adopt for

**Table 3.** Adopted masses and luminosities for the different PAGB populations of the Galaxy.

Population	Age (Gyr)	Metallicity Range [Fe/H]	Mass Range ( $M_{\odot}$ )	Initial Mass <sup>a</sup> ( $M_{\odot}$ )	PAGB Mass ( $M_{\odot}$ )	PAGB Luminosity ( $L_{\odot}$ )	Class <sup>b</sup>
Young Thin Disk	$\leq 0.7$	-0.2 to +0.5	3.0 – 8.0	3.0	0.70	12000	I
Intermediate Thin Disk	0.7 – 3.0	-0.2 to +0.5	1.6 – 3.0	2.0	0.61	6000	IIa
Old Thin Disk	3.0 – 8.0	-0.7 to +0.5	1.1 – 1.6	1.5	0.56	3500	IIb
Thick Disk	8 – 12	-1.6 to -0.3	0.9 – 1.1	1.0	0.53	1700	III
Bulge	2.0 – 12	-1.9 to +0.6	1.0 – 1.8	1.6	0.57	4000	V
Inner Halo	11 – 13	-2.4 to -0.6	$\sim 0.8$	0.8	0.54	1700	IV
Outer Halo	11 – 13	$\leq -1.5$	$\sim 0.8$	0.8	0.53:	1700	IV

<sup>a</sup>Adopted mass; <sup>b</sup> class according to the scheme of Peimbert (1978), as parameterized by Quireza et al. (2007).

PAGB objects located in the Galactic bulge the situation is more complicated due to the complex formation history of the Bulge. Bensby et al. (2013) found a population of old ( $> 10$  Gyr) metal-poor stars with several groups of younger higher metallicity stars with a broad distribution of ages, some as young as 2 Gyr (Bensby et al. 2013), corresponding to a progenitor mass of  $\sim 1.8 M_{\odot}$ . The age distribution of the metal-rich component peaks around 4 – 5 Gyr, with a progenitor mass of  $\sim 1.4 M_{\odot}$ . On the assumption that the observed Bulge population of PAGB stars and PNe derive from  $1.6 \pm 0.2 M_{\odot}$  stars, we infer an average core mass of  $0.57 M_{\odot}$ , and hence a PAGB luminosity of  $4000 L_{\odot}$ , again following VW94. Since the Bulge sample of compact, optically-thick PNe we have also analysed (§ 5.1) is dominated by helium-burning [WCL] stars, it would be useful to have an understanding of their mean mass. As far as we know there is no literature determination of the mean mass of these stars, but Althaus et al. (2009) have measured the average mass of a sample of 37 PG 1159 stars, the possible descendants of the [WCL] stars, to be  $0.573 M_{\odot}$ , in good agreement with our assumed Bulge mass. We hence assume a luminosity  $4000 L_{\odot}$  for all [WCL] stars, including those that belong to the Galactic disk.<sup>9</sup>

The adopted parameters of the sub-populations of the Galaxy used in this study are summarised in Table 3. The ages and metallicities have been adopted (or derived) from Carollo et al. (2007, 2010), Fuhrmann (2011), Ramírez & Allende Prieto (2011), Kalirai (2012), Bensby et al. (2013), and Hansen et al. (2013). We also give the inferred luminosities derived from the progenitor masses via an averaged IFMR (see the above references) and the core-luminosity relation of VW94, and we attempt to map our populations to the classes of Peimbert (1978), expected when the objects evolve into PNe (see also Casassus & Roche 2001; Quireza et al. 2007). Owing to various assumptions that differ between these studies, this can only be done approximately.

Based on the observed mass function of PN central stars, we consider it likely that almost all observed disk PAGB stars in the Toruń catalogue have luminosities between 3500 and 10000  $L_{\odot}$ , with only a few more luminous objects. Hence, at worst, the error on an individual distance is about 40 per cent, and significantly smaller if our classification into subgroups has been effective.

<sup>9</sup> We note there is still debate over which PPN precursors are destined to produce [WC] stars (e.g. Szczerba et al. 2003; Górný et al. 2010).

### 3.2 SED Fitting and Distance Determination

Dusty PPNe typically exhibit a double-peaked SED (Kwok 1993) and so would require two Planck functions to model the total flux of the object. However, some objects, e.g. those objects with circumstellar disks (e.g. Waters et al. 1993; de Ruyter et al. 2006; Van Winckel et al. 2006), require additional functions. We have modelled the SEDs of all 209 *likely* PAGB objects in the Toruń catalogue, as well as a number of candidate PPNe and young compact PNe (see Appendix A1), by fitting Planck functions to the observational data described in section 2.

The monochromatic flux for each SED component has been modelled by:

$$F_{\lambda} = CB_{\lambda}(T_c) \quad (1)$$

where  $B_{\lambda}(T_c)$  is the Planck function with a colour temperature  $T_c$  and  $C$  is a distance/angular size dependent scale factor. The total monochromatic flux,  $F(\lambda, \mathbf{p})$ , of each object is simply the superposition of each of the Planck functions for all components. The fitting of the Planck functions has been done using the *curve\_fit* function in the SciPy package<sup>10</sup> which uses the Levenberg-Marquardt algorithm (Marquardt 1963; Markwardt 2009). The algorithm optimises the parameters  $\mathbf{p}(C, T_c)$  such that the following function:

$$S(\mathbf{p}) = \sum_{n=1}^m [y_n(\lambda_n, f_n) - F(\lambda_n, \mathbf{p})]^2 \quad (2)$$

where  $y_n(\lambda_n, f_n)$  are the observational data such that  $y_n$  represents the wavelength ( $\lambda_n$ ) and flux ( $f_n$ ) of the nth data point, is minimised. This procedure is repeated for up to a maximum of four Planck functions after which equation 2 is applied to each scenario to determine which combination gives the minimum deviation between the observed data and the model data.

From the SED fitting process we were able to derive a number of parameters for each object. The total monochromatic flux of each object (in units of  $L_{\odot} \text{kpc}^{-2}$ ) was derived via numerical integration of the superposition of the Planck functions, integrated from 1000 Å through to infinity. The luminosity dependent distance is then simply:

$$D_L^2 = \frac{L_{\star}}{4\pi F} \quad (3)$$

where  $L_{\star}$  is the assumed stellar luminosity (in solar units) and

<sup>10</sup> <http://www.scipy.org/>

$F$  is the integrated flux expressed in  $L_{\odot}\text{kpc}^{-2}$ . For most disk objects, we used  $L_{\star} = 6000 L_{\odot}$  (but see § 3.1), while for low-mass Galactic thick disk objects and metal-poor Population II stars the assumed luminosity is  $1700 L_{\odot}$  and  $2000 L_{\odot}$  respectively, as discussed in section 3.1. The uncertainty in the distance is derived directly from the uncertainty in the flux, convolved with the uncertainties of the overall fit, and the assumed luminosity. The distance uncertainty is calculated from:

$$\sigma_{\text{Dist}} = (\sigma_{\text{Lum}}^2 + \sigma_{\text{Fit}}^2 + \sigma_{E(B-V)}^2)^{0.5} \quad (4)$$

where  $\sigma_{\text{Lum}}$  is the uncertainty on the assumed luminosity,  $\sigma_{\text{Fit}}$  is the uncertainty of the fitting function, and  $\sigma_{E(B-V)}$  is the interstellar reddening uncertainty, which can be neglected in those objects where the IR flux dominates. For objects with  $|b| > 4$  deg we have used the asymptotic reddening of Schlafly & Finkbeiner (2011) with an assumed uncertainty of 10% for high latitude objects ( $|b| > 10$  deg) and 20% for lower latitude objects (4 deg  $< |b| < 10$  deg). For objects in the plane of the Galaxy we have used the extinction model of Arenou, Grenon & Gomez (1992) to determine the line of sight reddening for a given distance. Generally the more obscured the central star the lower the Galactic latitude distribution (see figure 9 of Ramos-Larios et al. 2012). For Galactic plane objects the central star is in some cases completely obscured (e.g. IRAS 11544–6408 and IRAS 18450–0148 of Fig 1); for these objects the distance uncertainty will generally be  $< 10\%$  where  $F_{\text{IR}}/F_{\star} > 10$ . Note that we have not corrected for circumstellar extinction.

For the young PNe we have used the same method as above except for objects in the Galactic plane ( $|b| < 4$  deg). For these objects we have used the extinctions derived from the Balmer decrement, taken from Tylenda et al. (1992) and Frew, Bojićić & Parker (2013). We have adopted uncertainties ranging from 10–30% for the Tylenda et al. (1992) values, and adopt the reddening uncertainties unchanged from Frew et al. (2013). The SEDs have been dereddened using the extinction law of Cardelli, Clayton & Mathis (1989) with the updated NIR coefficients of O'Donnell (1994). Here we have assumed  $R_V = 3.09$ . Figure 1 shows representative SEDs and our model fits for nine representative PAGB objects: IRAS 06176-1036 (the Red Rectangle), IRAS 10158-2844 (HR 4049), IRAS 10256-5628, IRAS 11339-6004, IRAS 11544-6408, IRAS 13416-6243, IRAS 18071-1727, IRAS 18450-0148 and IRAS 19480+2504. The SED plots for all 209 likely and 87 possible PAGB objects will be made available through the worldwide web.

### 3.3 Other Derived Parameters

The dereddened photospheric temperature and the dust component temperatures were derived directly from the fitting process, as solutions to the least squares problem defined in section 3.2, along with their corresponding  $1\sigma$  uncertainties, which in some cases are quite large due to the inability to constrain one side of the Planck function. For those objects with a Planck function clearly representative of the central star, i.e. with a black-body temperature higher than an approximate sublimation temperature of  $T_{\text{subl}} \sim 1300$  K for silicate dust (Kama, Min & Dominik 2009), we have calculated the ratio of the infrared/dust flux to that of the central star,  $F_{\text{IR}}/F_{\star}$ . We define the  $F_{\text{IR}}/F_{\star}$  ratio as the ratio of the integrated flux from the photospheric Planck function(s), integrated from 1000 Å to infinity, to the integrated flux of the dust component(s) also integrated from 1000 Å to infinity. The ratio of IR to stellar flux was calculated after the application of the reddening correction.

For objects with a bipolar morphology,  $F_{\text{IR}}/F_{\star}$  can be used as an indication of the orientation of the object whether it be pole-on or edge-on (Su, Hrivnak & Kwok 2001). We also determined the height  $|z| = D \sin b$  above the Galactic mid-plane for each star from our distance and the Galactic latitude, to help ascertain the kinematic population that each object belongs to. A full analysis of the various PAGB subsamples will be given in a future paper.

## 4 DISTANCE CATALOGUE

In this section we provide a catalogue of distances to the PAGB objects listed in the Toruń catalogue. In the past, the distances to PAGB objects were difficult to determine, due to the near total obscuration of the central star by their surrounding nebula, and the inherent difficulty in their classification. The purpose of this work is to present a more accurate and homogenised SED method of calculating distances to PAGB objects. For the SED method to be applicable (without reddening correction) the objects require a larger infrared flux compared to the central star flux i.e.  $F_{\text{IR}}/F_{\star} > 1$ . For objects with no infrared excess the derived distances are questionable without applying an extinction correction to the stellar flux. In this section we provide a catalogue of distances to the PAGB objects listed in the Toruń catalogue.

Table 4 contains the first 10 rows of the SED derived parameters for the 209 *likely* PAGB objects. The entire table is available in the associate online supplement. Column 1 and 2 are the IRAS identifier and the other name listed in the Toruń catalogue based on an order of preference given in Szczerba et al. (2007). The longitude and latitude for each object are given in columns 3 and 4. The total integrated flux of each star is expressed in units of  $\text{erg s}^{-1} \text{cm}^{-2}$  and  $L_{\odot}\text{kpc}^{-2}$  (assuming an isotropic flux distribution) are presented in columns 5 and 6. In column 7 we give the adopted luminosity of the source, and the estimated reddening for each object is given in column 8. The derived distance and calculated uncertainty are given in column 9. The ratio of IR to stellar flux after reddening correction is listed in column 10. Finally we have listed the dust temperature and uncertainty if only one black body was applied, or a range of dust temperatures if multiple black bodies were applied, up to the sublimation temperature of astrophysical silicates,  $T_{\text{subl}} \sim 1300$  K as given by Kama, Min & Dominik (2009). We have also estimated distances in an identical fashion for the 87 *possible* PAGB objects in the Toruń catalogue, presented in Table 5. The meanings of the column headings are identical to those in Table 4.

### 4.1 Is the 22 μm Luminosity a Standard Candle for Dusty PAGB stars

Using the distance catalogue and the apparent WISE W4 magnitudes we have plotted a histogram (figure 3) of the absolute magnitudes at 22 μm for the *likely* and *possible* PAGB objects for which WISE 22 μm data were available. After inspecting the SEDs and the  $F_{\text{IR}}/F_{\star}$  ratio we have found that the objects with an absolute W4 magnitude fainter than 12th are those where a clear IR excess is absent, and therefore the optical and near-IR fluxes need to be dereddened before the distance can be considered reliable. Thus we assume that the W4 magnitude is representative of the IR excess and not the central star, and that the object must have a distinct IR excess i.e.  $F_{\text{IR}}/F_{\star} > 1$ . We were able to statistically determine an absolute brightness for each object using our distance and the

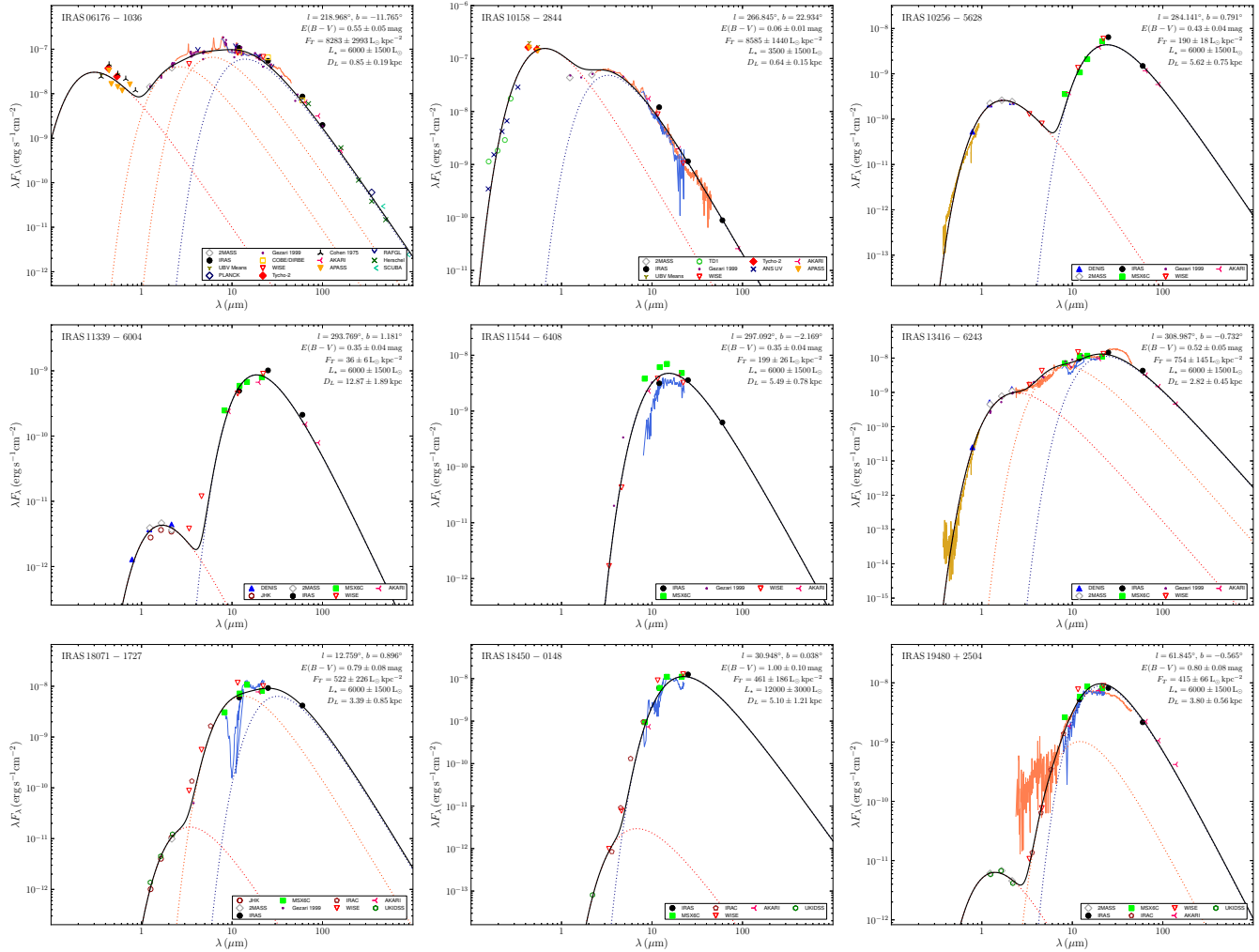


**Figure 1.** Representative SEDs for nine PAGB objects. Top row – IRAS 06176-1036 (the Red Rectangle), IRAS 10158-2844 (HR 4049), and IRAS 10256-5628; Middle row – IRAS 11339-6004, IRAS 11544-6408, and IRAS 13416-6243; Bottom row – IRAS 18071-1727, IRAS 18450-0148 and IRAS 19480+2504.

**Table 4.** Parameters and distances for 209 *likely* PAGB stars in the Toruń catalogue, ordered by Galactic longitude. The table is published in its entirety as an online supplement, and a portion is shown here for guidance regarding its form and content.

IRAS No.	Other Name	<i>l</i> ( $^{\circ}$ )	<i>b</i> ( $^{\circ}$ )	Flux (erg s\$^{-1}\$ cm\$^{-2}\$)	Flux (L\$_{\odot}\$ kpc\$^{-2}\$)	Luminosity (L\$_{\odot}\$)	<i>E(B-V)</i> (mag)	Distance (kpc)	<i>F</i> <sub>IR</sub> / <i>F</i> <sub>★</sub>	<i>T</i> <sub>D</sub> (K)
17581-2926	GLMP 688	1.293	-3.199	1.46E-09 $\pm$ 2.60E-10	45 $\pm$ 8	4000 $\pm$ 1500	0.51 $\pm$ 0.05	9.38 $\pm$ 1.95	1.49	113 $\pm$ 6
17291-2402	GLMP 575	2.518	5.120	4.22E-09 $\pm$ 5.85E-10	131 $\pm$ 18	4000 $\pm$ 1500	1.16 $\pm$ 0.23	5.52 $\pm$ 1.10	8.99	130-853
17349-2444	GLMP 593	2.652	3.637	2.17E-09 $\pm$ 3.81E-10	67 $\pm$ 12	4000 $\pm$ 1500	0.51 $\pm$ 0.05	7.70 $\pm$ 1.59	9.61	121 $\pm$ 6
18371-3159	LSE 63	2.918	-11.818	1.92E-09 $\pm$ 3.99E-10	60 $\pm$ 12	1700 $\pm$ 750	0.13 $\pm$ 0.01	5.34 $\pm$ 1.30	0.77	134 $\pm$ 7
17576-2653	...	3.472	-1.853	2.57E-09 $\pm$ 3.66E-10	80 $\pm$ 11	4000 $\pm$ 1500	0.51 $\pm$ 0.05	7.07 $\pm$ 1.42	2.32	187 $\pm$ 9
17516-2525	GLMP 662	4.038	0.056	4.91E-08 $\pm$ 7.06E-09	1528 $\pm$ 219	6000 $\pm$ 1500	0.50 $\pm$ 0.05	1.98 $\pm$ 0.29	7.07	141-749
17074-1845	LSE 3	4.100	12.263	4.07E-09 $\pm$ 9.59E-10	127 $\pm$ 30	6000 $\pm$ 1500	0.25 $\pm$ 0.02	6.88 $\pm$ 1.18	0.51	146 $\pm$ 7
17441-2411	Silkworm Nebula	4.223	2.145	3.27E-08 $\pm$ 3.97E-09	1018 $\pm$ 123	12000 $\pm$ 3000	1.65 $\pm$ 0.43	3.43 $\pm$ 0.48	17	208-962
17332-2215	GLMP 588	4.542	5.295	2.52E-09 $\pm$ 3.92E-10	78 $\pm$ 12	4000 $\pm$ 1500	0.78 $\pm$ 0.16	7.14 $\pm$ 1.45	8.97	137-833
17360-2142	GLMP 600	5.364	5.038	2.20E-09 $\pm$ 3.77E-10	69 $\pm$ 12	4000 $\pm$ 1500	0.72 $\pm$ 0.14	7.64 $\pm$ 1.57	4.12	141 $\pm$ 7

corresponding WISE 22  $\mu m$  magnitude. For W4 apparent magnitudes brighter  $m_{22} = -3.5$ , which suffer from saturation effects, we estimated the magnitude from the IRAS [25] magnitude, using the following transformation equation:

$$m_{22} = 1.07(0.01) m_{25} + 0.64(0.05) \quad (5)$$

which we derived from Figure 2. It is clear from figure 3 that PAGB objects appear to have a relatively narrow distribution of absolute brightness at 22  $\mu m$ . By applying a gaussian to the distribution we found the mean W4 magnitude to be  $-14.77$  mag with a standard deviation of 0.54 mag. This implies that the WISE W4

**Table 5.** Parameters and distances for 87 *possible* PAGB stars in the Toruń catalogue, ordered by Galactic longitude. The table is published in its entirety as an online supplement, and a portion is shown here for guidance regarding its form and content.

IRAS No.	Other Name	$l$ ( $^{\circ}$ )	$b$ ( $^{\circ}$ )	Flux ( $\text{erg s}^{-1} \text{cm}^{-2}$ )	Flux ( $L_{\odot} \text{kpc}^{-2}$ )	Luminosity ( $L_{\odot}$ )	$E(B - V)$ (mag)	Distance (kpc)	$F_{\text{IR}}/F_{\star}$	$T_{\text{D}}$ (K)
...	LS 4825	1.671	-6.628	3.09E-09 $\pm$ 6.10E-10	96 $\pm$ 19	4000 $\pm$ 1500	0.24 $\pm$ 0.05	6.45 $\pm$ 1.36	...	...
17550-2800	GLMP 676	2.205	-1.900	2.24E-09 $\pm$ 4.59E-10	70 $\pm$ 14	4000 $\pm$ 1500	0.51 $\pm$ 0.05	7.58 $\pm$ 1.62	...	125–1030
...	CD-30 15602	2.798	-7.675	1.26E-09 $\pm$ 1.79E-10	39 $\pm$ 6	3500 $\pm$ 1500	0.22 $\pm$ 0.04	9.44 $\pm$ 2.13	...	...
17376-2040	...	6.437	5.275	4.48E-09 $\pm$ 1.70E-09	139 $\pm$ 53	4000 $\pm$ 1500	0.65 $\pm$ 0.13	5.36 $\pm$ 1.43	5.71	161–1232
17416-2112	GLMP 625	6.469	4.198	2.14E-09 $\pm$ 2.34E-10	67 $\pm$ 7	4000 $\pm$ 1500	0.85 $\pm$ 0.17	7.75 $\pm$ 1.51	77	130–499
16476-1122	...	7.524	20.418	8.32E-09 $\pm$ 8.44E-10	259 $\pm$ 26	3500 $\pm$ 1500	0.70 $\pm$ 0.07	3.68 $\pm$ 0.81	0.11	186 $\pm$ 9
F16277-0724	LS IV -07 1	7.956	26.706	1.36E-07 $\pm$ 8.80E-09	4234 $\pm$ 274	3500 $\pm$ 1500	0.24 $\pm$ 0.02	0.91 $\pm$ 0.20	...	...
17433-1750	GLMP 637	9.562	5.612	5.73E-09 $\pm$ 3.22E-09	178 $\pm$ 100	4000 $\pm$ 1500	0.53 $\pm$ 0.11	4.74 $\pm$ 1.60	5.95	156–431
17364-1238	...	13.183	9.720	8.80E-10 $\pm$ 1.05E-10	27 $\pm$ 3	1700 $\pm$ 750	0.46 $\pm$ 0.09	7.88 $\pm$ 1.80	0.28	134 $\pm$ 7
18313-1738	...	15.322	-4.268	7.58E-09 $\pm$ 2.36E-09	236 $\pm$ 73	6000 $\pm$ 1500	0.64 $\pm$ 0.13	5.04 $\pm$ 1.01	6.39	412–1142

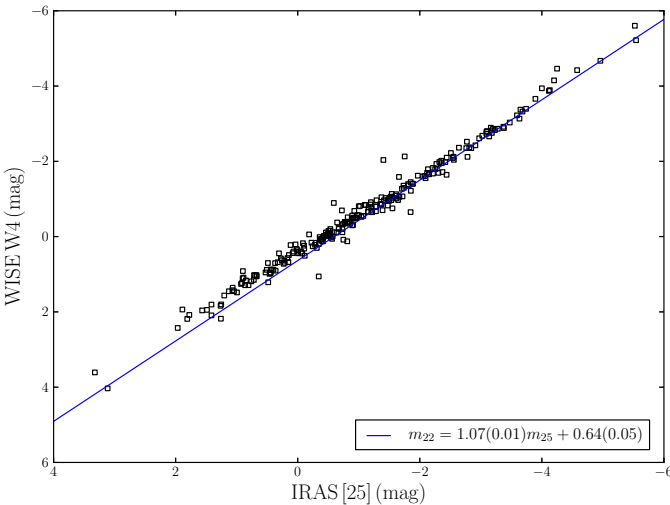


**Figure 2.** A comparison between WISE (W4) 22  $\mu\text{m}$  and IRAS 25  $\mu\text{m}$  apparent magnitudes shows surprisingly little scatter around a linear fit, described by  $m_{22} = 1.07(0.01)m_{25} + 0.64(0.05)$ . The W4 magnitudes saturate brighter than mag −3.5.

22  $\mu\text{m}$  magnitude has the potential to be used as a standard candle for dusty PAGB stars, and merits further investigation.

## 5 MIMICS

As discussed by Szczerba et al. (2007), several classes of objects can mimic PAGB stars in terms of their optical and IR colours, just as PNe are confused with a wide range of mimics (e.g. Cohen et al. 2007; Frew & Parker 2010; Frew et al. 2010; Parker et al. 2012; De Marco et al. 2013). While H II regions can be readily differentiated from PAGB stars and PNe (Anderson et al. 2012), some circumstellar nebulae around massive stars (e.g. Wachter et al. 2010), especially the rare class of yellow hypergiants with dusty ejecta, e.g. IRC+10420 (Jones et al. 1993; Oudmaijer & de Wit 2013), Hen 3-1379 (Lagadec et al. 2011b; Hutsemékers, Cox & Vamvatira-Nakou 2013) and probably AFGL 4106 (van Loon et al. 1999), have very similar MIR colours to some PPNe. For other objects their true nature remains uncertain, e.g. HD 179821 (AFGL 2343) (Kastner & Weintraub 1995; Hawkins et al. 1995; Reddy & Hrivnak 1999; Josselin & Lèbre 2001; Kipper 2008; Ferguson & Ueta 2010). Young stellar objects (YSOs) are the other

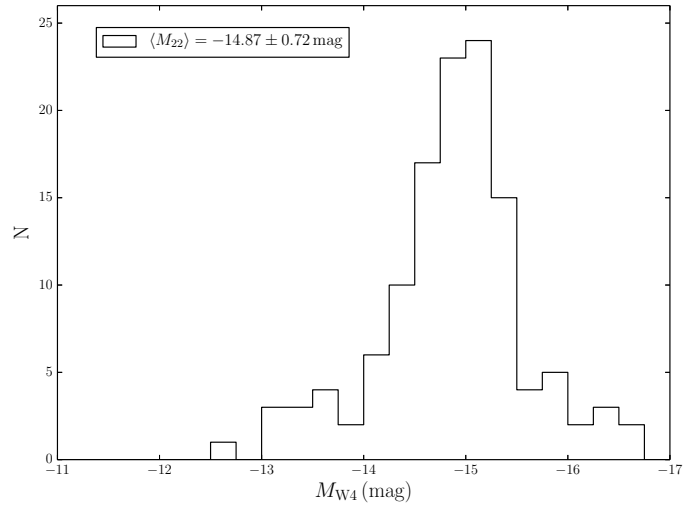


**Figure 3.** Histogram of WISE 22  $\mu\text{m}$  (W4) absolute magnitudes derived using our SED distances for all 209 *likely* and 87 *possible* objects. We have excluded those objects that do not show a significant IR excess, i.e.  $F_{\text{IR}}/F_{\star} < 1$ .

main contaminant in lists of PAGB stars (e.g. Adams, Lada & Shu 1987; Urquhart et al. 2007) often having quite similar SEDs and MIR colours. We differentiate the two classes on the basis of secondary criteria such as the  $z$ -height from the Galactic plane (after first estimating the distance), and the surrounding environment, particularly checking for areas of active star formation.

On the other hand, dusty D-type symbiotic stars (Corradi 1995; Belczyński et al. 2000), and some B[e] stars (Lamers et al. 1998), might be expected to have luminosities of  $10^3$  to  $10^4$   $L_{\odot}$ , at least if the accretion-disk luminosity is not too high. Hence the SED technique should be applicable to these objects too. Several objects with ambiguous classifications, such as the Ant nebula, Mz 3 (Cohen et al. 1978, 2011; Santander-García et al. 2004) and the Calabash Nebula, OH 231.8+4.2 (§ 5.3; Choi et al. 2012), have distances included in Table 4 as we base our classifications on the current edition of the Toruń catalogue. The yellow symbiotic stars, particularly the D'-symbiotic systems (e.g. Gutiérrez Moreno & Moreno 1998; Jorissen 2003; Pereira, Smith & Cunha 2005; Frankowski & Jorissen 2007; Miszalski et al. 2012), are more problematic as the assumption of optical thickness and the luminosity of the cool star are generally unknown *a priori*. Thus, we

have not determined distances to any of these stars, pending further analysis.

### 5.1 Derived parameters and distances for 69 miscellaneous nebulae

Several classes of objects are amenable to the SED distance technique, such as the dust-enshrouded AGB stars (Jura & Kleinmann 1989; Olivier, Whitelock & Marang 2001), and some B[e] and D-type symbiotic systems (e.g. Parthasarathy & Pottasch 1989; Miszalski, Mikolajewska & Udalski 2013). As long as the same assumptions apply to these objects as for PAGB stars, such as a typical PAGB luminosity, approximate isotropy, and optical thickness, as shown by a large thermal infrared excess, then a SED distance can be determined.

Of course the youngest, dustiest PNe (Kwok, Hrivnak & Milone 1986; Zhang & Kwok 1991; Sahai, Morris & Villar 2011) can be modelled, especially dusty PNe with very-late Wolf-Rayet (or [WCL]) and similar central stars (Kwok, Hrivnak & Langill 1993; De Marco, Barlow & Storey 1997; De Marco et al. 2002; Gesicki et al. 2006; De Pew et al. 2011), as these often show a very strong MIR excess (Zijlstra 2001; Clayton et al. 2011). As discussed in § 3.1 we assume an intrinsic luminosity of  $4000 L_\odot$  for these stars.

Other PNe and transitional objects with signatures of youth such as detectable OH maser emission (Zijlstra et al. 1989; Usanga et al. 2012), have also been investigated.<sup>11</sup> This approach is only approximately correct, as ionized nebulae reprocess the energy of their central stars in other components besides the thermal dust continuum, such as in emission lines and free- and bound-free continua, which may not be modelled correctly using our SED fitting method. Furthermore, for strongly anisotropic nebulae, this method will give an upper limit of the distance. To assess these caveats, we determined an SED distance to the strongly bipolar Type I nebula NGC 6302 (Wright et al. 2011), which exceeds the known distance of 1.17 kpc (Meaburn et al. 2008) by a factor of two. This large nebula is clearly not optically thick in all directions, illustrated in the difference between the total observed luminosity ( $5700 L_\odot$ ) and the assumed stellar luminosity of  $14300 L_\odot$  (see Wright et al. 2011).

Lastly, since several well-known objects formerly considered to be PPNe are excluded from the current edition of the Toruń catalogue, such as M 2-9 (Allen & Swings 1972; Balick 1989; Hora & Latter 1994; Corradi et al. 2011; Castro-Carrizo et al. 2012), and Hen 2-90 (Sahai & Nyman 1990; Costa, de Freitas-Pacheco & Maclie 1993; Sahai et al. 2002; Kraus et al. 2005), we have also determined distances to them. We also include the B[e] star MWC 922 (the Red Square; Tuthill & Lloyd 2007), as its nebular morphology and SED are remarkably similar to the better known Red Rectangle (Cohen et al. 2004), as well as the D-type symbiotic outflow Hen 2-147 (Corradi et al. 1999) as it has an independent distance estimate (Santander-García et al. 2007). We have added the final flash objects, FG Sge (included in the Toruń catalogue), as well as V605 Aql which is embedded in recently-formed hot dust (Clayton & De Marco 1997; Clayton et al. 2013), and is hosted by the old

faint planetary nebula, Abell 58 (Abell 1966; Bond 1976). In Table 6, we provide data for these additional sources taken from our extensive database of Galactic PNe and related objects (Bojičić et al. 2014, in preparation). The meanings of the column headings are identical to those in Table 4.

### 5.2 Comparison with Independent Distances

To assess the SED technique as a viable distance tool, we undertook a comparison of our estimated distances with the highest-quality, independent literature distances that were available. These distances are derived from several primary techniques, e.g. trigonometric and expansion parallaxes. We have compiled a sample of PAGB stars, supplemented with several (nascent)-pre-PNe<sup>12</sup> and young compact PNe, which have independently determined distances that we have deemed reliable.

We have omitted from the comparison the trigonometric distance calculated by Imai et al. (2011) for IRAS 19312+1950, as it is not clear if this is a bona fide PAGB star (Nakashima et al. 2011). We have ignored for now any kinematic distances derived from radial velocities and the assumption of circular motion around the Galaxy (e.g. Sahai, Sánchez Contreras & Morris 2005). We justify this by noting the peculiar velocities of many PAGB stars can be large, which will lead to inaccurate distances from this method. Only for PPNe with high-mass progenitors will this approach work (see also Frew et al. 2014b).

The literature objects that we have used for the distance comparisons are given in Table 7 along with their literature distances and the corresponding SED derived distance from this work, taken from Tables 4, 5, and 6. Extended notes on some of these objects are given in § 5.3. The sample of literature distances includes one object IRAS 07399–1435 (more commonly known as OH 231.8+4.2, Calabash, or Rotten Egg nebula) found in the *possible* section of the Toruń catalogue as well as three *likely* PAGB objects. The others are taken from Table 6. The distances for the globular clusters M 13 and ω Cen have been taken from the 2010 edition of the Harris (1996) catalogue. Our distance for the PAGB star in NGC 6712 is imprecise, owing to a lack of good photometry, so we have excluded it from the distance comparison. For the dust-enshrouded Miras and symbiotic outflows we have determined the luminosity for the SED fit from the period-luminosity relations of Feast et al. (1989) and Groenewegen & Whitelock (1996) for O-rich and C-rich stars respectively.

In Figure 4 we plot the SED derived distances against the independent literature distances given in Table 7. A least squares fit of the data with a slope of  $1.00 \pm 0.04$  indicating that the two data sets are in very good agreement. Figure 4 demonstrates clearly that the SED technique is a viable method for determining distances to dusty PAGB objects. In addition to the independent distance comparison we have compared our SED distances (with a default luminosity,  $L_* = 6000 L_\odot$ ) with those derived by Sahai et al. (2007), previously the largest sample of SED derived distances for PAGB objects. In the bottom panel of Figure 4 we show that our independent SED distances are in excellent agreement with those of Sahai et al. (2007). Note that we have excluded the distance of IRAS 22036+5306 from this comparison on the grounds that the

<sup>11</sup> Note that a young age alone is not enough of a discriminant to see if the SED distance technique is applicable. For example, Hen 3-1357 is a young, rapidly evolving PN (Parthasarathy & Pottash 1989; Parthasarathy et al. 1993) but has very little thermal dust emission, relative to its H $\alpha$  flux.

<sup>12</sup> The term nascent PPN has been applied by Sahai et al. (2006) to the most evolved dust-enshrouded AGB stars that are seen to have prominent surrounding reflection nebulae; see also Schmidt, Hines & Swift (2002) and Kim & Taam (2012).

**Table 6.** Parameters and distances for 69 miscellaneous objects not in the Toruń Catalogue, ordered by Galactic longitude. The table is published in its entirety as an online supplement, and a portion is shown here for guidance regarding its form and content.

IRAS No.	Other Name	<i>l</i> (°)	<i>b</i> (°)	Flux (erg s <sup>-1</sup> cm <sup>-2</sup> )	Flux (L <sub>⊙</sub> kpc <sup>-2</sup> )	Luminosity (L <sub>⊙</sub> )	<i>E(B - V)</i> (mag)	Distance (kpc)	<i>F<sub>IR</sub>/F<sub>★</sub></i>	<i>T<sub>D</sub></i> (K)
17371-2747	JaSt 23	0.344	1.566	2.27E-09 ± 9.27E-10	71 ± 29	4000 ± 1500	0.51 ± 0.05	7.52 ± 2.08	...	90–657
17574-2921	H 1-47	1.295	-3.040	9.11E-10 ± 3.08E-10	28 ± 10	4000 ± 1500	0.52 ± 0.05	11.88 ± 3.00	34	113–337
18129-3053	SwSt 1	1.591	-6.176	1.41E-08 ± 3.41E-09	437 ± 106	4000 ± 1500	0.30 ± 0.06	3.02 ± 0.68	15	200–861
18040-2941	H 1-55	1.714	-4.455	3.60E-10 ± 1.08E-10	11 ± 3	4000 ± 1500	0.45 ± 0.09	18.91 ± 4.54	15	87–325
18029-2840	M 1-38	2.483	-3.745	8.81E-08 ± 2.24E-08	2740 ± 697	4000 ± 1500	0.79 ± 0.08	1.21 ± 0.27	0.01	136±7
18022-2822	M 1-37	2.681	-3.468	1.56E-09 ± 6.39E-10	48 ± 20	4000 ± 1500	0.89 ± 0.09	9.09 ± 2.52	5.72	118–349
18084-2823	Ap 1-12	3.326	-4.660	1.64E-09 ± 2.92E-10	51 ± 9	4000 ± 1500	0.41 ± 0.08	8.86 ± 1.84	3.59	117–623
18213-2948	Hen 3-1688	3.392	-7.810	5.24E-08 ± 7.05E-09	1631 ± 219	6000 ± 1500	0.38 ± 0.08	1.92 ± 0.27	0.09	116–1090
17074-1845	Hen 3-1347	4.100	12.263	3.33E-09 ± 9.18E-10	104 ± 29	6000 ± 1500	0.25 ± 0.03	7.61 ± 1.42	0.34	146±7
19288-3419	Hen 2-436	4.871	-22.727	1.93E-10 ± 5.96E-11	6.00 ± 1.85	4000 ± 1500	0.41 ± 0.04	25.81 ± 6.27	9.75	267–880

**Table 7.** Objects used in literature distance comparison, arranged in order of increasing distance.

IRAS No.	Common Name	<i>L<sub>★</sub></i> (L <sub>⊙</sub> )	<i>D<sub>SED</sub></i> (kpc)	<i>D<sub>Lit</sub></i> (kpc)	Method	Reference
(nascent)-PPNe / PAGB objects						
09452+1330	CW Leo (IRC+10216)	9800±3000	0.13 ± 0.02	0.123 ± 0.014	G	Groenewegen et al. (2012)
03507+1115	IK Tau (NML Tau)	9100±3000	0.24 ± 0.06	0.265 ± 0.02	E	Hale et al. (1997)
21003+3630	CRL 2688	6000±1500	0.61 ± 0.08	0.42 ± 0.06	E	Ueta et al. (2006)
10158–2844	HR 4049	6000±1500	0.67 ± 0.17	0.64 ± 0.19	D	Acke et al. (2013)
18460–0151	OH 31.0-0.2	6000±1500	3.02 ± 0.40	2.1 ± 0.6	S	Imai et al. (2013b)
18286–0959	OH 21.80-0.13	6000±1500	3.42 ± 0.56	3.61 <sup>+0.63</sup> <sub>-0.47</sub>	T	Imai et al. (2013a)
...	NGC 5139 WOR 1957	2000±750	6.64 ± 1.36	5.2 ± 0.5	M	Harris (1996)
19134+2131	[HSD93b] 16	6000±1500	7.99 ± 1.30	8.00 <sup>+0.90</sup> <sub>-0.70</sub>	T	Imai et al. (2007)
17423–1755	Hen 3-1475	20000±5000	8.07 ± 1.40	8.30(±1.0)	E	Borkowski & Harrington (2001)
...	NGC 6205 BARN 29	2000±750	8.54 ± 1.74	7.1 ± 0.7	M	Harris (1996)
Young PNe						
...	NGC 7027	6000±1500	0.95 ± 0.15	0.87 ± 0.10 <sup>b</sup>	E	Zijlstra et al. (2008, and references therein)
19327+3024	BD+30 3639	4000±1500	1.20 ± 0.29	1.52 ± 0.21	V	Akras & Steffen (2012)
19219+0947	Vy 2-2	6000±1500	3.37 ± 0.55	3.6 ± 0.4	E	Christianto & Seaquist (1998)
18240–0244	M 2-43	3500±1500	4.27 ± 0.70	6.9 ± 1.5	E	Guzmán et al. (2006)
19255+2123	K 3-35	6000±1500	5.78 ± 0.94	3.90 <sup>+0.70</sup> <sub>-0.50</sub>	T	Tafoya et al. (2011)
19288–3419	Hen 2-436	4000±1500	25.8 ± 6.3	26.0 ± 2.0 <sup>c</sup>	M	Zijlstra et al. (2006)
Symbiotic stars / Other objects						
07399–1435	OH 231.8+4.2 <sup>a</sup>	15000±3000	2.20 ± 0.40	1.54 <sup>+0.02</sup> <sub>-0.01</sub>	T	Choi et al. (2012)
20097+2010	Hen 1-5 (FG Sge)	6000±1500	2.23 ± 0.36	2.5 (±0.5)	P	Mayor & Acker (1980)
17028–1004	M 2-9	2000±750	2.26 ± 0.30	1.3 ± 0.2	G	Corradi et al. (2011)
16099–5651	Hen 2-147	7000±1500	3.50 ± 0.50	3.0 ± 0.4	PL	Santander-Garcia et al. (2007)
17317–3331	V1018 Sco	35000±5000	3.76 ± 0.66	3.20 ± 0.64	L	Cohen et al. (2005)
19158+0141	Abell 58 (V605 Aql)	4000±1500	5.25 ± 0.80	4.60 ± 0.60	E	Clayton et al. (2013)

**Notes:** D: dynamical parallax; E: expansion parallax; G: geometric model; L: phase-lag method; M: membership of system at known distance; P: pulsation theory; PL: Mira period-luminosity relationship; S: statistical parallax; T: trigonometric parallax; V: velocity field mapping. <sup>a</sup>physical member of the open cluster M 46; <sup>b</sup>This is the average of the distances given in Zijlstra et al. (2008); <sup>c</sup> Refer to the text.

Sahai et al. (2007) distance was not derived using the SED technique.

### 5.3 Notes on Individual Objects with Independent Distances

#### 5.3.1 IRAS 03507+1115 (NML Tau)

This nearby dust-enshrouded Mira (Decin et al. 2010), or nascent PPN, is historically known as NML Tau (Neugebauer, Martz & Leighton 1965). The 469-d pulsation period leads to a bolomet-

ric luminosity of 9100 ± 3000 L<sub>⊙</sub> from the P-L relation of Feast et al. (1989), and a distance of 240 ± 0.60 pc, in good agreement with the expansion distance from Hale et al. (1997) of 265 ± 20 pc.

#### 5.3.2 IRAS 06176-1036 (HD 44179)

This is the Red Rectangle, quite possibly the most famous pre-PN for its beautiful reflection nebulosity (Cohen et al. 2004; Van Winckel 2014). We required two black body curves to represent the dust component,  $T \approx 950$  K and  $T \approx 290$  K, to repre-

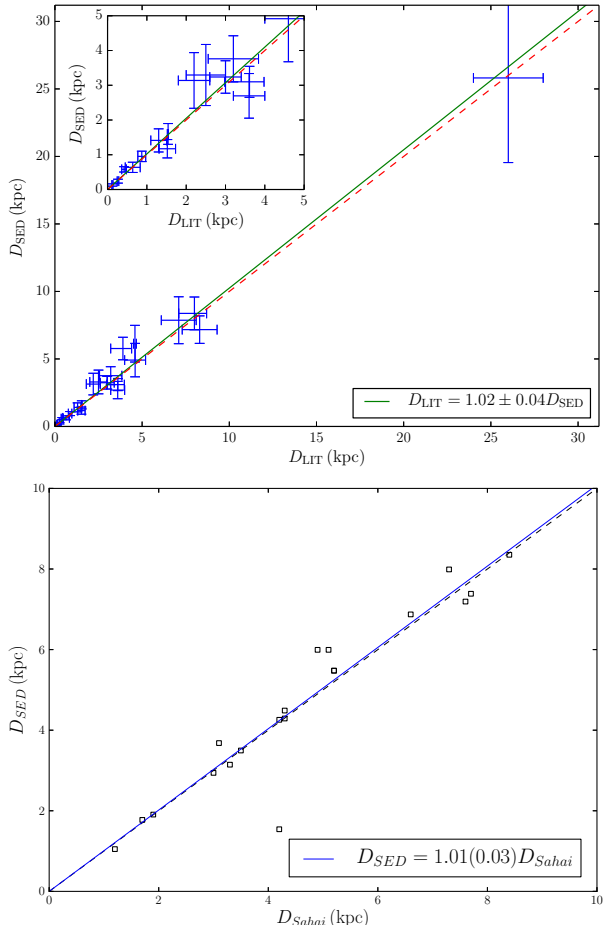


**Figure 4.** Top: Literature comparison of distances listed in Table 7. *Inset:* zoom of objects inside 5 kpc. Bottom: Comparison of distances from this work with the SED distances from Sahai et al. (2007) using the same method and with an assumed luminosity ( $L_{\star} = 6000 L_{\odot}$ ) for both data sets. The blue line is a linear fit to the data, which has a slope close to unity.

sent the Keplerian disk in this system (Men'shchikov et al. 2002). The integrated flux of the Red Rectangle gives a distance of  $D_{\text{SED}} = 0.83^{+0.12}_{-0.14}$  kpc compared to the currently accepted distance of 0.73 kpc derived by Men'shchikov et al. (2002). These authors also derived a core mass of  $0.58 M_{\odot}$  which corresponds to a luminosity of  $\approx 4000 L_{\odot}$  using our prescription, whereas those authors used a higher luminosity of  $6050 L_{\odot}$ . Using a luminosity of  $4000 L_{\odot}$ , we derive a distance to the Red Rectangle of  $D_{\text{SED}} = 0.74$  kpc, in excellent agreement with their distance.

### 5.3.3 IRAS 09452+1330 (IRC+10216)

CW Leo is the nearest dust-enshrouded AGB star to the Sun (Becklin et al. 1969; Morris 1975; Menten et al. 2012). The surrounding bipolar nebula (Christou et al. 1991; Kastner & Weintraub 1994; Osterbart et al. 2000) indicates the star is very close to leaving the AGB and becoming a bona fide PPN. We use the distance from Groenewegen et al. (2012) as a comparison with our own distance. By modelling the time-lag between the star and surrounding bow-shock, these authors determined a distance of  $123 \pm 14$  pc. We refine our SED distance by estimating the bolometric luminosity directly from the 630-d pulsation period and adopting the revised

**Table 8.** Comparison of our SED derived distances and those derived by Sahai et al. (2007).

IRAS No.	$D_{\text{SED}}$ (kpc)	$D_{\text{Sahai}}$ (kpc)	$\Delta D$ (kpc)	Morph
01037+1219	...	0.65	...	E
11385-5517	1.05	1.20	0.15	I
13428-6232	1.91	1.90	0.01	B
13557-6442	3.14	3.30	0.16	B
15045-4945	...	4.90	...	B
15452-5459	1.77	1.70	0.07	B
15553-5230	4.49	4.30	0.19	B
16559-2957	5.48	5.20	0.28	B
17253-2831	7.39	7.70	0.31	E
17347-3139	3.68	3.10	0.58	B
17440-3310	7.19	7.60	0.41	B
17543-3102	7.99	7.30	0.69	B
18276-1431	2.94	3.00	0.06	B
18420-0512	6.87	6.60	0.27	E
19024+0044	5.99	5.10	0.89	M
19134+2131	8.35	8.40	0.05	B
19292+1806	5.48	5.20	0.28	B
19306+1407	5.99	4.90	1.09	B
19475+3119	1.54	4.20	2.66	M
20000+3239	3.50	3.50	0.00	E
22036+5306 <sup>a</sup>	3.83	...	...	B
22223+4327	4.29	4.30	0.01	E
23304+6147	4.26	4.20	0.06	M

**Notes:** <sup>a</sup>The Sahai et al. (2007) distance for IRAS 22036+5306 has been excluded since it was not derived via the SED technique.

period-luminosity relation for carbon-rich Miras from Groenewegen & Whitelock (1996). We determine  $L = 9800 L_{\odot}$ , and a distance  $D_{\text{SED}} = 133 \pm 13$  pc, in excellent agreement.

### 5.3.4 IRAS 10158-2844 (HR 4049)

AG Ant is a long-period spectroscopic binary with a core mass of  $0.58 M_{\odot}$  and a secondary mass of  $0.34 M_{\odot}$  (Hinkle et al. 2007). The large infrared excess of HR 4049 has been modelled using a black body of  $T \sim 1100$  K by Dominik et al. (2003), De Ruyter et al. (2006), and Hinkle, Brittain & Lambert (2007) in agreement with our SED modelling. Several authors have determined the stellar parameters of HR 4049 (Lambert et al. 1988; Waelkens et al. 1991) finding an effective temperature;  $T_{\text{eff}} \approx 7500$  K slightly higher than the photospheric temperature determined via black body fitting. Our SED distance of 0.67 kpc is in good agreement with a new dynamical parallax distance of 0.64 kpc from Acke et al. (2013).

### 5.3.5 IRAS 17028-1004 (M 2-9)

An extensive literature (e.g. Allen & Swings 1972; Schwarz et al. 1997; Smith & Gehrz 2005, and references therein) exists on this beautiful and remarkable bipolar nebula. It is considered here to be a resolved symbiotic outflow, based on its spectral characteristics and red NIR colours (see Schmeja & Kimeswenger 2001). Corradi, Balick & Santander-García (2011) have modelled the light changes of the Butterfly Nebula to determine a distance of  $1.3 \pm 0.2$  kpc. The physical properties of this system are then consistent with a symbiotic-like interacting binary as the central engine, but the implied luminosity ( $2500 L_{\odot}$ ) is less than expected for a TP-AGB

star. It may be a RGB or early-AGB star, or alternatively a thick-disk TP-AGB star.

### 5.3.6 IRAS 17317–3331 (V1018 Sco)

This heavily obscured, high-mass, oxygen-rich OH/IR star is surrounded by an ionized ring nebula (Cohen, Parker & Chapman 2005; Cohen et al. 2006), which is either an unusual PN, or a symbiotic outflow. Our SED distance compares well with the phase-lag distance of  $3.2 \pm 0.6$  kpc from Cohen et al. (2005). Assuming the pulsation period of the star is given by the maser light curve, the 1486-d period (Chapman, Habing & Killeen 1995) leads to a bolometric luminosity of  $35000 L_\odot$  adopting the Mira period-luminosity relation for O-rich stars of Feast et al. (1989). Our measured bolometric flux,  $F_{\text{tot}} = 2475 L_\odot \text{kpc}^{-2}$  leads directly to a distance of  $3.76 \pm 0.66$  kpc, in agreement with the phase-lag distance within the uncertainties.

### 5.3.7 IRAS 17423–1755 (Hen 3-1475)

This is a particularly interesting example of an oxygen-rich PAGB star with highly collimated outflows (Riera et al. 1995; Manteiga et al. 2011). Assuming  $L = 20000 L_\odot$ , appropriate for a high-mass progenitor, we estimate a distance of 8.0 kpc, in excellent agreement with the expansion parallax distance of Borkowski & Harrington (2001). Similar objects to Hen 3-1475 are IRAS 19343+2926 and IRAS 17393–2727,<sup>13</sup> which shows a strong  $12.8 \mu\text{m}$  [Ne II] nebular emission line, showing its central region is already ionized by its fast-evolving central star (García-Hernández et al. 2007).

### 5.3.8 IRAS 19288–3419 (Hen 2-436)

Hen 2-436 is the optically brightest PN in the Sagittarius dwarf spheroidal galaxy (see Zijlstra et al. 2006, and references therein). Though not in the Toruń catalogue, this dusty object belongs to the rare group of IR-[WC] PNe (Zijlstra 2001), so is amenable to the SED technique. Recent distances to the Sgr dSph galaxy range from 24.3 kpc (McDonald et al. 2013) to 28–30 kpc (Siegel et al. 2011), suggesting there is considerable line-of-sight depth. We adopt a distance of  $26 \pm 2$  kpc which is the average of the values tabulated by Kunder & Chaboyer (2009) and McDonald et al. (2013). This is in very good agreement with our SED distance to Hen 2-436 of 27 kpc, after assuming a stellar luminosity of  $4000 L_\odot$  for its [WC] nucleus (see § 3.1).

### 5.3.9 IRAS 21003+3630 (CRL 2688)

The Cygnus Egg is the closest PPN to the Sun, with a distance of 0.42 kpc, derived from two-epoch *HST* proper motions of the expanding system of nebular features (Ueta et al. 2006). Our bolometric flux,  $F_{\text{tot}} = 16300 L_\odot \text{kpc}^{-2}$  combined with an assumed luminosity of  $6000 L_\odot$  leads to an estimated distance of  $0.61 \pm 0.08$  kpc. It appears the intrinsic luminosity must be less than our assumed value, despite CRL 2668 having a DUPLEX morphology.

### 5.3.10 OH 231.8+04.2, a Bipolar Outflow in an Open Cluster

There is an extensive literature on this object so only a brief sketch is provided here. Commonly known as the Calabash or Rotten Egg Nebula, this strongly bipolar reflection/emission nebulosity lies in the outskirts of the rich open cluster, M 46 (NGC 2437), and is generally regarded as a PPN (Sánchez Contreras et al. 2000; Bujarrabal et al. 2002; Meakin et al. 2003). However, the fact that there is a binary system at the centre, comprising a very late-type (M9–10 III) Mira star (Cohen 1981; Kastner et al. 1998) with a 700-d pulsation period, and an A0 V companion (Saánchez Contreras, Gil de Paz & Sahai 2004), seems to indicate that the nebula has more in common with D-type symbiotic outflows (Corradi 1995), than with true PPNe.

Unlike the case of the planetary, NGC 2438 which is projected on M 46 (Kiss et al. 2008), the systemic radial velocity of the Calabash nebula (Jura & Morris 1985; Morris et al. 1987; Sánchez Contreras, Bujarrabal & Alcolea 1997; Zijlstra et al. 2001; Bujarrabal et al. 2012) is consistent with the mean radial velocity of M 46 (Mermilliod et al. 2007; Frinchaboy & Majewski 2008; Kiss et al. 2008). Both the phase-lag distance to OH 231.8 of 1.3–1.5 kpc (Bowers & Morris 1984; Kastner et al. 1992), and the much more accurate maser trigonometric distance of 1.54 kpc from Choi et al. (2012) are in good agreement with recent distance determinations to M 46 from Sharma et al. (2006) and Davidge (2013). Lastly, the proper motions of its associated water masers (Choi et al. 2012) also agree with the cluster’s proper motion (Dias, Lépine & Alessi 2002). As the membership of OH 231.8+04.2 in M 46 is now secure, we can use the age of the cluster ( $2.2\text{--}2.5 \times 10^8$  yrs; Sharma et al. 2006; Davidge 2013) to infer the progenitor mass of the Mira, which turns out to be  $\sim 3.4 M_\odot$ , in agreement with previous mass estimates (Kastner et al. 1998). The substantial nitrogen enrichment compared to the solar abundance (Cohen et al. 1985) seen in the shock-ionized lobes of the Calabash (Reipurth 1987; Bujarrabal et al. 2002), is consistent with mild HBB in this star. Hence, this observation may indicate that nitrogen enrichment can occur at stellar masses under  $\sim 4.0 M_\odot$  (see Karakas et al. 2011).

## 6 SUMMARY AND FUTURE WORK

The compilation of the Toruń catalogue (Szczerba et al. 2007, 2012) gathered a wide assortment of flux data for all Galactic PAGB objects known at that time. We have used these data, adding more recent fluxes from the literature to build an homogenised set of distances by modelling their observed SEDs with one or more black body curves. Total fluxes were calculated for each object by numerically integrating the fitted curves. In a follow up paper we investigate the potential discrepancy in the integrated fluxes when using model atmospheres to model the central star as opposed to black body fitting. We expect that for severely reddened stars and stars with a high  $F_{\text{IR}}/F_\star$  model atmospheres will make little difference compared to the UV-bright stars where we expect a larger difference in integrated fluxes. The assumed luminosity (in solar units) was derived using the empirical core-mass luminosity relation for PAGB evolution from VW94, and a set of criteria separating the different populations of PAGB objects. Distances were computed by equating an assumed luminosity with the integrated flux of each source thus creating a homogenised set of distances, presented in full as an online supplement. The calculated distances were compared to several independently derived literature values measured using a variety of methods, in order to ascertain the ac-

<sup>13</sup> This object is not in the current edition of the Toruń catalogue.

curacy of our approach. In Section 5.2, we showed that our derived distances are in good agreement with a range of literature values. In this way we have effectively demonstrated that the SED technique is a valid method for calculating statistical distances to PAGB and related objects. In a follow-up paper (Vickers et al., in preparation), we will determine distances to the remaining objects in the Toruń Catalogue, namely the RV Tauri stars, using instead empirical period-luminosity relations, as well as the R CrB stars (and related hydrogen-deficient objects).

In a further paper, we will investigate the population characteristics of a relatively complete volume-limited sample of Galactic disk PAGB objects for the first time. Such a census can be used for understanding the population demographics of Galactic PAGB objects, and their relationships with their precursor AGB stars and descendent PNe (Frew & Parker 2006; Frew 2008; Frew et al. 2014b). Volume-limited samples are an under-appreciated tool for studying stellar populations (Frew & Parker 2012), having the power to unlock the vital characteristics of Galactic PAGB objects, needed to understand the possible shaping mechanisms of their progenitors (Balick & Frank 2002). Specifically we will endeavour to determine the scale heights (and hence progenitor ages and masses) of the various subgroups of PAGB stars and relate these to the morphological and dust properties of the resolved nebulae (Ueta et al. 2000; Siódmiak et al. 2008), and those objects that possess Keplerian dust disks (see Van Winckel et al. 2006; Hinkle et al. 2007; van Aarle et al. 2011; Acke et al. 2013). Our upcoming analysis will be undertaken with much larger samples than have been utilised previously (Likkel, te Lintel Hekkert & Chapman 1993).

Finally we expect the data avalanche from modern multi-wavelength surveys to aid in the discovery of many more PAGB stars and PPNe in the Galaxy. These will be incorporated into our new relational database of PNe and PAGB stars currently under construction at Macquarie University, in conjunction with the CDS, Strasbourg (Bojičić et al., in preparation).

## ACKNOWLEDGEMENTS

This research has made use of the SIMBAD database and the VizieR service, operated at CDS, Strasbourg, France. Additional data were obtained from the Mikulski Archive for Space Telescopes (MAST). STScI is operated by the Association of Universities for Research in Astronomy, Inc. Support for MAST for non-HST data is provided by the NASA Office of Space Science. D.J.F. thanks Macquarie University for a MQ Research Fellowship and I.S.B. is the recipient of an Australian Research Council Super Science Fellowship (project ID FS100100019), while Q.A.P acknowledges additional support from the Australian Astronomical Observatory.

## REFERENCES

- Abell G.O., 1966, *ApJ*, 144, 259  
 Acke B. et al., 2013, *A&A*, 551, A76  
 Adams F.C., Lada C.J., Shu F.H., 1987, *ApJ*, 312, 788  
 Akras S., Steffen W., 2012, *MNRAS*, 423, 925  
 Alcock C. et al., 1998, *AJ*, 115, 1921  
 Alcolea J., Bujarrabal V., 1991, *A&A*, 245, 499  
 Allen D.A., Swings J.P., 1972, *ApJ*, 174, 583  
 Althaus L.G., Panei J.A., Miller Bertolami M.M., García-Berro E., Córscico A.H., Romero A.D., Kepler S.O., Rohrmann R.D., 2009, *ApJ*, 704, 1605  
 Alves D.R., Bond H.E., Livio M., 2000, *AJ*, 120, 2044  
 Alves D.R., Bond H.E., Onken C., 2001, *AJ*, 121, 318  
 Anderson L.D., Zavagno A., Barlow M.J., Garca-Lario P., Noriega-Crespo A., 2012, *A&A*, 537, A1  
 Arenou F., Grenon M., Gomez A., 1992, *A&A*, 258, 104  
 Balick B., 1987, *AJ*, 94, 671  
 Balick B., 1989, *AJ*, 97, 476  
 Balick B., Frank A., 2002, *ARA&A*, 40, 439  
 Barnbaum C., Zuckerman B., Kastner J.H., 1991, *AJ*, 102, 289  
 Becklin E.E., Frogel J.A., Hyland, A. R.; Kristian J., Neugebauer G., 1969, *ApJ*, 158, L133  
 Beichman C.A., Neugebauer G., Habing H.J., Clegg P.E., Chester T.J., eds, 1988, *Infrared Astronomical Satellite (IRAS) Catalogs and Atlases*, Vol. 1: Explanatory Supplement. US Government Printing Office, Washington, DC  
 Belczyński K., Mikołajewska J., Munari U., Ivison R.J., Friedjung M., 2000, *A&AS*, 146, 407  
 Bensby T. et al., 2013, *A&A*, 549, A147  
 Bianchi L., Efremova B., Herald J., Girardi L., Zabot A., Marigo P., Conti A., Martin C., 2011a, *MNRAS*, 411, 2770  
 Bianchi L., Herald J., Efremova B., Girardi L., Zabot A., Marigo P., Conti A., Shiao B., 2011b, *Ap&SS*, 335, 161  
 Blöcker T., 1995, *A&A*, 299, 755  
 Boksenberg A. et al., 1973, *MNRAS*, 163, 291  
 Bond H.E., 1976, *PASP*, 88, 192  
 Boothroyd A.I., Sackmann I.-J., Ahern S.C., 1993, *ApJ*, 416, 762  
 Borkowski K.J., Harrington J.P., 2001, *ApJ*, 550, 778  
 Boyer M.L. et al., 2013, *ApJ*, 774, 83  
 Bujarrabal V. et al., 2012, *A&A*, 537, A8  
 Bujarrabal V., Alcolea J., Sánchez Contreras C., Sahai R., 2002, *A&A*, 389, 271  
 Bujarrabal V., Van Winckel H., Neri R., Alcolea J., Castro-Carrizo A., Deroo P., 2007, *A&A*, 468, L45  
 Bujarrabal V., Alcolea J., Van Winckel H., Santander-Garcia M., Castro-Carrizo A., 2013, *A&A*, 557, A104  
 Cardelli J.A., Clayton G. C., Mathis J. S., 1989, *ApJ*, 345, 245  
 Carey S.J. et al., 2009, *PASP*, 121, 76  
 Carollo D. et al., 2007, *Nature*, 450, 1020  
 Carollo D. et al., 2010, *ApJ*, 712, 692  
 Casassus S., Roche P.F., 2001, *MNRAS*, 320, 435  
 Castro-Carrizo A., Neri R., Bujarrabal V., Chesneau O., Cox P., Bachiller R., 2012, *A&A*, 545, A1  
 Cerrigone L., Umana, G., Trigilio C., Leto P., Buemi C. S., Hora J. L., 2008, *MNRAS*, 390, 363  
 Cerrigone L., Hora J.L., Umana G., Trigilio C., 2009, *ApJ*, 703, 585  
 Cerrigone L., Hora J.L., Umana G., Trigilio C., Hart A., Fazio G., 2011, *ApJ*, 738, 121  
 Choi Y.K., Brunthaler A., Menten K.M., Reid M.J., 2012, *Proc. IAU Symposium*, 287, 407  
 Christianto, H., & Sequist, E. R. 1998, *AJ*, 115, 2466  
 Christou J.C., Ridgway S.T., Buscher D.F., Haniff C.A., McCarthy Jr. D.W., 1991, In Elston R. (ed.) *Astrophysics with infrared arrays*. ASP Conf. Series 14, ASP, San Francisco, p. 133  
 Clayton G.C., 1996, *PASP*, 108, 225  
 Clayton G.C., 2012, *JAVSO*, 40, 539  
 Clayton G.C., De Marco O., 1997, *AJ*, 114, 2679  
 Clayton G.C. et al., 2011, *AJ*, 142, 54  
 Clayton G.C. et al., 2013, *ApJ*, 771, 130  
 Cohen M., 1981, *PASP* 93, 288  
 Cohen M., Kuhi L. V., 1977, *ApJ*, 213, 79  
 Cohen M. et al., 1975, *ApJ*, 196, 179  
 Cohen M. et al., 2007, *ApJ* 669, 343  
 Cohen M., Chapman J.M., Deacon R.M., Sault R.J., Parker Q.A., Green A.J., 2006, *MNRAS*, 369, 189  
 Cohen M., Dopita M.A., Schwartz R.D., Tielens A.G.G.M., 1985, *ApJ*, 297, 702  
 Cohen M., Kunkel W., Lasker B. M., Osmer P. S., Fitzgerald M. P., 1978, *ApJ*, 221, 151  
 Cohen M., Parker Q.A., Chapman J., 2005, *MNRAS*, 357, 1189

- Cohen M., Parker Q.A., Green A.J., Miszalski B., Frew D.J., Murphy T., 2011, MNRAS, 413, 514
- Cohen M., Van Winckel H., Bond, H.E., Gull T.R., 2004, AJ, 127, 2362
- Cohen M., Walker R. G., Witteborn F. C., 1992, AJ, 104, 2030
- Corradi R.L.M., 1995, MNRAS, 276, 521
- Corradi R.L.M., Ferrer O.E., Schwarz H.E., Brandi E., García L., 1999, A&A, 348, 978
- Corradi R.L.M., Schwarz H.E., 1995, A&A, 293, 871
- Corradi R.L.M., Schönberner D., Steffen M., Perinotto M., 2003, MNRAS, 340, 417
- Corradi R.L.M., Balick B., Santander-García M., 2011, A&A, 529, A43
- Costa R.D.D., de Freitas-Pacheco J.A., Maciel W.J., 1993, A&A, 276, 184
- Cox N.L.J. et al., 2012, A&A, 537, A35
- Cutri R. M. 2003, Explanatory Supplement to the 2MASS All Sky Data Release (Pasadena: Caltech), <http://www.ipac.caltech.edu/2mass/releases/allsky/do>
- Cutri R. M. et al., 2003, 2MASS All Sky Catalog of point sources (NASA/IPAC Infrared Science Archive)
- Decin L. et al., 2010, A&A, 521, L4
- De Marco O., Barlow M. J., Storey P. J., 1997, MNRAS, 292, 86
- De Marco O., Clayton G.C., Herwig F., Pollacco D.L., Clark J.S., Kilkenny D., 2002, AJ, 123, 3387
- De Marco O., Passy J.-C., Frew D.J., Moe M.M., Jacoby G.H., 2013, MNRAS, 428, 2118
- DePew K., Parker Q.A., Miszalski B., De Marco O., Frew D.J., Acker A., Kovacevic A.V., Sharp R.G., 2011, MNRAS, 414, 2812
- De Ruyter S., van Winckel H., Dominik C., Waters L. B. F. M., Dejonghe H., 2005, A&A, 435, 161
- De Ruyter S., van Winckel H., Maas T., Lloyd Evans T., Waters L. B. F. M., Dejonghe H., 2006, A&A, 448, 641
- Dias W.S., Lépine J.R.D. Alessi B.S., 2002, A&A, 388, 168
- Dominik C., Dullemond, C. P., Cami J., van Winckel H., 2003, A&A, 397, 595
- Edwards J.L., Ziurys L.M., 2013, ApJL, 770, L5
- Egan M.P. et al., 2003, Air Force Research Laboratory Technical Report AFRL-VS-TR-2003-1589
- Engelke C.W., Kraemer K.E., Price S.D., 2004, ApJS, 150, 343
- Epcleitn N. et al., 1997, The Messenger, 87, 27
- Epcleitn N. et al., 1999, A&A, 349, 236
- Fazio G.G. et al., 2004, ApJS, 154, 10
- Feast M.W., Glass I.S., Whitelock P.A., Catchpole R.M., 1989, MNRAS, 241, 375
- Ferguson B.A., Ueta T., 2010, ApJ, 711, 613
- Frankowski A., Jorissen A., 2007, BaltA, 16, 104
- Frew D.J., 2008, PhD Thesis, Macquarie University
- Frew D.J., Parker Q.A., 2006, in Barlow M.J., Méndez R.H., eds, Proc. IAU Symp. 234, Planetary Nebulae in our Galaxy and Beyond. Cambridge Univ. Press, Cambridge, p. 49
- Frew D.J., Parker Q.A., 2010, PASA, 27, 129
- Frew D.J., Parker Q.A., 2012, in Proc. IAU Symp. 283, Planetary Nebulae: An Eye to the Future. Cambridge Univ. Press, Cambridge, p. 192
- Frew D.J., Madsen G.J., O'Toole S.J., Parker Q.A., 2010, PASA, 27, 203
- Frew D.J., Bojićić I.S., Parker Q.A., 2013, MNRAS, 431, 2
- Frew D.J. et al., 2014a, MNRAS, in press (arXiv:1301.3994)
- Frew D.J., Parker Q.A., Bojićić I.S., 2014b, MNRAS, submitted
- Frinchaboy P.M., Majewski S.R., 2008, AJ, 136, 118
- Fuhrmann K., 2011, MNRAS, 414, 2893
- García-Hernández D.A., Perea-Calderón J.V., Bobrowsky M., García-Lario P., 2007, ApJ, 666, L33
- García-Lario P., Manchado A., Pych W., Pottasch S.R., 1997, A&AS, 126, 479
- Gesicki K., Zijlstra A.A., 2007, A&A, 467, L29
- Gesicki K. et al., 2006, A&A, 451, 925
- Gezari D. Y., Pitts P. S., Schmitz M., 1999, VizieR On-line Data Catalog: II/225
- Gielen C. et al., 2011, A&A, 533, A99
- Gillett F.C., Hyland A.R., Stein W.A., 1970, ApJ, 162, L21
- Gledhill T.M., 2005, MNRAS, 356, 883
- Goldsmith M. J., Evans A., Albinson J. S., Bode M. F., 1987, MNRAS, 227, 143
- Górny S.K., Schwarz H. E., Corradi R. L. M., Van Winckel H., 1999, A&AS, 136, 145
- Górny S.K., Perea-Calderón J.V., García-Hernández D.A., García-Lario P., Szczepańska R., 2010, A&A, 516, A39
- Griffin M.J. et al., 2010, A&A, 518, L3
- Groenewegen M.A.T., Whitelock P.A., 1996, MNRAS, 281, 1347
- Groenewegen M.A.T. et al., 2011, A&A, 526, 162
- Groenewegen M.A.T. et al., 2012, A&A, 543, L8
- Gutiérrez-Moreno A., Moreno H., 1998, PASP, 110, 458
- Guzmán L., Gómez Y., Rodríguez L.F., 2006, RMxAA, 42, 127
- Hale D.D.S. et al., 1997, ApJ, 490, 407
- Hansen B.M.S. et al., 2013, Nature, 500, 51
- Harris W.E., 1996, AJ, 112, 1487
- Hawkins G., UpWhitaker C. J., Meixner M. M., Jernigan J. G., Arens J. F., Keto E., Graham J. R., 1995, ApJ, 452, 314
- Henden A.A., Levine S.E., Terrell D., Smith T.C., Welch D., 2012, JAVSO, 40, 430
- Hinkle K. H., Brittain S. D., Lambert D. L., 2007, ApJ, 664, 501
- Hillen M. et al. 2013, A&A, A&A, 559, A111
- Høg E., et al., 2000, A&A, 355, L27
- Holland W. S. et al., 1999, MNRAS, 303, 659
- Hora J.L., Latter W.B., 1994, ApJ, 437, 281
- Hora J.L. et al., 2008, AJ, 135, 726
- Hrivnak B.J., Kwok S., Volk K.M., 1989, 346, 265
- Hrivnak B.J., Kwok S., Su K.Y.L., 2001, AJ, 121, 2775
- Hrivnak B.J., Langill P.P., Su K.Y.L., Kwok S., 1999, ApJ, 513, 421
- Hu J. Y., Slijkhuis S., de Jong T., Jiang B. W., 1993, A&AS, 100, 413
- Humphreys R. M. Warner J. W., Gallagher J. S., 1976, PASP, 88, 380
- Hutsemékers D., Cox N.L.J., Vamvatira-Nakou C., 2013, A&A, 552, L6
- Imai H., Sahai R., Morris M., 2007, ApJ, 669, 424
- Imai H., Tafoya D., Honma M., Hirota T., Miyaji T., 2011, PASJ, 63, 81
- Imai H., Chong S.N., He J.-H., Nakashima J., Hsia C.-H., Sakai T., Deguchi S., Koning N., 2012, PASJ, 64, 98
- Imai H., Kurayama T., Honma M., Miyaji T., 2013a, PASJ, 65, 28
- Imai H., Deguchi S., Nakashima J., Kwok S., Diamond P.J., 2013b, ApJ, 773, 182
- IPAC, 1986, IRAS Catalog of Point Sources, Version 2.0, VizieR online catalogue, II/125
- Ishihara D., Onaka T., Kataza H., et al., 2010, A&A, 514
- Izzard R.G., Tout C.A., Karakas A.I., Pols O.R., 2004, MNRAS, 350, 407
- Jacoby G.H., Morse J.A., Fullton L. K., Kwitter K. B., Henry R. B. C., 1997, AJ, 114, 2611
- Jacoby G.H. et al., 2010, PASA, 27, 156
- Jeffery C. S., 2008, in ASP Conf. Series, 391, p. 53
- Jeffery C. S., Karakas A. I., Saio H., 2011, MNRAS, 414, 3599
- Johansson L.E.B., Andersson C., Goss W.M., Winnberg A., 1977, A&A, 54, 323
- Jones T.J. et al., 1993, ApJ, 411, 323
- Jorissen A., 2003, in ASP Conf. Ser., 303, p. 25
- Josselin E., Lèbre A., 2001, A&A, 367, 826
- Justtanont K., Teyssier D., Barlow M.J., Matsuura M., Swinyard B., Waters L.B.F.M., Yates J., 2013, A&A, 556, A101
- Jura M., 1986, ApJ, 309, 732
- Jura M., Morris M., 1985, ApJ, 292, 487
- Jura M., Kleinmann S.G., 1989, ApJ, 341, 359
- Kalirai J.S., 2012, Nature, 486, 90
- Kalirai J.S., Hansen B.M.S., Kelson D.D., Reitzel D.B., Rich R.M., Richer H.B., 2008, ApJ, 676, 594
- Kalirai J.S., Davis D.S., Richer H.B., Bergeron P., Catelan M., Hansen B.M.S., Rich R.M., 2009, ApJ, 705, 408
- Kalirai J.S., Hansen B.M.S., Kelson D.D., Reitzel D.B., Rich R.M., Richer H.B., 2008, ApJ, 676, 594
- Kama M., Min M., Dominik C., 2009, A&A, 506, 1199
- Kamath D., Wood P.R., Van Winckel H., 2014, MNRAS, in press
- Karakas, A.I., van Raaij, M.A., Lugaro M., Sterling N.C., Dinerstein H.L., 2009, ApJ, 690, 1130

- Kastner J.H., Weintraub D.A., 1994, ApJ, 434, 719  
 Kastner J.H., Weintraub D.A., 1995, ApJ, 452, 833  
 Kastner J.H., Weintraub D.A., Zuckerman B., Becklin E.E., McLean I., Gatley I., 1992, ApJ, 398, 552  
 Kastner J.H., Weintraub D.A., Merrill K.M., Gatley I., 1998, AJ, 116, 1412  
 Kepler S. O., Kleinman S. J., Nitta A., et al., 2007, MNRAS, 375, 1315  
 Kim H., Taam R.E., 2012, ApJ, 759, L22  
 Kingsburgh R.L., Barlow M.J., 1994, MNRAS, 271, 257  
 Kipper T., 2008, BaltA, 17, 87  
 Kiss L.L., Szabó G.M., Balog Z., Parker Q.A., Frew D.J., 2008, MNRAS, 391, 399  
 Kleinman S.J. et al., 2013, ApJS, 204, 5  
 Kleinmann S. G., Gillett F. C., Joyce R. R., 1981, ARA&A, 19, 411  
 Klochova V. G., Panchuk V. E., Chentsov E. L., 1997, A&A, 323, 789  
 Kohoutek L., 2001, A&A, 378, 843  
 Kraus M., Borges Fernandes M., de Araújo F.X., Lamers H.J.G.L.M., 2005, A&A, 441, 289  
 Kunder A., Chaboyer B., 2009, AJ, 137, 4478  
 Kwok S., 1982, ApJ, 258, 280  
 Kwok S., 1993, ARA&A, 31, 63  
 Kwok S., 2010, PASA, 27, 174  
 Kwok S., Hrivnak B. J., Milone E. F., 1986, ApJ, 303, 451  
 Kwok S., Hrivnak B. J., Langill P.P., 1993, ApJ, 408, 586  
 Kwok S., Hrivnak B.J., Su K. Y. L., 2000, ApJ, 544, L149  
 Kwok S., Purton C.R., Fitzgerald P.M., 1978, ApJ, 219, L125  
 Kwok S., Volk K., Bidelman W.P., 1997, ApJS, 112, 557  
 Kwok S., Volk K.M., Hrivnak B.J., 1989, ApJ, 345, L51  
 Lagadec E. et al., 2011a, MNRAS, 417, 32  
 Lagadec E., Zijlstra A.A., Oudmaijer R.D., Verhoelst T., Cox N.L.J., Szczerba R., Mękarnia D., van Winckel H., 2011b, A&A, 534, L10  
 Lambert D.L., Hinkle K.H., Luck R.E., 1988, ApJ 333, 917  
 Lamers H.J.G.L.M., Zickgraf F.-J., de Winter D., Houziaux L., Zorec J., 1998, A&A, 340, 117  
 Lasker B.M. et al., 2008, AJ, 136, 735  
 Lawrence A. et al., 2007, MNRAS, 379, 1599  
 Liebert J., Bergeron P., Holberg J. B., 2005, ApJS, 156, 47  
 Likkel L., te Lintel Hekkert P., Chapman J.M., 1993, ASP Conf. Ser., 45, 159  
 Lucas P. W. et al., 2008, MNRAS, 391, 136  
 Maas T., Giridhar S., Lambert D.L., 2007, ApJ, 666, 378  
 Manchado A., García-Lario P., Esteban C., Mampaso A., Pottasch S.R., 1989, A&A, 214, 139  
 Manchado A., Guerrero M. A., Stanghellini L., Serra-Ricart M., 1996. The IAC morphological catalog of northern Galactic planetary nebulae. La Laguna: Instituto de Astrofísica de Canarias  
 Manteiga M., García-Hernández D.A., Ulla A., Manchado A., García-Lario P., 2011, AJ, 141, 80  
 Markwardt C.B. 2009, in ASP Conference Series, 411, Astronomical Data Analysis Software and Systems XVIII, ed. D.A. Bohlander, D. Durand & P. Dowler, 251  
 Marquardt D., 1963, SIAM Journal on Applied Mathematics, 11, 431  
 Matsunaga N. et al., 2006, MNRAS, 370, 1979  
 Matsunaga N., Feast M.W., Menzies J.W., 2009, MNRAS, 397, 933  
 Matsuura M., Yamamura I., Zijlstra A. A., Bedding T. R., 2002, A&A, 387, 1022  
 Mauron N., Huggins P. J., 2006, A&A, 452, 257  
 Mauron N., Huggins P. J., Cheung C.-L., 2013, A&A, 551, A110  
 Mayor M., Acker A., 1980, A&A, 92, 1  
 Mazzitelli I., D'Antona F., Ventura P., 1999, A&A, 348, 846  
 McDonald I. et al., 2013, MNRAS, 436, 413  
 McSaveney J.A., Wood P.R., Scholz M., Lattanzio J.C., Hinkle K.H., 2007, MNRAS, 378, 1089  
 Meaburn J., Lloyd M., Vaytet N. M. H., López J. A., 2008, MNRAS, 385, 269  
 Meakin C.A., Bieging J.H., Latter W.B., Hora J.L., Tielens A.G.G.M., 2003, ApJ, 585, 482  
 Meixner M. et al., 1999, ApJS, 122, 221  
 Meixner M., Ueta T., Bobrowsky M., Speck A., 2002, ApJ, 571, 936  
 Men'schikov A. B., Schertl D., Tuthill P. G., Weigelt G., Yungelson L. R., 2002, A&A, 393, 867  
 Menten K.M., Reid M.J., Kamiński T., Claussen M.J., 2012, A&A, 543, A73  
 Mermilliod J.-C., 2006, VizieR On-line Data Catalog: II/168  
 Mermilliod J.-C., Mermilliod M., Hauck B., 1997, A&AS, 124, 349  
 Mermilliod J.-C., Andersen J., Latham D. W., Mayor M., 2007, A&A, 473, 829  
 Miszalski B., Boffin H.M.J., Frew D.J., Acker A., Köppen J., Moffat A.F.J., Parker Q.A., 2012, MNRAS, 419, 39  
 Miszalski B., Mikołajewska J., Udalski A., 2013, MNRAS, 432, 3186  
 Morris M., 1975, ApJ, 197, 603  
 Morris M., Guilloteau S., Lucas R., Omont A., 1987, ApJ, 321, 888  
 Morrissey P. et al., 2007, ApJS, 173, 682  
 Nakashima J., Deguchi S., Imai H., Kemball A., Lewis B.M., 2011, ApJ, 728, 76  
 Neugebauer G., Martz D.E., Leighton R.B., 1965, ApJ, 142, 399  
 Neugebauer G., et al., 1984, ApJL, 278, 1  
 Ney E. P., Merrill K. M., Becklin E. E., Neugebauer G., Wynn-Williams C. G., 1975, ApJ, 198, L129  
 O'Donnell J.E., 1994, ApJ, 422, 158  
 Olivier E. A., Whitelock P., Marang F., 2001, MNRAS, 326, 490  
 Osterbart R., Balega Y.Y., Blöcker T., Menshchikov A.B., Weigelt G., 2000, A&A, 357, 169  
 Oudmaijer R.D., de Wit W.J., 2013, A&A, 551, A69  
 Oudmaijer R.D., van der Veen W. E. C. J., Waters L. B. F. M., Trams N. R., Waelkens C., Engelsman E., 1992, A&AS, 96, 625  
 Paczyński B., 1971, Aca, 21, 417  
 Pandey G., Kameswara Rao N., Lambert D.L., Jeffery C.S., Asplund M., 2001, MNRAS, 324, 937  
 Parker Q.A. et al., 2006, MNRAS, 373, 79  
 Parker Q.A. et al., 2012, MNRAS, 427, 3016  
 Parthasarathy M., Pottasch S.R., 1986, A&A, 154, L16  
 Parthasarathy M., Pottasch S.R., 1989, A&A, 225, 521  
 Parthasarathy M., Garcia-Lario P., Pottasch S.R., Manchado A., Clavel J., de Martino D., van de Steene G.C.M., Sahu K.C., 1993, A&A, 267, L19  
 Peimbert M., 1978, Proc. IAU Symp., 76, 215  
 Pereira C. B., Smith V. V., Cunha K., 2005, A&A, 429, 993  
 Phillips J.P., 2001, PASP, 113, 839  
 Pilbratt G. L. et al., 2010, A&A, 518, L1  
 Planck Collaboration I, 2011, A&A, 536, A1  
 Planck Collaboration VII, 2011, A&A, 536, A7  
 Poglitsch A. et al., 2010, A&A, 518, L2  
 Pottasch S.R., Parthasarathy M., 1988, 192, 182  
 Preite-Martinez A., 1988, A&AS, 76, 317  
 Preston G.W., Krzeminski W., Smak J., Williams J. A., 1963, ApJ, 137, 401  
 Price S.D., Murdock T. L., 1983, The Revised AFGL Infrared Sky Survey Catalog, AFGL-TR-83-0161  
 Price S.D., Egan M. P., Carey S. J., Mizuno D. R., Kuchar T. A., 2001, AJ, 121, 2819  
 Quireza C., Rocha-Pinto H.J., Maciel W.J., 2007, A&A, 475, 217  
 Ramírez I., Allende Prieto C., 2011, ApJ, 743, 135  
 Ramos-Larios G., Guerrero M.A., Suárez O., Miranda L.F., Gómez J.F., 2009, A&A, 501, 1207  
 Ramos-Larios G., Guerrero M.A., Suárez O., Miranda L.F., Gómez J.F., 2012, A&A, 545, A20  
 Reddy B.E., Hrivnak B.J., 1999, AJ, 117, 1834  
 Reipurth B., 1987, Nature, 325, 787  
 Renedo I., Althaus L.G., Miller Bertolami M.M., Romero A.D., Córscico A.H., Rohrmann R.D., García-Berro E., 2010, ApJ, 717, 183  
 Renzini A., 1981, in Iben I., Jr., Renzini A., eds, Physical Processes in Red Giants. Dordrecht: Riedel, p. 431  
 Rieke G.H. et al. 2004, ApJS, 154, 25  
 Riera A., García-Lario P., Manchado A., Pottasch S.R., Raga A.C., 1995, A&A, 302, 137  
 Sahai R., Nyman L.-Å., 2000, ApJ, 538, L145  
 Sahai R., Trauger J.T., 1998, AJ, 116, 1357

- Sahai R., Brilliant S., Livio M., Grebel E.K., Brandner W., Tingay S., Nyman L.-Å., 2002, *ApJ*, 573, L123
- Sahai R., Morris M., Sánchez Contreras C., Claussen M., 2006, *Proc. IAU Symp.*, 234, 499
- Sahai R., Morris M., Sánchez Contreras C., Claussen M., 2007, *AJ*, 134, 2200
- Sahai R., Morris M.R., Villar G.G., 2011, *AJ*, 141, 134
- Sahai R., Sánchez Contreras C., Morris M., 2005, *ApJ*, 620, 948
- Sahai R., te Lintel Hekkert P., Morris M., Zijlstra A., Likkel L., 1999, *ApJ*, 514, L115
- Sánchez Contreras C., Bujarrabal V., Alcolea J., 1997, *A&A*, 327, 689
- Sánchez Contreras C., Bujarrabal V., Miranda L.F., Fernández-Figueroa M.J., 2000, *A&A*, 355, 1103
- Sánchez Contreras C., Gil de Paz A., Sahai R., 2004, *ApJ*, 616, 519
- Santander-García M., Corradi R.L.M., Balick B., Mampaso A., 2004, *A&A*, 426, 185
- Santander-García M., Corradi R.L.M., Whitelock P.A., Munari U., Mampaso A., Marang F., Boffi F., Livio M., 2007, *A&A*, 465, 481
- Sasselov D.D., 1984, *Ap&SS*, 102, 161
- Schlafly E.D., Finkbeiner D.P., 2011, *ApJ*, 737, 103
- Schmeja S., Kimeswenger S., 2001, *A&A*, 377, L18
- Schmidt G.D., Hines D.C., Swift S., 2002, *ApJ*, 576, 429
- Schönberner D., 1983, *ApJ*, 272, 708
- Schwarz H.E., Aspin C., Corradi R.L.M., Reipurth B., 1997, *A&A*, 319, 267
- Sevenster M.N., 2002, *AJ*, 123, 2772
- Sharma S., Pandey A. K., Ogura K., Mito H., Tarusawa K., Sagar R., 2006, *AJ*, 132, 1669
- Siegel M.H. et al., 2011, *ApJ*, 743, 20
- Siódmiak N., Meixner M., Ueta T., Sugerman B.E.K., Van de Steene G.C., Szczerba R., 2008, *ApJ*, 677, 382
- Skrutskie M.F. et al., 2006, *AJ*, 131, 1163
- Smith B.J., 2003, *AJ*, 126, 935
- Smith B.J., Price S.D., Baker R.I., 2004, *ApJS*, 154, 673
- Smith N., Gehrz R.D., 2005, *AJ*, 129, 969
- Soszyński I. et al., 2008, *AcA*, 58, 293
- Stasińska G., Górný S.K., Tylenda R., 1997, *A&A*, 327, 736
- Su K.Y.L., Hrivnak B.J., Kwok S., 2001, *AJ*, 122, 1525
- Su K.Y.L., Volk K., Kwok S., Hrivnak B.J., 1998, *ApJ*, 508, 744
- Suárez O., García-Lario P., Manchado A., Manteiga M., Ulla A., Pottasch S.R., 2006, *A&A*, 458, 173
- Szczerba R., Górný S.K., Zalfresco-Jundziłł M., 2001, *ASSL*, 265, 13
- Szczerba R., Stasińska G., Siódmiak N., Górný S.K., 2003, *ESA SP-511*, 149
- Szczerba R., Siódmiak N., Stasińska G., Borkowski J., 2007, *A&A*, 469, 799
- Szczerba R. et al., 2012, *IAUS*, 283, 506
- Tafoya D. et al., 2011, *PASJ*, 63, 71
- Tafoya D., Loinard L., Fonfría J. P., Vlemmings W. H. T., Martí-Vidal I., Pech G., 2013, *A&A*, 556, A35
- te Lintel Hekkert P., Versteegen-Hensel H.A., Habing H.J., Wiertz M., 1989, *A&AS*, 78, 399
- Thompson G. I., Nandy K., Jamar C., Monfils A., Houziaux L., Carnochan D. J., Wilson R., 1978, *Catalogue of Stellar Ultraviolet Fluxes* (London: Sci. Res. Council)
- Tisserand P. et al., 2011, *A&A*, 529, A118
- Tisserand P., 2012, *A&A*, 539, 51
- Tisserand P., Clayton G. C., Welch D. L., Pilecki B., Wyrzykowski L., Kilkenny D., 2013, *A&A*, 551, A77
- Tremblay P.-E., Bergeron P., Gianninas A., 2011, *ApJ*, 730, 128
- Tuthill P.G., Lloyd J.P., 2007, *Science*, 316, 247
- Ueta T., Meixner M., Bobrowsky M., 2000, *ApJ*, 528, 861
- Ueta T., Murakawa K., Meixner M., 2006, *ApJ*, 641, 1113
- Urquhart J. S., Busfield A. L., Hoare M. G., Lumsden S. L., Clarke A. J., Moore T. J. T., Mottram J. C., Oudmaijer R. D., 2007, *A&A*, 461, 11
- Uscanga L., Gómez J.F., Suárez O., Miranda L.F., 2012, *A&A*, 547, A40
- van Aarle E., van Winckel H., Lloyd Evans T., Ueta T., Wood P. R., Ginsburg A. G., 2011, *A&A*, 530, A90
- Van de Steene G. C., van Hoof P. A. M., Wood P. R., 2000, *A&A*, 362, 984
- van der Veen W.E.C.J., Habing H.J., 1988, *A&A*, 194, 125
- van der Veen W.E.C.J., Habing H.J., Geballe T.R., 1989, *A&A*, 226, 108
- Van Hoof P. A. M., Oudmaijer R. D., Waters L. B. F. M., 1997, *MNRAS*, 289, 371
- van Leeuwen F., 2007, *A&A*, 474, 653
- van Loon J. Th., Molster F.J., Van Winckel H., Waters L.B.F.M., 1999, *A&A*, 350, 120
- Van Winckel H., 2003, *ARA&A*, 41, 391
- Van Winckel H., 2014, *Proc. IAU Symp.*, 297, 180
- Van Winckel H., Lloyd Evans T., Reyniers M., Deroo P., Gielen C., 2006, *MmSAI*, 77, 943
- Van Winckel H., Waelkens C., Fernie J. D., Waters L. B. F. M., 1999, *A&A*, 343, 202
- Van Winckel H. et al., 2009, *A&A*, 505, 1221
- Vassiliadis E., Wood P.R., 1994, *ApJS*, 92, 125 (VW94)
- Vennes S., Smith R.J., Boyle B.J., Croom S.M., Kawka A., Shanks T., Miller L., Loaring N., 2002, *MNRAS*, 335, 673
- Volk K., Cohen M., 1989, *AJ*, 98, 1918
- Volk K.M., Kwok S., 1989, *ApJ*, 342, 345
- Waelkens C., van Winckel H., Bogaert E., Trams N.R., 1991, *A&A*, 251, 495
- Wachter S., Mauerhan J.C., Van Dyk S.D., Hoard D.W., Kafka S., Morris P.W., 2010, *AJ*, 139, 2330
- Wallerstein G., 2002, *PASP*, 114, 689
- Waters L.B.F.M., Waelkens C., Mayor M., Trams N.R., 1993, *A&A*, 269, 242
- Wesselius P. R., van Duinen R. J., de Jonge A. R. W., Aalders J. W. G., Luinge W., Wildeman K. J., 1982, *A&AS*, 49, 427
- Westbrook W. E., Willner S. P., Merrill K. M., Schmidt M., Becklin E. E., Neugebauer G., Wynn-Williams C. G., 1975, *ApJ*, 202, 407
- Witt A.N., Vijh U.P., Hobbs L.M., Aufdenberg J.P., Thorburn J.A., York D.G., 2009, *ApJ*, 693, 1946
- Wright E.L., et al., 2010, *AJ*, 140, 1868
- Wood P.R., Bessell M.S., Fox M.W., 1983, *ApJ*, 272, 99
- Wright N.J., Barlow M.J., Ercolano B., Rauch T., 2011, *MNRAS*, 418, 370
- Zhang C.Y., Kwok S., 1991, *A&A*, 250, 179
- Zijlstra A.A., 2001, *Ap&SS*, 275, 79
- Zijlstra A.A., te Lintel Hekkert P., Pottasch S.R., Caswell J.L., Ratag M., Habing H.J., 1989, *A&A*, 217, 157
- Zijlstra A.A., Chapman J.M., te Lintel Hekkert P., Likkel L., Comeron F., Norris R.P., Molster F.J., Cohen R.J., 2001, *MNRAS*, 322, 280
- Zijlstra A.A., Gesicki K., Walsh J.R., Péquignot D., van Hoof P.A.M., Minniti D., 2006, *MNRAS*, 369, 875
- Zijlstra A.A., van Hoof P.A.M., Perley R.A., 2008, *ApJ*, 681, 1296
- Zuckerman B., 1978, *IAUS*, 76, 305
- Zuckerman B., Gilra D. P., Turner B. E., Morris M., Palmer P., 1976, *ApJ*, 205, L15

## APPENDIX A: ONLINE SUPPLEMENT: CATALOGUE OF SED DISTANCES

Table A1: Parameters and distances for 209 *likely* PAGB objects, ordered by Galactic longitude.

IRAS No.	Other Name	<i>l</i> ( $^{\circ}$ )	<i>b</i> ( $^{\circ}$ )	Flux ( $\text{erg s}^{-1} \text{cm}^{-2}$ )	Flux ( $L_{\odot} \text{kpc}^{-2}$ )	Luminosity ( $L_{\odot}$ )	$E(B - V)$ (mag)	Distance (kpc)	$F_{IR}/F_{\star}$	$T_D$ (K)
17581-2926	GLMP 688	1.293	-3.199	1.46E-09 $\pm$ 2.60E-10	45 $\pm$ 8	4000 $\pm$ 1500	0.51 $\pm$ 0.05	9.38 $\pm$ 1.95	1.49	113 $\pm$ 6
17291-2402	GLMP 575	2.518	5.120	4.22E-09 $\pm$ 5.85E-10	131 $\pm$ 18	4000 $\pm$ 1500	1.16 $\pm$ 0.23	5.52 $\pm$ 1.10	8.99	130-853
17349-2444	GLMP 593	2.652	3.637	2.17E-09 $\pm$ 3.81E-10	67 $\pm$ 12	4000 $\pm$ 1500	0.51 $\pm$ 0.05	7.70 $\pm$ 1.59	9.61	121 $\pm$ 6
18371-3159	LSE 63	2.918	-11.818	1.92E-09 $\pm$ 3.99E-10	60 $\pm$ 12	1700 $\pm$ 750	0.13 $\pm$ 0.01	5.34 $\pm$ 1.30	0.77	134 $\pm$ 7
17576-2653	...	3.472	-1.853	2.57E-09 $\pm$ 3.66E-10	80 $\pm$ 11	4000 $\pm$ 1500	0.51 $\pm$ 0.05	7.07 $\pm$ 1.42	2.32	187 $\pm$ 9
17516-2525	GLMP 662	4.038	0.056	4.91E-08 $\pm$ 7.06E-09	1528 $\pm$ 219	6000 $\pm$ 1500	0.50 $\pm$ 0.05	1.98 $\pm$ 0.29	7.07	141-749
17074-1845	LSE 3	4.100	12.263	4.07E-09 $\pm$ 9.59E-10	127 $\pm$ 30	6000 $\pm$ 1500	0.25 $\pm$ 0.02	6.88 $\pm$ 1.18	0.51	146 $\pm$ 7
17441-2411	Silkworm Nebula	4.223	2.145	3.27E-08 $\pm$ 3.97E-09	1018 $\pm$ 123	12000 $\pm$ 3000	1.65 $\pm$ 0.43	3.43 $\pm$ 0.48	17	208-962
17332-2215	GLMP 588	4.542	5.295	2.52E-09 $\pm$ 3.92E-10	78 $\pm$ 12	4000 $\pm$ 1500	0.78 $\pm$ 0.16	7.14 $\pm$ 1.45	8.97	137-833
17360-2142	GLMP 600	5.364	5.038	2.20E-09 $\pm$ 3.77E-10	69 $\pm$ 12	4000 $\pm$ 1500	0.72 $\pm$ 0.14	7.64 $\pm$ 1.57	4.12	141 $\pm$ 7
17388-2203	GLMP 616	5.393	4.314	2.86E-09 $\pm$ 4.39E-10	89 $\pm$ 14	4000 $\pm$ 1500	0.85 $\pm$ 0.17	6.70 $\pm$ 1.36	1.25	138 $\pm$ 7
18113-2503	...	6.566	-3.642	2.38E-09 $\pm$ 6.31E-10	74 $\pm$ 20	4000 $\pm$ 1500	0.51 $\pm$ 0.05	7.34 $\pm$ 1.68	12	159 $\pm$ 10
18384-2800	V4728 Sgr	6.725	-10.372	2.45E-08 $\pm$ 9.66E-09	762 $\pm$ 300	4000 $\pm$ 1500	0.18 $\pm$ 0.02	2.29 $\pm$ 0.62	0.06	373 $\pm$ 37
17456-2037	...	7.467	3.701	2.46E-09 $\pm$ 4.69E-10	76 $\pm$ 15	4000 $\pm$ 1500	0.51 $\pm$ 0.05	7.23 $\pm$ 1.52	100	172-527
17203-1534	...	8.548	11.486	4.68E-09 $\pm$ 7.53E-10	146 $\pm$ 23	6000 $\pm$ 1500	0.39 $\pm$ 0.04	6.42 $\pm$ 0.95	0.35	132 $\pm$ 7
17487-1922	...	8.905	3.712	3.21E-09 $\pm$ 3.32E-10	100 $\pm$ 10	4000 $\pm$ 1500	0.51 $\pm$ 0.05	6.33 $\pm$ 1.23	145	174-938
18083-2155	GLMP 728	8.979	-1.515	5.29E-09 $\pm$ 1.37E-09	165 $\pm$ 43	6000 $\pm$ 1500	0.51 $\pm$ 0.05	6.04 $\pm$ 1.08	2695	136-345
18043-2116	OH 9.1 -0.4	9.097	-0.393	1.91E-09 $\pm$ 3.94E-10	60 $\pm$ 12	4000 $\pm$ 1500	0.51 $\pm$ 0.05	8.20 $\pm$ 1.75	144	110-318
17423-1755	Hen 3-1475	9.364	5.779	1.25E-08 $\pm$ 1.69E-09	389 $\pm$ 52	20000 $\pm$ 5000	0.60 $\pm$ 0.12	7.17 $\pm$ 1.02	7.92	109-865
17381-1616	LS 4331	10.255	7.493	2.31E-09 $\pm$ 1.01E-09	72 $\pm$ 32	6000 $\pm$ 1500	0.48 $\pm$ 0.10	9.15 $\pm$ 2.32	0.38	171 $\pm$ 9
17488-1741	...	10.373	4.554	1.82E-09 $\pm$ 3.47E-10	57 $\pm$ 11	6000 $\pm$ 1500	0.71 $\pm$ 0.14	10.29 $\pm$ 1.62	0.64	113 $\pm$ 6
18071-1727	...	12.759	0.896	1.68E-08 $\pm$ 7.26E-09	522 $\pm$ 226	6000 $\pm$ 1500	0.79 $\pm$ 0.08	3.39 $\pm$ 0.85	...	115-1076
18139-1816	OH 12.8 -0.9	12.816	-0.895	7.00E-09 $\pm$ 1.43E-09	218 $\pm$ 45	6000 $\pm$ 1500	0.79 $\pm$ 0.08	5.25 $\pm$ 0.85	...	135-480
17279-1119	V340 Ser	13.230	12.174	1.64E-08 $\pm$ 1.73E-09	511 $\pm$ 54	6000 $\pm$ 1500	0.45 $\pm$ 0.05	3.43 $\pm$ 0.47	0.35	171-855
...	LS IV -04 1	14.403	22.856	1.16E-09 $\pm$ 6.50E-11	36 $\pm$ 2	1700 $\pm$ 750	0.28 $\pm$ 0.03	6.86 $\pm$ 1.53	...	...
18135-1456	...	15.701	0.770	2.16E-08 $\pm$ 4.43E-09	672 $\pm$ 138	6000 $\pm$ 1500	0.79 $\pm$ 0.08	2.99 $\pm$ 0.48	...	143-584
18379-1707	LS 5112	16.503	-5.421	3.66E-09 $\pm$ 5.63E-10	114 $\pm$ 18	6000 $\pm$ 1500	0.36 $\pm$ 0.07	7.26 $\pm$ 1.06	3.87	171-776
18276-1431	V445 Sct	17.687	-2.032	2.23E-08 $\pm$ 1.19E-09	694 $\pm$ 37	6000 $\pm$ 1500	0.79 $\pm$ 0.08	2.94 $\pm$ 0.38	59	161-692
18321-1401	...	18.627	-2.758	5.46E-10 $\pm$ 6.29E-11	17 $\pm$ 2	6000 $\pm$ 1500	0.79 $\pm$ 0.08	18.79 $\pm$ 2.59	0.45	112 $\pm$ 6
18075-0924	GLMP 726	19.845	4.734	6.45E-09 $\pm$ 1.70E-09	201 $\pm$ 53	6000 $\pm$ 1500	1.26 $\pm$ 0.25	5.47 $\pm$ 0.99	0.43	142-1235
18386-1253	GLMP 818	20.362	-3.653	4.13E-09 $\pm$ 6.87E-10	129 $\pm$ 21	6000 $\pm$ 1500	0.91 $\pm$ 0.09	6.83 $\pm$ 1.03	0.66	124-465
17542-0603	GLMP 669	21.187	9.223	4.40E-09 $\pm$ 1.61E-09	137 $\pm$ 50	6000 $\pm$ 1500	0.83 $\pm$ 0.17	6.62 $\pm$ 1.47	0.89	185-1128
18286-0959	OH 21.80 -0.13	21.797	-0.127	2.01E-08 $\pm$ 2.87E-09	625 $\pm$ 89	6000 $\pm$ 1500	0.91 $\pm$ 0.09	3.10 $\pm$ 0.45	1794	160-342
F15240+1452	BD+15 2862	21.866	51.930	2.67E-08 $\pm$ 3.33E-09	829 $\pm$ 104	1700 $\pm$ 750	0.04 $\pm$ 0.01	1.43 $\pm$ 0.33	0.00	91-899
19500-1709	V5112 Sgr	23.984	-21.036	3.29E-08 $\pm$ 2.19E-09	1023 $\pm$ 68	6000 $\pm$ 1500	0.18 $\pm$ 0.02	2.42 $\pm$ 0.31	1.18	190 $\pm$ 10
18489-0629	...	27.224	-2.977	1.29E-08 $\pm$ 1.10E-09	401 $\pm$ 34	6000 $\pm$ 1500	0.91 $\pm$ 0.09	3.87 $\pm$ 0.51	0.06	112 $\pm$ 6
19590-1249	LS IV -12 111	29.180	-21.264	2.52E-09 $\pm$ 3.38E-10	78 $\pm$ 11	1700 $\pm$ 750	0.17 $\pm$ 0.02	4.66 $\pm$ 1.07	0.40	133 $\pm$ 7
19005-0445	GLMP 864	30.086	-4.738	1.68E-09 $\pm$ 2.46E-10	52 $\pm$ 8	6000 $\pm$ 1500	0.66 $\pm$ 0.13	10.72 $\pm$ 1.55	69	127-1195
18450-0148	W 43A	30.948	0.038	1.48E-08 $\pm$ 5.98E-09	461 $\pm$ 186	12000 $\pm$ 3000	1.00 $\pm$ 0.10	5.10 $\pm$ 1.21	...	164-540
18460-0151	OH 31.0 -0.2	31.013	-0.220	1.96E-08 $\pm$ 8.72E-09	609 $\pm$ 271	6000 $\pm$ 1500	1.00 $\pm$ 0.10	3.14 $\pm$ 0.80	...	62-281
...	PHL 1580	31.334	-43.479	7.63E-10 $\pm$ 6.97E-11	24 $\pm$ 2	1700 $\pm$ 750	0.04 $\pm$ 0.01	8.46 $\pm$ 1.91	...	...
...	PHL 174	33.165	-48.122	2.72E-10 $\pm$ 1.56E-11	8.47 $\pm$ 0.48	1700 $\pm$ 750	0.03 $\pm$ 0.01	14.17 $\pm$ 3.15	...	...
18514+0019	GLMP 841	33.568	-0.384	4.08E-09 $\pm$ 1.11E-09	127 $\pm$ 34	6000 $\pm$ 1500	1.00 $\pm$ 0.10	6.87 $\pm$ 1.27	...	154-417
18582+0001	GLMP 858	34.094	-2.039	4.88E-09 $\pm$ 8.89E-10	152 $\pm$ 28	6000 $\pm$ 1500	1.00 $\pm$ 0.10	6.29 $\pm$ 0.97	0.23	112 $\pm$ 6
19024+0044	GLMP 870	35.208	-2.653	5.38E-09 $\pm$ 1.02E-09	167 $\pm$ 32	12000 $\pm$ 3000	1.00 $\pm$ 0.10	8.47 $\pm$ 1.33	35	146-365
19114+0002	V1427 Aql	35.620	-4.956	2.96E-07 $\pm$ 7.22E-08	9209 $\pm$ 2245	6000 $\pm$ 1500	0.96 $\pm$ 0.19	0.81 $\pm$ 0.14	0.36	143 $\pm$ 7
18596+0315	OH 37.12 -0.85	37.119	-0.847	2.81E-09 $\pm$ 6.60E-10	87 $\pm$ 21	6000 $\pm$ 1500	1.00 $\pm$ 0.10	8.29 $\pm$ 1.42	...	125-926
18533+0523	GLMP 849	38.278	1.152	1.77E-09 $\pm$ 3.28E-10	55 $\pm$ 10	6000 $\pm$ 1500	1.00 $\pm$ 0.10	10.45 $\pm$ 1.63	22	132-325
18485+0642	GLMP 838	38.910	3.178	3.70E-09 $\pm$ 8.43E-10	115 $\pm$ 26	6000 $\pm$ 1500	1.00 $\pm$ 0.10	7.22 $\pm$ 1.22	119	129-278
19386+0155	V1648 Aql	40.505	-10.086	1.77E-08 $\pm$ 3.42E-09	550 $\pm$ 106	6000 $\pm$ 1500	0.36 $\pm$ 0.04	3.30 $\pm$ 0.52	2.26	222-948
...	PG 1704+222	43.056	32.356	7.14E-10 $\pm$ 3.07E-11	22 $\pm$ 1	1700 $\pm$ 750	0.07 $\pm$ 0.01	8.75 $\pm$ 1.94	...	...
22327-1731	HM Aqr	43.229	-57.133	1.19E-08 $\pm$ 2.25E-09	369 $\pm$ 70	1700 $\pm$ 750	0.03 $\pm$ 0.01	2.15 $\pm$ 0.52	0.53	242-949
18385+1350	GLMP 817	44.193	8.583	6.12E-10 $\pm$ 1.93E-10	19 $\pm$ 6	6000 $\pm$ 1500	0.64 $\pm$ 0.13	17.75 $\pm$ 3.57	7.78	119-965
19356+0754	GLMP 935	45.454	-6.559	2.30E-09 $\pm$ 8.48E-10	72 $\pm$ 26	6000 $\pm$ 1500	0.33 $\pm$ 0.07	9.15 $\pm$ 2.04	...	140-869
19190+1102	...	46.256	-1.476	2.43E-09 $\pm$ 4.26E-10	75 $\pm$ 13	6000 $\pm$ 1500	0.72 $\pm$ 0.07	8.92 $\pm$ 1.36	...	124-483
19306+1407	GLMP 923	50.303	-2.477	5.37E-09 $\pm$ 7.12E-10	167 $\pm$ 22	6000 $\pm$ 1500	0.03 $\pm$ 0.01	5.99 $\pm$ 0.85	29	150 $\pm$ 8
18062+2410	V886 Her	50.675	19.790	5.87E-09 $\pm$ 2.42E-09	183 $\pm$ 75	1700 $\pm$ 750	0.10 $\pm$ 0.01	3.05 $\pm$ 0.92	2.16	200-289
17534+2603	89 Her	51.434	23.188	2.88E-07 $\pm$ 5.87E-08	8973 $\pm$ 1826	3500 $\pm$ 1500	0.08 $\pm$ 0.01	0.62 $\pm$ 0.15	0.31	474-1056
19422+1438	...	52.141	-4.671	1.34E-09 $\pm$ 1.42E-10	42 $\pm$ 4	6000 $\pm$ 1500	0.34 $\pm$ 0.07	12.02 $\pm$ 1.63	0	

IRAS No.	Other Name	<i>l</i> ( $^{\circ}$ )	<i>b</i> ( $^{\circ}$ )	Flux (erg s $^{-1}$ cm $^{-2}$ )	Flux (L $_{\odot}$ kpc $^{-2}$ )	Luminosity (L $_{\odot}$ )	<i>E(B - V)</i> (mag)	Distance (kpc)	<i>F<sub>IR</sub></i> / <i>F<sub>★</sub></i>	T <sub>D</sub> (K)
20462+3416	V1853 Cyg	76.601	-5.747	6.38E-09 $\pm$ 8.89E-10	198 $\pm$ 28	3500 $\pm$ 1500	0.29 $\pm$ 0.06	4.20 $\pm$ 0.95	0.39	122 $\pm$ 6
17436+5003	V814 Her	77.133	30.870	6.08E-08 $\pm$ 7.92E-09	1891 $\pm$ 247	3500 $\pm$ 1500	0.03 $\pm$ 0.01	1.36 $\pm$ 0.30	0.47	130 $\pm$ 9
Z21003+3630	Egg Nebula	80.168	-6.503	5.74E-07 $\pm$ 5.17E-08	17847 $\pm$ 1609	6000 $\pm$ 1500	0.25 $\pm$ 0.05	0.58 $\pm$ 0.08	...	186-401
20461+3853	GLMP 1007	80.191	-2.816	1.96E-09 $\pm$ 2.03E-10	61 $\pm$ 6	6000 $\pm$ 1500	0.79 $\pm$ 0.08	9.91 $\pm$ 1.34	6.76	191 $\pm$ 10
20259+4206	...	80.396	2.191	4.17E-09 $\pm$ 2.49E-09	130 $\pm$ 77	6000 $\pm$ 1500	0.79 $\pm$ 0.08	6.80 $\pm$ 2.20	0.44	208 $\pm$ 10
21546+4721	GLMP 1047	95.013	-5.563	6.73E-10 $\pm$ 1.77E-10	21 $\pm$ 5	6000 $\pm$ 1500	0.21 $\pm$ 0.04	16.93 $\pm$ 3.07	2.98	202-896
22223+4327	BD+42 4388	96.754	-11.559	1.05E-08 $\pm$ 6.67E-10	326 $\pm$ 21	6000 $\pm$ 1500	0.15 $\pm$ 0.02	4.29 $\pm$ 0.55	0.71	147 $\pm$ 7
...	BD+39 4926	98.409	-16.726	5.72E-09 $\pm$ 6.92E-10	178 $\pm$ 22	1700 $\pm$ 750	0.12 $\pm$ 0.01	3.09 $\pm$ 0.71	...	...
22023+5249	LS III +52 24	99.303	-1.956	4.93E-09 $\pm$ 1.02E-09	153 $\pm$ 32	6000 $\pm$ 1500	0.62 $\pm$ 0.06	6.26 $\pm$ 1.01	0.76	141 $\pm$ 7
22036+5306	GLMP 1052	99.633	-1.835	1.32E-08 $\pm$ 2.48E-09	410 $\pm$ 77	12000 $\pm$ 3000	0.61 $\pm$ 0.06	5.41 $\pm$ 0.85	...	111-1293
22272+5435	V354 Lac	103.349	-2.518	9.97E-08 $\pm$ 1.33E-08	3102 $\pm$ 413	6000 $\pm$ 1500	0.65 $\pm$ 0.07	1.39 $\pm$ 0.20	0.80	194 $\pm$ 17
21537+6435	GLMP 1044	105.540	8.097	3.81E-09 $\pm$ 5.52E-10	118 $\pm$ 17	6000 $\pm$ 1500	0.55 $\pm$ 0.11	7.12 $\pm$ 1.03	...	195-760
22574+6609	...	112.040	5.959	4.95E-09 $\pm$ 1.48E-09	154 $\pm$ 46	12000 $\pm$ 3000	1.58 $\pm$ 0.32	8.83 $\pm$ 1.72	120	148-626
23304+6147	GLMP 1078	113.857	0.587	1.06E-08 $\pm$ 1.06E-09	331 $\pm$ 33	6000 $\pm$ 1500	0.80 $\pm$ 0.08	4.26 $\pm$ 0.57	1.65	190 $\pm$ 10
23321+6545	...	115.207	4.322	1.08E-08 $\pm$ 1.25E-09	335 $\pm$ 39	12000 $\pm$ 3000	1.86 $\pm$ 0.37	5.99 $\pm$ 0.82	...	176-545
23541+7031	RAFGL 3181	118.415	8.416	3.93E-08 $\pm$ 8.13E-09	1223 $\pm$ 253	6000 $\pm$ 1500	0.50 $\pm$ 0.10	2.21 $\pm$ 0.36	378	196-604
01005+7910	...	123.568	16.591	5.85E-09 $\pm$ 6.79E-10	182 $\pm$ 21	6000 $\pm$ 1500	0.21 $\pm$ 0.02	5.74 $\pm$ 0.79	0.78	197-1013
Z02229+6208	...	133.733	1.499	4.64E-08 $\pm$ 6.18E-09	1442 $\pm$ 192	6000 $\pm$ 1500	0.74 $\pm$ 0.07	2.04 $\pm$ 0.29	1.51	231 $\pm$ 12
05040+4820	LS V +48 26	159.750	4.756	2.10E-08 $\pm$ 1.57E-09	652 $\pm$ 49	6000 $\pm$ 1500	0.51 $\pm$ 0.10	3.03 $\pm$ 0.40	0.07	95 $\pm$ 5
06338+5333	V382 Aur	161.983	19.592	8.93E-09 $\pm$ 7.25E-10	278 $\pm$ 23	1700 $\pm$ 750	0.08 $\pm$ 0.01	2.47 $\pm$ 0.56	0.02	421 $\pm$ 37
04296+3429	GLMP 74	166.237	-9.048	7.77E-09 $\pm$ 8.21E-10	242 $\pm$ 26	6000 $\pm$ 1500	0.71 $\pm$ 0.14	4.98 $\pm$ 0.68	3.85	211-571
04395+3601	RAFGL 618	166.446	-6.527	2.61E-07 $\pm$ 2.32E-08	8131 $\pm$ 722	12000 $\pm$ 3000	0.64 $\pm$ 0.13	1.22 $\pm$ 0.16	1210	134-878
05113+1347	GLMP 88	188.857	-14.294	3.92E-09 $\pm$ 4.18E-10	122 $\pm$ 13	1700 $\pm$ 750	0.38 $\pm$ 0.04	3.73 $\pm$ 0.85	0.99	209 $\pm$ 10
05381+1012	GLMP 117	195.524	-10.607	4.62E-09 $\pm$ 6.24E-10	144 $\pm$ 19	3500 $\pm$ 1500	0.29 $\pm$ 0.03	4.93 $\pm$ 1.11	0.15	183-506
05341+0852	GLMP 106	196.189	-12.141	2.64E-09 $\pm$ 2.39E-10	82 $\pm$ 7	1700 $\pm$ 750	0.25 $\pm$ 0.02	4.55 $\pm$ 1.02	2.62	284 $\pm$ 14
07008+1050	PS Gem	204.671	7.575	3.98E-08 $\pm$ 6.46E-09	1237 $\pm$ 201	3500 $\pm$ 1500	0.09 $\pm$ 0.02	1.68 $\pm$ 0.39	0.11	722 $\pm$ 71
07134+1005	LS VI +10 15	206.746	9.995	2.41E-08 $\pm$ 2.09E-09	748 $\pm$ 65	6000 $\pm$ 1500	0.07 $\pm$ 0.01	2.83 $\pm$ 0.38	1.27	181 $\pm$ 14
07430+1115	GLMP 192	208.931	17.067	5.01E-09 $\pm$ 5.32E-10	156 $\pm$ 17	6000 $\pm$ 1500	0.04 $\pm$ 0.01	6.20 $\pm$ 0.84	1.94	223 $\pm$ 11
06530-0213	GLMP 161	215.437	-0.135	5.17E-09 $\pm$ 3.99E-10	161 $\pm$ 12	6000 $\pm$ 1500	0.80 $\pm$ 0.08	6.11 $\pm$ 0.80	2.23	196 $\pm$ 10
06176-1036	Red Rectangle	218.968	-11.765	2.66E-07 $\pm$ 9.62E-08	8283 $\pm$ 2993	6000 $\pm$ 1500	0.55 $\pm$ 0.05	0.85 $\pm$ 0.19	5.47	264-607
07018-0513	...	219.127	0.443	7.01E-08 $\pm$ 4.27E-08	2182 $\pm$ 1329	6000 $\pm$ 1500	0.45 $\pm$ 0.04	1.66 $\pm$ 0.55	0.00	112 $\pm$ 20
09371+1212	Frosty Leo	221.890	42.727	5.74E-09 $\pm$ 8.11E-10	179 $\pm$ 25	1700 $\pm$ 750	0.03 $\pm$ 0.01	3.08 $\pm$ 0.71	0.87	75 $\pm$ 4
05208-2035	BD-20 1073	222.848	-28.277	1.39E-08 $\pm$ 2.19E-09	434 $\pm$ 68	6000 $\pm$ 1500	0.06 $\pm$ 0.01	3.72 $\pm$ 0.55	0.31	331 $\pm$ 17
07253-2001	GLMP 183	234.863	-1.475	4.01E-09 $\pm$ 6.29E-10	125 $\pm$ 20	6000 $\pm$ 1500	0.46 $\pm$ 0.05	6.93 $\pm$ 1.02	5.78	222-825
08187-1905	V552 Pup	240.581	9.762	1.13E-08 $\pm$ 1.07E-09	351 $\pm$ 33	6000 $\pm$ 1500	0.10 $\pm$ 0.02	4.13 $\pm$ 0.55	0.30	138 $\pm$ 7
08005-2356	V510 Pup	242.365	3.583	2.07E-08 $\pm$ 2.66E-09	643 $\pm$ 83	12000 $\pm$ 3000	0.20 $\pm$ 0.04	4.32 $\pm$ 0.61	3.90	181-974
07577-2806	GLMP 200	245.567	0.831	8.69E-10 $\pm$ 1.73E-10	27 $\pm$ 5	6000 $\pm$ 1500	0.88 $\pm$ 0.09	14.90 $\pm$ 2.38	1.08	175-491
08057-3417	GLMP 204	251.699	-1.041	1.26E-08 $\pm$ 1.76E-09	392 $\pm$ 55	6000 $\pm$ 1500	0.81 $\pm$ 0.08	3.91 $\pm$ 0.56	0.05	206-441
07582-4059	GLMP 201	256.573	-5.878	2.18E-09 $\pm$ 3.53E-10	68 $\pm$ 11	6000 $\pm$ 1500	0.86 $\pm$ 0.17	9.40 $\pm$ 1.40	7.74	172 $\pm$ 9
08143-4406	GLMP 206	260.830	-5.066	6.35E-09 $\pm$ 4.08E-10	197 $\pm$ 13	6000 $\pm$ 1500	0.97 $\pm$ 0.19	5.51 $\pm$ 0.71	0.29	143 $\pm$ 7
09032-3953	GLMP 241	263.090	4.670	2.33E-08 $\pm$ 2.39E-09	725 $\pm$ 74	6000 $\pm$ 1500	0.70 $\pm$ 0.14	2.88 $\pm$ 0.39	988	193-987
...	BD+13 2491	264.549	72.472	3.74E-08 $\pm$ 3.49E-09	1163 $\pm$ 108	1700 $\pm$ 750	0.03 $\pm$ 0.01	1.21 $\pm$ 0.27	...	...
08281-4850	GLMP 218	266.077	-5.823	2.05E-09 $\pm$ 3.20E-10	64 $\pm$ 10	6000 $\pm$ 1500	0.78 $\pm$ 0.16	9.70 $\pm$ 1.43	2.19	198 $\pm$ 10
10158-2844	HR 4049	266.845	22.934	2.76E-07 $\pm$ 4.63E-08	8585 $\pm$ 1440	3500 $\pm$ 1500	0.06 $\pm$ 0.01	0.64 $\pm$ 0.15	0.31	1120 $\pm$ 113
...	CPD-61 455	269.968	-34.078	1.57E-09 $\pm$ 6.62E-11	49 $\pm$ 2	1700 $\pm$ 750	0.03 $\pm$ 0.01	5.91 $\pm$ 1.31	...	...
09370-4826	GLMP 255	273.434	2.857	7.93E-09 $\pm$ 1.94E-09	247 $\pm$ 60	6000 $\pm$ 1500	0.31 $\pm$ 0.03	4.93 $\pm$ 0.86	43	220 $\pm$ 19
08275-6206	GLMP 217	277.063	-13.509	5.29E-09 $\pm$ 5.79E-10	165 $\pm$ 18	3500 $\pm$ 1500	0.23 $\pm$ 0.02	4.61 $\pm$ 1.02	0.42	236 $\pm$ 14
11472-0800	...	277.910	51.563	2.93E-09 $\pm$ 7.59E-10	91 $\pm$ 24	1700 $\pm$ 750	0.04 $\pm$ 0.01	4.32 $\pm$ 1.10	2.41	335 $\pm$ 18
10194-5625	GLMP 271	283.372	0.381	8.94E-09 $\pm$ 2.06E-09	278 $\pm$ 64	6000 $\pm$ 1500	0.43 $\pm$ 0.04	4.64 $\pm$ 0.79	...	210-478
10256-5628	GLMP 277	284.141	0.791	6.11E-09 $\pm$ 5.90E-10	190 $\pm$ 18	6000 $\pm$ 1500	0.43 $\pm$ 0.04	5.62 $\pm$ 0.75	17	152 $\pm$ 8
10197-5750	Roberts 22	284.177	-0.790	1.90E-07 $\pm$ 1.88E-08	5904 $\pm$ 584	12000 $\pm$ 3000	0.25 $\pm$ 0.03	1.43 $\pm$ 0.19	109	203-702
10178-5958	GLMP 270	285.119	-2.716	9.21E-09 $\pm$ 1.46E-09	287 $\pm$ 45	6000 $\pm$ 1500	0.43 $\pm$ 0.04	4.58 $\pm$ 0.68	13	110-604
...	EC 11507-2253	285.948	37.781	8.79E-11 $\pm$ 1.64E-11	2.74 $\pm$ 0.51	1700 $\pm$ 750	0.05 $\pm$ 0.01	24.93 $\pm$ 5.97	...	...
11385-5517	V885 Cen	293.028	5.937	1.75E-07 $\pm$ 2.85E-08	5454 $\pm$ 886	3500 $\pm$ 1500	0.33 $\pm$ 0.07	0.80 $\pm$ 0.18	0.78	128-921
11339-6004	GLMP 303	293.769	1.181	1.16E-09 $\pm$ 1.78E-10	36 $\pm$ 6	6000 $\pm$ 1500	0.35 $\pm$ 0.04	12.87 $\pm$ 1.89	205	196 $\pm$ 10
11201-6545	...	294.041	-4.709	4.37E-09 $\pm$ 5.15E-10	136 $\pm$ 16	6000 $\pm$ 1500	0.74 $\pm$ 0.15	6.64 $\pm$ 0.92	2.38	149 $\pm$ 7
11353-6037	...	294.086	0.702	2.81E-09 $\pm$ 5.12E-10	87 $\pm$ 16	6000 $\pm$ 1500	0.35 $\pm$ 0.04	8.29 $\pm$ 1.28	2.66	123-1212
11387-6113	GLMP 307	294.650	0.231	4.13E-09 $\pm$ 5.25E-10	129 $\pm$ 16	6000 $\pm$ 1500	0.35 $\pm$ 0.04	6.83 $\pm$ 0.96	1.19	143 $\pm$ 7
11381-6401	...	295.3								

IRAS No.	Other Name	<i>l</i> ( $^{\circ}$ )	<i>b</i> ( $^{\circ}$ )	Flux ( $\text{erg s}^{-1} \text{cm}^{-2}$ )	Flux ( $L_{\odot} \text{kpc}^{-2}$ )	Luminosity ( $L_{\odot}$ )	$E(B - V)$ (mag)	Distance (kpc)	$F_{IR}/F_{\star}$	$T_D$ (K)
14104-5819	GLMP 375	313.537	2.595	2.83E-09 $\pm$ 7.90E-10	88 $\pm$ 25	6000 $\pm$ 1500	0.74 $\pm$ 0.07	8.25 $\pm$ 1.55	...	217-571
14331-6435	LS 3268	313.887	-4.203	1.55E-08 $\pm$ 5.76E-09	483 $\pm$ 179	6000 $\pm$ 1500	0.57 $\pm$ 0.11	3.52 $\pm$ 0.79	0.96	144 $\pm$ 7
14072-5446	CD-54 5573	314.200	6.122	8.29E-09 $\pm$ 8.82E-10	258 $\pm$ 27	6000 $\pm$ 1500	0.50 $\pm$ 0.10	4.82 $\pm$ 0.66	0.12	122 $\pm$ 6
14341-6211	...	314.933	-2.053	1.90E-09 $\pm$ 2.13E-10	59 $\pm$ 7	6000 $\pm$ 1500	0.84 $\pm$ 0.08	10.08 $\pm$ 1.38	40	189-800
14527-6204	...	316.944	-2.869	3.10E-08 $\pm$ 5.53E-09	966 $\pm$ 172	3500 $\pm$ 1500	0.46 $\pm$ 0.05	1.90 $\pm$ 0.44	...	...
...	BPS CS 22877-0023	317.105	53.105	2.87E-10 $\pm$ 1.21E-11	8.93 $\pm$ 0.38	1700 $\pm$ 750	0.04 $\pm$ 0.01	13.80 $\pm$ 3.06	...	...
15210-6554	...	317.691	-7.737	2.64E-09 $\pm$ 6.84E-10	82 $\pm$ 21	6000 $\pm$ 1500	0.18 $\pm$ 0.04	8.55 $\pm$ 1.54	1.20	198-965
14482-5725	...	318.525	1.538	2.22E-09 $\pm$ 5.14E-10	69 $\pm$ 16	6000 $\pm$ 1500	0.88 $\pm$ 0.09	9.32 $\pm$ 1.59	0.76	200 $\pm$ 10
15066-5532	GLMP 403	321.662	1.996	6.22E-09 $\pm$ 1.54E-09	193 $\pm$ 48	6000 $\pm$ 1500	0.38 $\pm$ 0.04	5.57 $\pm$ 0.98	26	120 $\pm$ 6
14429-4539	...	322.959	12.492	6.67E-09 $\pm$ 1.35E-09	207 $\pm$ 42	6000 $\pm$ 1500	0.15 $\pm$ 0.01	5.38 $\pm$ 0.86	15	244-590
15039-4806	LS 3309	325.038	8.649	5.73E-08 $\pm$ 8.62E-09	1784 $\pm$ 268	3500 $\pm$ 1500	0.27 $\pm$ 0.05	1.40 $\pm$ 0.32	0.01	137 $\pm$ 7
15482-5741	...	325.159	-3.007	1.36E-09 $\pm$ 2.59E-10	42 $\pm$ 8	6000 $\pm$ 1500	0.55 $\pm$ 0.06	11.92 $\pm$ 1.87	1.07	156 $\pm$ 8
15452-5459	...	326.518	-0.633	6.13E-08 $\pm$ 1.58E-08	1908 $\pm$ 491	6000 $\pm$ 1500	0.30 $\pm$ 0.03	1.77 $\pm$ 0.32	...	144-471
15445-5449	OH 326.5 -0.4	326.536	-0.428	1.00E-08 $\pm$ 1.89E-09	312 $\pm$ 59	6000 $\pm$ 1500	0.35 $\pm$ 0.04	4.38 $\pm$ 0.69	...	133-966
16206-5956	LS 3591	326.770	-7.487	7.69E-09 $\pm$ 7.84E-10	239 $\pm$ 24	3500 $\pm$ 1500	0.19 $\pm$ 0.04	3.83 $\pm$ 0.84	0.38	136 $\pm$ 6
...	LS 3593	330.644	-3.672	3.13E-08 $\pm$ 3.68E-09	974 $\pm$ 115	1700 $\pm$ 750	0.53 $\pm$ 0.05	1.32 $\pm$ 0.30	...	...
...	LSE 237	331.555	-27.219	8.31E-10 $\pm$ 8.22E-11	26 $\pm$ 3	1700 $\pm$ 750	0.04 $\pm$ 0.01	8.11 $\pm$ 1.83	...	...
16115-5044	...	332.284	-0.001	4.55E-08 $\pm$ 6.58E-09	1416 $\pm$ 205	6000 $\pm$ 1500	0.53 $\pm$ 0.05	2.06 $\pm$ 0.30	2.86	100 $\pm$ 9
16127-5021	...	332.692	0.148	3.90E-09 $\pm$ 8.44E-10	121 $\pm$ 26	6000 $\pm$ 1500	0.53 $\pm$ 0.05	7.04 $\pm$ 1.16	...	135-996
16279-4757	...	336.144	0.083	4.57E-08 $\pm$ 8.77E-09	1421 $\pm$ 273	6000 $\pm$ 1500	0.53 $\pm$ 0.05	2.06 $\pm$ 0.32	...	173-1296
16029-4101	...	337.800	8.145	1.67E-09 $\pm$ 1.68E-10	52 $\pm$ 5	6000 $\pm$ 1500	0.61 $\pm$ 0.12	10.75 $\pm$ 1.45	3.06	207-610
16328-4517	...	338.660	1.290	2.62E-09 $\pm$ 2.76E-10	82 $\pm$ 9	6000 $\pm$ 1500	0.53 $\pm$ 0.05	8.58 $\pm$ 1.16	10	189 $\pm$ 9
16283-4424	...	338.770	2.466	1.86E-09 $\pm$ 3.26E-10	58 $\pm$ 10	6000 $\pm$ 1500	0.53 $\pm$ 0.05	10.18 $\pm$ 1.55	3.27	172 $\pm$ 9
16594-4656	Water Lily Nebula	340.392	-3.289	2.83E-08 $\pm$ 3.36E-09	879 $\pm$ 105	12000 $\pm$ 3000	0.51 $\pm$ 0.05	3.69 $\pm$ 0.51	33	200-1067
17311-4924	LSE 76	341.406	-9.037	2.15E-08 $\pm$ 2.04E-09	669 $\pm$ 64	6000 $\pm$ 1500	0.19 $\pm$ 0.04	3.00 $\pm$ 0.40	8.81	192-1214
16342-3814	Water Fountain Nebula	344.073	5.847	3.39E-08 $\pm$ 3.17E-09	1053 $\pm$ 99	12000 $\pm$ 3000	0.65 $\pm$ 0.13	3.38 $\pm$ 0.45	144	131-1003
17009-4154	GLMP 509	344.534	-0.420	1.61E-08 $\pm$ 2.77E-09	501 $\pm$ 86	6000 $\pm$ 1500	0.51 $\pm$ 0.05	3.46 $\pm$ 0.53	...	134-1269
16494-3930	...	345.055	2.783	2.22E-09 $\pm$ 3.61E-10	69 $\pm$ 11	6000 $\pm$ 1500	0.51 $\pm$ 0.05	9.31 $\pm$ 1.39	9.87	190 $\pm$ 9
17476-4446	...	346.880	-9.053	8.55E-10 $\pm$ 1.17E-10	27 $\pm$ 4	1700 $\pm$ 750	0.25 $\pm$ 0.05	7.99 $\pm$ 1.85	1.49	191 $\pm$ 10
17234-4008	GLMP 563	348.452	-2.818	1.77E-09 $\pm$ 1.97E-10	55 $\pm$ 6	6000 $\pm$ 1500	0.51 $\pm$ 0.05	10.43 $\pm$ 1.43	...	148-1095
17245-3951	Walnut Nebula	348.813	-2.840	5.03E-09 $\pm$ 6.48E-10	157 $\pm$ 20	12000 $\pm$ 3000	0.51 $\pm$ 0.05	8.76 $\pm$ 1.23	18	148-814
17208-3859	...	349.128	-1.756	4.09E-09 $\pm$ 1.16E-09	127 $\pm$ 36	6000 $\pm$ 1500	0.51 $\pm$ 0.05	6.86 $\pm$ 1.30	40	111-323
16552-3050	GLMP 498	352.567	7.298	1.81E-09 $\pm$ 2.85E-10	56 $\pm$ 9	4000 $\pm$ 1500	0.40 $\pm$ 0.08	8.43 $\pm$ 1.72	559	147 $\pm$ 7
18025-3906	GLMP 713	353.268	-8.725	7.14E-09 $\pm$ 7.08E-10	222 $\pm$ 22	6000 $\pm$ 1500	0.14 $\pm$ 0.03	5.20 $\pm$ 0.70	1.93	159 $\pm$ 8
16559-2957	GLMP 500	353.367	7.727	6.44E-09 $\pm$ 1.28E-09	200 $\pm$ 40	6000 $\pm$ 1500	0.32 $\pm$ 0.06	5.47 $\pm$ 0.87	16	189-1122
17150-3224	Cotton Candy Nebula	353.844	2.984	4.39E-08 $\pm$ 3.45E-09	1367 $\pm$ 107	12000 $\pm$ 3000	0.57 $\pm$ 0.06	2.96 $\pm$ 0.39	132	168-409
17310-3432	...	353.944	-0.970	1.47E-09 $\pm$ 3.73E-10	46 $\pm$ 12	4000 $\pm$ 1500	0.83 $\pm$ 0.08	9.35 $\pm$ 2.12	27	150 $\pm$ 7
17106-3046	GLMP 531	354.624	4.701	7.94E-09 $\pm$ 9.06E-10	247 $\pm$ 28	12000 $\pm$ 3000	1.16 $\pm$ 0.23	6.97 $\pm$ 0.96	4.92	143 $\pm$ 7
17149-3053	GLMP 539	355.066	3.878	1.63E-09 $\pm$ 3.35E-10	51 $\pm$ 10	4000 $\pm$ 1500	0.83 $\pm$ 0.08	8.90 $\pm$ 1.90	...	156-1136
17370-3357	...	355.110	-1.697	2.13E-09 $\pm$ 4.03E-10	66 $\pm$ 13	4000 $\pm$ 1500	0.85 $\pm$ 0.09	7.76 $\pm$ 1.63	0.89	116 $\pm$ 6
...	LSE 148	355.547	-20.421	3.16E-08 $\pm$ 1.43E-09	982 $\pm$ 44	1700 $\pm$ 750	0.09 $\pm$ 0.01	1.31 $\pm$ 0.29	...	...
17385-3332	...	355.641	-1.743	2.13E-09 $\pm$ 3.78E-10	66 $\pm$ 12	4000 $\pm$ 1500	0.78 $\pm$ 0.08	7.78 $\pm$ 1.61	2.75	138 $\pm$ 7
17440-3310	...	356.562	-2.527	3.74E-09 $\pm$ 4.98E-10	116 $\pm$ 15	4000 $\pm$ 1500	0.71 $\pm$ 0.07	5.86 $\pm$ 1.17	5.48	109 $\pm$ 5
18023-3409	LS 4634	357.614	-6.306	8.53E-09 $\pm$ 4.10E-09	265 $\pm$ 127	4000 $\pm$ 1500	0.39 $\pm$ 0.08	3.88 $\pm$ 1.18	0.06	161-1052
17195-2710	...	358.701	5.170	5.49E-09 $\pm$ 1.51E-09	171 $\pm$ 47	6000 $\pm$ 1500	1.22 $\pm$ 0.24	5.93 $\pm$ 1.10	35	187-1093
17317-2743	GLMP 584	359.750	2.628	4.03E-09 $\pm$ 5.07E-10	125 $\pm$ 16	4000 $\pm$ 1500	0.69 $\pm$ 0.07	5.65 $\pm$ 1.12	4.86	120 $\pm$ 6
17580-3111	GLMP 687	359.780	-4.073	2.49E-09 $\pm$ 3.85E-10	77 $\pm$ 12	4000 $\pm$ 1500	0.71 $\pm$ 0.14	7.19 $\pm$ 1.46	...	189-1099
18096-3230	GLMP 737	359.814	-6.871	1.35E-09 $\pm$ 2.16E-10	42 $\pm$ 7	4000 $\pm$ 1500	0.35 $\pm$ 0.07	9.77 $\pm$ 1.99	148	124 $\pm$ 6

Table A2: Parameters and distances for 87 possible PAGB objects, ordered by Galactic longitude.

IRAS No.	Other Name	<i>l</i> ( $^{\circ}$ )	<i>b</i> ( $^{\circ}$ )	Flux ( $\text{erg s}^{-1} \text{cm}^{-2}$ )	Flux ( $L_{\odot} \text{kpc}^{-2}$ )	Luminosity ( $L_{\odot}$ )	<i>E(B - V)</i> (mag)	Distance (kpc)	$F_{IR}/F_{\star}$	$T_D$ (K)
...	LS 4825	1.671	-6.628	3.09E-09 $\pm$ 6.10E-10	96 $\pm$ 19	4000 $\pm$ 1500	0.24 $\pm$ 0.05	6.45 $\pm$ 1.36	...	...
17550-2800	GLMP 676	2.205	-1.900	2.24E-09 $\pm$ 4.59E-10	70 $\pm$ 14	4000 $\pm$ 1500	0.51 $\pm$ 0.05	7.58 $\pm$ 1.62	...	125-1030
...	CD-30 15602	2.798	-7.675	1.26E-09 $\pm$ 1.79E-10	39 $\pm$ 6	3500 $\pm$ 1500	0.22 $\pm$ 0.04	9.44 $\pm$ 2.13	...	...
17376-2040	...	6.437	5.275	4.48E-09 $\pm$ 1.70E-09	139 $\pm$ 53	4000 $\pm$ 1500	0.65 $\pm$ 0.13	5.36 $\pm$ 1.43	5.71	161-1232
17416-2112	GLMP 625	6.469	4.198	2.14E-09 $\pm$ 2.34E-10	67 $\pm$ 7	4000 $\pm$ 1500	0.85 $\pm$ 0.17	7.75 $\pm$ 1.51	77	130-499
16476-1122	...	7.524	20.418	8.32E-09 $\pm$ 8.44E-10	259 $\pm$ 26	3500 $\pm$ 1500	0.70 $\pm$ 0.07	3.68 $\pm$ 0.81	0.11	186 $\pm$ 9
F16277-0724	LS IV -07 1	7.956	26.706	1.36E-07 $\pm$ 8.80E-09	4234 $\pm$ 274	3500 $\pm$ 1500	0.24 $\pm$ 0.02	0.91 $\pm$ 0.20	...	...
17433-1750	GLMP 637	9.562	5.612	5.73E-09 $\pm$ 3.22E-09	178 $\pm$ 100	4000 $\pm$ 1500	0.53 $\pm$ 0.11	4.74 $\pm$ 1.60	5.95	156-431
17364-1238	...	13.183	9.720	8.80E-10 $\pm$ 1.05E-10	27 $\pm$ 3	1700 $\pm$ 750	0.46 $\pm$ 0.09	7.88 $\pm$ 1.80	0.28	134 $\pm$ 7
18313-1738	...	15.322	-4.268	7.58E-09 $\pm$ 2.36E-09	236 $\pm$ 73	6000 $\pm$ 1500	0.64 $\pm$ 0.13	5.04 $\pm$ 1.01	6.39	412-1142
...	BPS CS 29493-0046	16.451	-50.434	9.03E-11 $\pm$ 4.87E-12	2.81 $\pm$ 0.15	1700 $\pm$ 750	0.02 $\pm$ 0.01	24.59 $\pm$ 5.46	...	...
...	NGC 6712 SS C26	25.353	-4.325	4.00E-10 $\pm$ 5.33E-11	12 $\pm$ 2	1700 $\pm$ 750	0.36 $\pm$ 0.07	11.68 $\pm$ 2.69	...	...
18420-0512	GLMP 823	27.577	-0.853	4.07E-09 $\pm$ 5.44E-10	127 $\pm$ 17	6000 $\pm$ 1500	0.91 $\pm$ 0.09	6.88 $\pm$ 0.98	3.25	127 $\pm$ 6
20023-1144	V1401 Aql	30.599	-21.534	1.07E-07 $\pm$ 1.22E-08	3332 $\pm$ 379	3500 $\pm$ 1500	0.13 $\pm$ 0.01	1.02 $\pm$ 0.23	...	...
18435-0052	...	31.605	0.811	1.56E-09 $\pm$ 5.76E-10	49 $\pm$ 18	6000 $\pm$ 1500	1.00 $\pm$ 0.10	11.11 $\pm$ 2.47	...	293-1191
18454+0001	GLMP 830	32.614	0.797	1.86E-09 $\pm$ 4.85E-10	58 $\pm$ 15	6000 $\pm$ 1500	1.00 $\pm$ 0.10	10.19 $\pm$ 1.84	71	121 $\pm$ 6
18539+0549	...	38.731	1.585	1.09E-09 $\pm$ 5.85E-10	34 $\pm$ 18	6000 $\pm$ 1500	1.00 $\pm$ 0.10	13.28 $\pm$ 3.92	...	100-308
19075+0432	GLMP 880	39.161	-2.008	7.13E-09 $\pm$ 1.24E-09	222 $\pm$ 39	6000 $\pm$ 1500	1.00 $\pm$ 0.10	5.20 $\pm$ 0.79	8.62	129-700
19176+1251	GLMP 898	47.688	-0.302	1.02E-09 $\pm$ 1.80E-10	32 $\pm$ 6	6000 $\pm$ 1500	0.76 $\pm$ 0.08	13.74 $\pm$ 2.10	...	168 $\pm$ 8
20547+0247	U Equ	51.363	-26.113	1.73E-08 $\pm$ 5.80E-09	539 $\pm$ 180	6000 $\pm$ 1500	0.08 $\pm$ 0.01	3.34 $\pm$ 0.70	124	281-1113
19181+1806	GLMP 900	52.367	2.050	8.78E-10 $\pm$ 1.25E-10	27 $\pm$ 4	6000 $\pm$ 1500	0.80 $\pm$ 0.08	14.82 $\pm$ 2.13	13	116-560
Z15500+3305	BD+33 2642	52.731	50.788	6.05E-09 $\pm$ 2.43E-09	188 $\pm$ 76	1700 $\pm$ 750	0.02 $\pm$ 0.01	3.00 $\pm$ 0.90	0.00	95 $\pm$ 5
...	BD+32 2754	53.575	41.502	3.52E-09 $\pm$ 3.09E-10	110 $\pm$ 10	1700 $\pm$ 750	0.02 $\pm$ 0.01	3.94 $\pm$ 0.89	...	...
19312+1950	...	55.371	0.186	3.31E-08 $\pm$ 1.06E-08	1029 $\pm$ 331	6000 $\pm$ 1500	0.80 $\pm$ 0.08	2.42 $\pm$ 0.49	...	74-998
19225+3013	...	63.564	6.889	1.83E-09 $\pm$ 2.30E-10	57 $\pm$ 7	1700 $\pm$ 750	0.25 $\pm$ 0.05	5.46 $\pm$ 1.25	0.34	208 $\pm$ 10
...	V534 Lyr	66.184	18.581	1.90E-08 $\pm$ 2.07E-09	591 $\pm$ 64	6000 $\pm$ 1500	0.05 $\pm$ 0.01	3.19 $\pm$ 0.43	...	...
19200+3457	LS II +34 1	67.572	9.511	2.18E-09 $\pm$ 6.35E-10	68 $\pm$ 20	1700 $\pm$ 750	0.12 $\pm$ 0.02	5.00 $\pm$ 1.32	0.16	144-326
19410+3733	LS II +37 1	71.909	7.003	3.65E-08 $\pm$ 1.37E-08	1137 $\pm$ 426	1700 $\pm$ 750	0.23 $\pm$ 0.05	1.22 $\pm$ 0.35	0.15	237-784
20244+3509	GLMP 996	74.586	-1.649	3.34E-09 $\pm$ 1.02E-09	104 $\pm$ 32	6000 $\pm$ 1500	0.89 $\pm$ 0.09	7.60 $\pm$ 1.50	1.00	134-1078
20094+3721	GLMP 976	74.682	2.103	1.42E-08 $\pm$ 3.23E-09	442 $\pm$ 72	6000 $\pm$ 1500	0.89 $\pm$ 0.09	3.69 $\pm$ 0.55	0.18	220-1293
20144+4656	GLMP 985	83.191	6.637	2.78E-09 $\pm$ 3.37E-10	86 $\pm$ 10	6000 $\pm$ 1500	0.60 $\pm$ 0.12	8.33 $\pm$ 1.16	23	126-553
20572+4919	V2324 Cyg	89.443	2.394	9.80E-09 $\pm$ 1.56E-09	305 $\pm$ 48	6000 $\pm$ 1500	0.79 $\pm$ 0.08	4.44 $\pm$ 0.66	0.69	170-929
20490+5934	GLMP 1012	96.570	9.900	2.09E-08 $\pm$ 2.79E-09	652 $\pm$ 87	6000 $\pm$ 1500	0.54 $\pm$ 0.11	3.03 $\pm$ 0.43	0.04	123-557
21289+5815	GLMP 1034	99.122	5.238	7.67E-10 $\pm$ 2.82E-10	24 $\pm$ 9	1700 $\pm$ 750	0.59 $\pm$ 0.12	8.44 $\pm$ 2.42	0.97	205 $\pm$ 11
21525+5643	GLMP 1043	100.534	2.000	3.17E-09 $\pm$ 1.01E-09	98 $\pm$ 32	6000 $\pm$ 1500	0.65 $\pm$ 0.07	7.80 $\pm$ 1.58	...	157-1218
20559+6416	GLMP 1013	100.816	12.233	8.34E-09 $\pm$ 1.23E-09	259 $\pm$ 38	1700 $\pm$ 750	0.63 $\pm$ 0.06	2.56 $\pm$ 0.59	0.19	157-1081
01259+6823	...	126.406	6.040	4.12E-09 $\pm$ 3.43E-10	128 $\pm$ 11	1700 $\pm$ 750	0.89 $\pm$ 0.18	3.64 $\pm$ 0.82	0.12	205 $\pm$ 10
02143+5852	GLMP 26	133.851	-1.927	3.85E-09 $\pm$ 8.86E-09	120 $\pm$ 28	6000 $\pm$ 1500	0.74 $\pm$ 0.07	7.07 $\pm$ 1.20	4.38	226-953
02528+4350	GLMP 34	145.419	-13.309	2.90E-09 $\pm$ 2.79E-10	90 $\pm$ 9	1700 $\pm$ 750	0.17 $\pm$ 0.02	4.34 $\pm$ 0.98	0.29	116-470
...	BPS CS 22946-0005	173.864	-82.408	2.08E-10 $\pm$ 1.70E-11	6.45 $\pm$ 0.53	1700 $\pm$ 750	0.02 $\pm$ 0.01	16.23 $\pm$ 3.64	...	...
05140+2851	LS V +28 2	176.626	-5.211	3.98E-07 $\pm$ 7.74E-08	12374 $\pm$ 2406	3500 $\pm$ 1500	0.60 $\pm$ 0.12	0.53 $\pm$ 0.12	...	...
05089+0459	GLMP 87	196.280	-19.505	4.01E-09 $\pm$ 4.22E-10	125 $\pm$ 13	1700 $\pm$ 750	0.10 $\pm$ 0.01	3.69 $\pm$ 0.84	5.80	206 $\pm$ 10
07131-0147	...	217.380	4.533	1.77E-09 $\pm$ 3.54E-10	55 $\pm$ 11	6000 $\pm$ 1500	0.13 $\pm$ 0.03	10.44 $\pm$ 1.67	2.86	112-404
07506-0345	GLMP 197	223.612	11.839	4.37E-10 $\pm$ 1.65E-10	14 $\pm$ 5	1700 $\pm$ 750	0.05 $\pm$ 0.01	11.18 $\pm$ 3.24	1.37	182-501
07227-1320	GLMP 182	228.698	1.176	3.22E-09 $\pm$ 2.28E-10	100 $\pm$ 7	3500 $\pm$ 1500	0.34 $\pm$ 0.03	5.91 $\pm$ 1.28	0.42	225 $\pm$ 11
07399-1435	Rotten Egg Nebula	231.836	4.220	7.54E-08 $\pm$ 2.09E-09	2347 $\pm$ 652	6000 $\pm$ 1500	1.55 $\pm$ 0.31	1.60 $\pm$ 0.30	6.19	120-612
F05338-3051	RV Col	234.985	-28.786	1.93E-08 $\pm$ 9.94E-10	599 $\pm$ 31	3500 $\pm$ 1500	0.03 $\pm$ 0.01	2.42 $\pm$ 0.52	...	...
07140-2321	CD-23 5180	236.569	-5.373	1.17E-08 $\pm$ 2.11E-09	364 $\pm$ 66	3500 $\pm$ 1500	0.53 $\pm$ 0.11	3.10 $\pm$ 0.72	0.13	179-496
08242-3828	GLMP 214	257.256	-0.336	1.88E-08 $\pm$ 4.02E-09	584 $\pm$ 125	3500 $\pm$ 1500	0.23 $\pm$ 0.02	2.45 $\pm$ 0.59	0.43	145-395
08351-4634	GLMP 222	264.958	-3.533	6.98E-09 $\pm$ 4.21E-10	217 $\pm$ 13	6000 $\pm$ 1500	0.47 $\pm$ 0.05	5.25 $\pm$ 0.68	...	230-593
10456-5712	NSV 4975	286.871	1.492	4.44E-07 $\pm$ 1.56E-07	13799 $\pm$ 4862	6000 $\pm$ 1500	0.16 $\pm$ 0.02	0.66 $\pm$ 0.14	0.13	378 $\pm$ 51
11000-6153	LS 2105	290.540	-1.951	3.92E-08 $\pm$ 8.81E-09	1220 $\pm$ 274	6000 $\pm$ 1500	0.35 $\pm$ 0.04	2.22 $\pm$ 0.37	0.83	120-739
11159-5954	...	291.573	0.620	2.91E-09 $\pm$ 6.09E-10	91 $\pm$ 19	6000 $\pm$ 1500	0.35 $\pm$ 0.04	8.13 $\pm$ 1.32	...	125 $\pm$ 9
12145-5834	...	298.516	3.721	3.32E-10 $\pm$ 4.92E-11	10 $\pm$ 2	1700 $\pm$ 750	0.35 $\pm$ 0.04	12.82 $\pm$ 2.98	4.51	149-1186
12262-6417	...	300.532	-1.793	2.21E-09 $\pm$ 3.45E-10	69 $\pm$ 11	6000 $\pm$ 1500	0.58 $\pm$ 0.06	9.35 $\pm$ 1.38	25	152-773
12360-5740	GLMP 334	301.261	4.889	1.76E-09 $\pm$ 1.37E-10	55 $\pm$ 4	3500 $\pm$ 1500	0.50 $\pm$ 0.10	8.00 $\pm$ 1.74	0.41	163 $\pm$ 8
13010-6012	...	304.491	2.354	5.82E-10 $\pm$ 1.24E-10	18 $\pm$ 4	6000 $\pm$ 1500	0.68 $\pm$ 0.07	18.21 $\pm$ 2.99	1.88	157-311
13258-8103	...	304.505	-18.558	1.79E-09 $\pm$ 2.85E-10	56 $\pm$ 9	1700 $\pm$ 750	0.42 $\pm$ 0.04	5.53 $\pm$ 1.30	17	170-770
12584-4837	V1028 Cen	304.601	13.951	1.84E-08 $\pm$ 3.10E-09	572 $\pm$ 96	3500 $\pm$ 1500	0.16 $\pm$ 0.02	2.47 $\pm$ 0.57	6.41	326-828
13313-5838	...	308.496	3.512	2.50E-09 $\pm$ 5.34E-10	78 $\pm$ 17	6000 $\pm$ 1500	0.59 $\pm$ 0.06	8.78 <		

IRAS No.	Other Name	$l$ ( $^{\circ}$ )	$b$ ( $^{\circ}$ )	Flux ( $\text{erg s}^{-1} \text{cm}^{-2}$ )	Flux ( $L_{\odot} \text{kpc}^{-2}$ )	Luminosity ( $L_{\odot}$ )	$E(B - V)$ (mag)	Distance (kpc)	$F_{IR}/F_{\star}$	$T_D$ (K)
17277-3506	Hen 3-1418	353.106	-0.715	2.01E-10 $\pm$ 6.80E-11	6.27 $\pm$ 2.11	4000 $\pm$ 1500	0.85 $\pm$ 0.09	25.27 $\pm$ 6.37	...	...
17287-3443	GLMP 574	353.542	-0.677	1.36E-08 $\pm$ 3.93E-09	423 $\pm$ 122	6000 $\pm$ 1500	0.57 $\pm$ 0.06	3.77 $\pm$ 0.72	7.31	113 $\pm$ 6
18019-3403	...	357.664	-6.181	1.28E-09 $\pm$ 5.64E-10	40 $\pm$ 18	4000 $\pm$ 1500	0.37 $\pm$ 0.07	10.04 $\pm$ 2.91	1.00	175-1050
17253-2831	...	358.311	3.361	3.52E-09 $\pm$ 4.24E-10	110 $\pm$ 13	4000 $\pm$ 1500	0.72 $\pm$ 0.07	6.04 $\pm$ 1.19	1.67	140 $\pm$ 7
17223-2659	GLMP 558	359.201	4.777	5.03E-09 $\pm$ 1.88E-09	156 $\pm$ 59	4000 $\pm$ 1500	1.45 $\pm$ 0.29	5.06 $\pm$ 1.34	0.20	189-1285
17543-3102	GLMP 670	359.499	-3.302	3.02E-09 $\pm$ 5.49E-10	94 $\pm$ 17	4000 $\pm$ 1500	0.73 $\pm$ 0.07	6.53 $\pm$ 1.36	118	145-751

Table A3: Parameters and distances for 69 Miscellaneous objects not in the Toruń Catalogue, ordered by Galactic longitude.

IRAS No.	Other Name	<i>l</i> ( $^{\circ}$ )	<i>b</i> ( $^{\circ}$ )	Flux ( $\text{erg s}^{-1} \text{cm}^{-2}$ )	Flux ( $L_{\odot} \text{kpc}^{-2}$ )	Luminosity ( $L_{\odot}$ )	$E(B - V)$ (mag)	Distance (kpc)	$F_{\text{IR}}/F_{\star}$	$T_{\text{D}}$ (K)
17371-2747	JaSt 23	0.344	1.566	$2.27E-09 \pm 9.27E-10$	$71 \pm 29$	$4000 \pm 1500$	$0.51 \pm 0.05$	$7.52 \pm 2.08$	...	90–657
17574-2921	H 1-47	1.295	-3.040	$9.11E-10 \pm 3.08E-10$	$28 \pm 10$	$4000 \pm 1500$	$0.52 \pm 0.05$	$11.88 \pm 3.00$	34	113–337
18129-3053	SwSt 1	1.591	-6.176	$1.41E-08 \pm 3.41E-09$	$437 \pm 106$	$4000 \pm 1500$	$0.30 \pm 0.06$	$3.02 \pm 0.68$	15	200–861
18040-2941	H 1-55	1.714	-4.455	$3.60E-10 \pm 1.08E-10$	$11 \pm 3$	$4000 \pm 1500$	$0.45 \pm 0.09$	$18.91 \pm 4.54$	15	87–325
18022-2822	M 1-37	2.681	-3.468	$1.56E-09 \pm 6.39E-10$	$48 \pm 20$	$4000 \pm 1500$	$0.89 \pm 0.09$	$9.09 \pm 2.52$	5.72	118–349
18084-2823	Ap 1-12	3.326	-4.660	$1.64E-09 \pm 2.92E-10$	$51 \pm 9$	$4000 \pm 1500$	$0.41 \pm 0.08$	$8.86 \pm 1.84$	3.59	117–623
18213-2948	Hen 3-1688	3.392	-7.810	$5.24E-08 \pm 7.05E-09$	$1631 \pm 219$	$6000 \pm 1500$	$0.38 \pm 0.08$	$1.92 \pm 0.27$	0.09	116–1090
17074-1845	Hen 3-1347	4.100	12.263	$3.33E-09 \pm 9.18E-10$	$104 \pm 29$	$6000 \pm 1500$	$0.25 \pm 0.03$	$7.61 \pm 1.42$	0.34	146±7
19288-3419	Hen 2-436	4.871	-22.727	$1.93E-10 \pm 5.96E-11$	$6.00 \pm 1.85$	$4000 \pm 1500$	$0.41 \pm 0.04$	$25.81 \pm 6.27$	9.75	267–880
18061-2502	MaC 1-10	5.974	-2.611	$2.93E-09 \pm 4.54E-10$	$91 \pm 14$	$4000 \pm 1500$	$0.51 \pm 0.05$	$6.62 \pm 1.34$	196	227–781
18170-2416	H 1-65	7.883	-4.407	$1.42E-09 \pm 4.06E-10$	$44 \pm 13$	$4000 \pm 1500$	$0.65 \pm 0.13$	$9.51 \pm 2.24$	2.24	116–356
...	M 2-9	10.900	18.055	$3.22E-08 \pm 9.23E-09$	$1002 \pm 287$	$2000 \pm 750$	$0.50 \pm 0.05$	$1.41 \pm 0.33$	146	169–767
17514-1555	PM 1-188	12.219	4.923	$6.55E-09 \pm 1.92E-09$	$204 \pm 60$	$4000 \pm 1500$	$1.72 \pm 0.34$	$4.43 \pm 1.05$	34	183–706
19016-2330	GLMP 869	13.134	-13.219	$8.94E-09 \pm 2.43E-09$	$278 \pm 76$	$4000 \pm 1500$	$0.21 \pm 0.02$	$3.79 \pm 0.88$	109	196–659
18240-2424	M 2-43	27.679	4.260	$1.92E-08 \pm 5.92E-09$	$598 \pm 184$	$4000 \pm 1500$	$1.80 \pm 0.36$	$2.59 \pm 0.63$	0.85	216–858
18096+0650	NGC 6572	34.621	11.847	$3.00E-08 \pm 8.59E-09$	$933 \pm 267$	$6000 \pm 1500$	$0.28 \pm 0.03$	$2.54 \pm 0.48$	2.72	178–894
17317-3331	V1018 Sco	35.884	-0.539	$7.95E-08 \pm 2.56E-08$	$2475 \pm 797$	$35000 \pm 5000$	$0.76 \pm 0.08$	$3.76 \pm 0.66$	...	187–482
18538+0703	K 3-17	39.828	2.167	$5.78E-09 \pm 1.37E-09$	$180 \pm 43$	$6000 \pm 1500$	$1.00 \pm 0.10$	$5.78 \pm 0.99$	...	139–447
19219+0947	Vy 2-2	45.498	-2.703	$2.65E-08 \pm 1.08E-08$	$826 \pm 335$	$6000 \pm 1500$	$1.06 \pm 0.11$	$2.69 \pm 0.64$	0.74	189–998
19396+1637	HM Sge	53.566	-3.150	$5.79E-08 \pm 1.85E-08$	$1800 \pm 575$	$6000 \pm 1500$	$0.57 \pm 0.06$	$1.83 \pm 0.37$	12	488–1296
19255+2123	K 3-35	56.096	2.094	$5.79E-09 \pm 8.38E-10$	$180 \pm 26$	$6000 \pm 1500$	$1.52 \pm 0.30$	$5.77 \pm 0.83$	83	110–460
19309+2646	M 1-91	61.396	3.619	$3.31E-09 \pm 7.56E-10$	$103 \pm 24$	$4000 \pm 1500$	$1.10 \pm 0.33$	$6.23 \pm 1.37$	...	112–594
19376+2622	Hen 2-442	61.793	2.111	$1.49E-08 \pm 1.52E-09$	$463 \pm 47$	$6000 \pm 1500$	$0.80 \pm 0.08$	$3.60 \pm 0.49$	52	609±30
19327+3024	BD+30-3639	64.785	5.019	$8.18E-08 \pm 1.15E-08$	$2546 \pm 358$	$4000 \pm 1500$	$0.36 \pm 0.07$	$1.25 \pm 0.25$	1.32	205–707
20406+2953	...	72.400	-7.535	$1.00E-08 \pm 1.47E-09$	$311 \pm 46$	$6000 \pm 1500$	$0.66 \pm 0.13$	$4.39 \pm 0.64$	8.88	177±9
20145+3656	M 1-76	74.906	1.020	$2.18E-08 \pm 2.52E-09$	$677 \pm 79$	$6000 \pm 1500$	$0.89 \pm 0.09$	$2.98 \pm 0.41$	12	846±42
...	NGC 7027	84.930	-3.497	$2.13E-07 \pm 4.09E-08$	$6611 \pm 1271$	$6000 \pm 1500$	$0.83 \pm 0.08$	$0.95 \pm 0.15$	...	217–660
21306+4422	IC 5117	89.873	-5.134	$7.65E-09 \pm 8.88E-10$	$238 \pm 28$	$6000 \pm 1500$	$0.42 \pm 0.08$	$5.02 \pm 0.69$	12	205–887
21282+5050	PK 093-00 2	93.987	-0.118	$2.15E-08 \pm 3.34E-09$	$669 \pm 104$	$4000 \pm 1500$	$0.59 \pm 0.06$	$2.44 \pm 0.50$	50	276–679
21554+6204	GLMP 1048	104.131	5.992	$2.48E-08 \pm 5.50E-09$	$772 \pm 171$	$6000 \pm 1500$	$0.66 \pm 0.13$	$2.79 \pm 0.47$	5517	261±22
23239+5754	Hb 12	111.877	-2.849	$2.05E-08 \pm 6.01E-09$	$639 \pm 187$	$6000 \pm 1500$	$0.83 \pm 0.25$	$3.06 \pm 0.59$	1.05	203–846
01427+4633	BD+46 442	132.514	-15.041	$6.49E-09 \pm 8.67E-10$	$202 \pm 27$	$1700 \pm 750$	$0.11 \pm 0.01$	$2.90 \pm 0.67$	0.09	312±36
04215+6000	M 4-18	146.795	7.601	$2.71E-09 \pm 5.16E-10$	$84 \pm 16$	$4000 \pm 1500$	$0.54 \pm 0.11$	$6.89 \pm 1.45$	2.34	210–638
03507+1115	IK Tau	177.955	-31.412	$5.06E-06 \pm 1.68E-06$	$157424 \pm 52311$	$9100 \pm 3000$	$0.23 \pm 0.02$	$0.24 \pm 0.06$	707610	451±151
...	CW Leo	221.449	45.060	$1.86E-05 \pm 7.44E-06$	$578035 \pm 231629$	$9800 \pm 3000$	$0.04 \pm 0.01$	$0.13 \pm 0.03$	...	385–635
09102-5101	...	272.122	-2.003	$6.57E-10 \pm 1.75E-10$	$20 \pm 5$	$6000 \pm 1500$	$0.35 \pm 0.04$	$17.14 \pm 3.13$	53	118–302
09394-4909	Hen 2-34	274.189	2.577	$2.15E-08 \pm 3.92E-09$	$669 \pm 122$	$6000 \pm 1500$	$0.70 \pm 0.14$	$2.99 \pm 0.46$	6.50	890±72
10214-6017	Hen 2-47	285.669	-2.743	$7.75E-09 \pm 1.79E-09$	$241 \pm 56$	$6000 \pm 1500$	$0.56 \pm 0.06$	$4.99 \pm 0.85$	1.92	148–1040
07027-7934	Vo 1	291.375	-26.294	$1.52E-08 \pm 2.03E-09$	$474 \pm 63$	$4000 \pm 1500$	$0.29 \pm 0.03$	$2.91 \pm 0.58$	139	210–765
13064-6103	Hen 2-90	305.110	1.468	$2.45E-08 \pm 7.07E-09$	$763 \pm 220$	$6000 \pm 1500$	$1.10 \pm 0.11$	$2.81 \pm 0.54$	4.07	272–788
13398-5951	...	309.343	2.108	$1.38E-09 \pm 2.66E-10$	$43 \pm 8$	$4000 \pm 1500$	$0.58 \pm 0.06$	$9.66 \pm 2.04$	19	189–514
14103-6311	Hen 2-106	312.026	-2.028	$2.18E-08 \pm 4.73E-09$	$678 \pm 147$	$6000 \pm 1500$	$0.48 \pm 0.05$	$2.97 \pm 0.49$	58	330–1028
14149-6253	Hen 2-107	312.613	-1.900	$1.64E-09 \pm 4.03E-10$	$51 \pm 13$	$4000 \pm 1500$	$0.29 \pm 0.03$	$8.85 \pm 1.98$	13	136–1139
15103-5754	...	320.907	-0.293	$1.69E-08 \pm 2.46E-09$	$524 \pm 77$	$6000 \pm 1500$	$0.34 \pm 0.03$	$3.38 \pm 0.49$	...	123–1038
14562-5406	Hen 2-113	321.048	3.988	$5.85E-08 \pm 8.43E-09$	$1821 \pm 262$	$4000 \pm 1500$	$0.75 \pm 0.08$	$1.48 \pm 0.30$	8.83	198–711
15198-5658	Pe 2-8	322.469	-0.178	$8.83E-09 \pm 2.68E-09$	$275 \pm 83$	$6000 \pm 1500$	$2.76 \pm 0.28$	$4.67 \pm 0.92$	23	189±11
15154-5258	PM 1-89	324.086	3.531	$2.25E-09 \pm 3.62E-10$	$70 \pm 11$	$4000 \pm 1500$	$0.43 \pm 0.04$	$7.55 \pm 1.54$	12	158–728
15534-5422	...	327.829	-0.888	$1.20E-09 \pm 3.29E-10$	$37 \pm 10$	$6000 \pm 1500$	$0.53 \pm 0.05$	$12.65 \pm 2.34$	62	156–791
16099-5651	Hen 2-147	327.920	-4.298	$1.84E-08 \pm 2.64E-09$	$572 \pm 82$	$7000 \pm 1500$	$0.45 \pm 0.09$	$3.50 \pm 0.45$	...	...
15405-4945	OH 329.14+3.92	329.142	3.949	$5.81E-09 \pm 9.63E-10$	$181 \pm 30$	$6000 \pm 1500$	$0.39 \pm 0.04$	$5.76 \pm 0.86$	208	107–685
16133-5151	Mz 3	331.727	-1.011	$7.99E-08 \pm 1.88E-08$	$2486 \pm 584$	$12000 \pm 3000$	$1.32 \pm 0.13$	$2.20 \pm 0.38$	26	173–813
17047-5650	Hen 3-1333	332.915	-9.908	$8.15E-08 \pm 1.63E-08$	$2534 \pm 507$	$4000 \pm 1500$	$0.33 \pm 0.07$	$1.26 \pm 0.27$	48	176–597
16333-4807	[VP93]1633-4807	336.644	-0.696	$9.57E-09 \pm 2.27E-09$	$298 \pm 71$	$3500 \pm 1500$	$0.53 \pm 0.05$	$3.43 \pm 0.84$	...	110–1000
17150-3754	PBZ 1	349.351	-0.211	$6.79E-09 \pm 1.33E-09$	$211 \pm 41$	$6000 \pm 1500$	$0.51 \pm 0.05$	$5.33 \pm 0.85$	143	84–319
17340-3757	...	351.412	-3.340	$4.09E-09 \pm 6.23E-10$	$127 \pm 19$	$4000 \pm 1500$	$0.71 \pm 0.07$	$5.61 \pm 1.14$	10	81–558
17251-3505	H 1-13	352.828	-0.260	$1.30E-08 \pm 2.23E-09$	$404 \pm 69$	$4000 \pm 1500$	$2.34 \pm 0.23$	$3.15 \pm 0.65$	20	162–429
16416-2758	K 2-16	352.947	11.396	$8.07E-09 \pm 1.19E-09$	$251 \pm 37$	$4000 \pm 1500$	$0.34 \pm 0.03$	$3.99 \pm 0.80$	2.68	183±9
17567-3849	Fg 3	352.958	-7.060	$4.26E-09 \pm 5.07E-10$	$133 \pm 16$	$6000 \pm 1500$	$0.32 \pm 0.06$	$6.73 \pm 0.93$	7.53	160–1055
17463-3700	H 1-36	353.514	-4.921	$7.57E-09 \pm 1.89E-09$	$235 \pm 59$	$6000 \pm 1500$	$0.55 \pm 0.11$	$5.05 \pm 0.89$	34	262–845
17183-3017	H 1-9	355.969	3.626	$4.10E-09 \pm 1.83E-09$	$128 \pm 57$	$4000 \pm 1500$	$1.16 \pm 0.12$	$5.60 \pm 1.63$	0.90	159–1021
17221-3038	Th 3-13	356.155	2.765	$1.42E-09 \pm 4.56E-10$	$44 \pm 14$	$4000 \pm 1500$	$2.41 \pm 0.48$ </			